

BLDSC no:- DX 177517

**LOUGHBOROUGH  
UNIVERSITY OF TECHNOLOGY  
LIBRARY**

**AUTHOR/FILING TITLE**

ERTAS, F.W.

**ACCESSION/COPY NO.**

040081955

**VOL. NO.**

**CLASS MARK**

25 JUN 1999

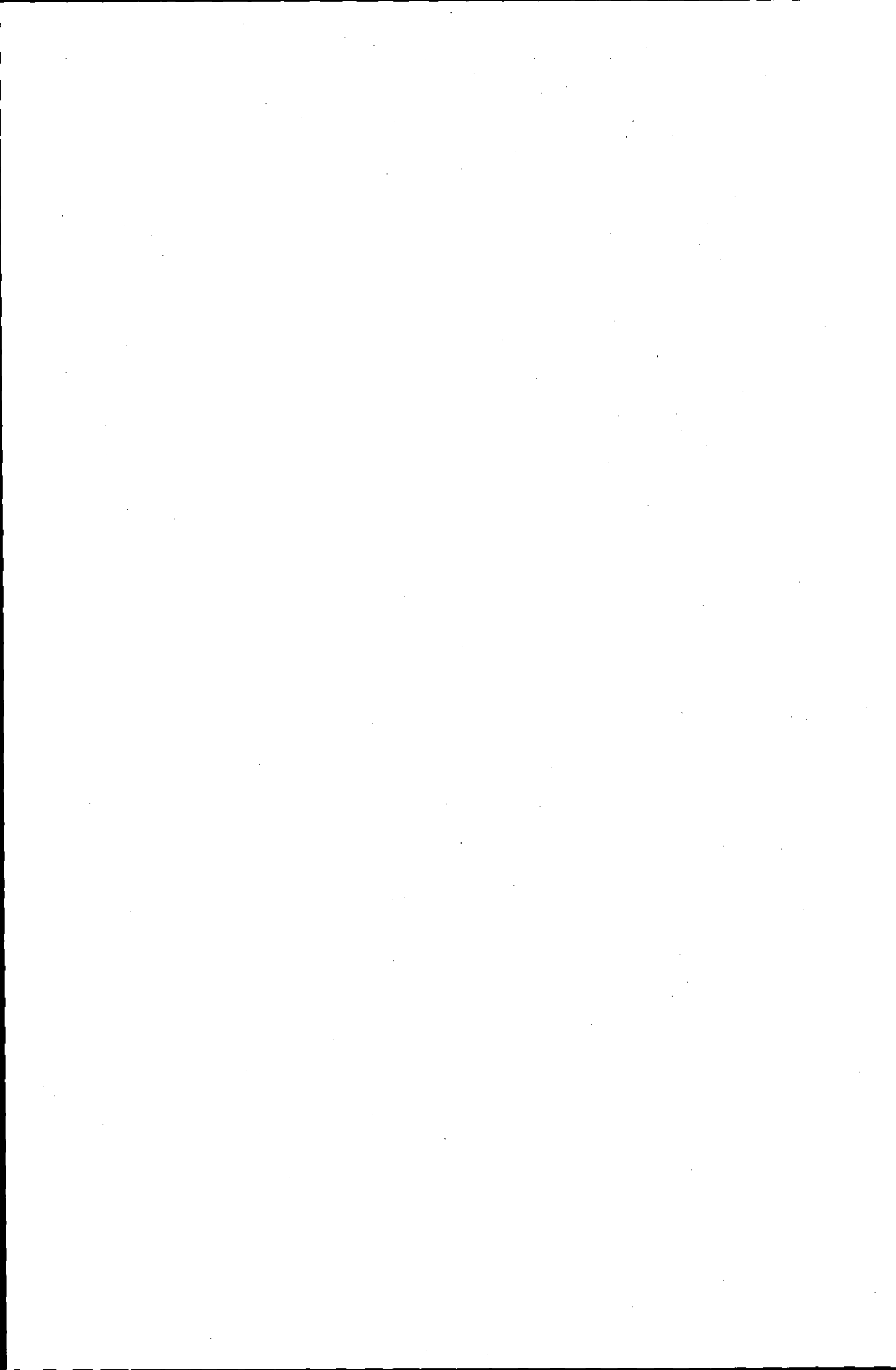
Loan copy

14 JAN 2000  
31 MAY 2000

0400819554



BADMINTON PRESS  
18 THE HALFCROFT  
SYSTON  
LEICESTER LE7 8LD  
ENGLAND  
TEL: 0533 602917  
FAX: 0533 696635



CATHODIC STRIPPING VOLTAMMETRY OF PEPTIDE  
COMPLEXES

BY

Fatma Nil Ertas, B.Sc., M.Sc.

submitted in partial fulfilment of the requirements for the award of

Doctor of Philosophy  
of the  
Loughborough University of Technology

July 1993

Supervisor : Dr. Arnold G. Fogg, B.Sc., Ph.D., D.Sc., C.Chem., FRSC.

Reader in Analytical Chemistry

Department of Chemistry

Loughborough University of Technology Library	
Date	Dec 93
Class	
Acc. No.	04 00 81955

29919756

## Acknowledgements

I would like to express my deep gratitude to Dr. Arnold G. Fogg for his valuable advice, guidance and encouragement throughout this study.

I thank Josino C. Moreira and Jiri Barek for their friendship and valuable help which contributed greatly to the preparation of this thesis.

I also would like to thank my colleagues in the laboratory, mainly Hasan, Ramin, Alan, Shereen, Valnice, Aini, Arginder, David, Paul, and Li for their friendship.

I am grateful to Ege University, Türkiye for financial support during my study.

## TABLE OF CONTENTS

### Chapter 1

#### Introduction to the voltammetric methods

Direct current polarography	1
Pulse polarography	4
Other wave forms	8
Sweep techniques	8
Voltammetry with solid electrodes	9
Stripping Voltammetry	10

### Chapter 2

#### Copper interaction with imidazole containing ligands

Introduction	22
Copper(II) complexes of imidazole and imidazole containing ligands	23
Copper(I) complexes	24

### Chapter 3

#### Experimental

Apparatus and reagents	37
Procedures	38

### Chapter 4

Adsorptive stripping voltammetric behaviour of copper(II) at a hanging mercury drop electrode in the presence of excess of imidazole

Introduction	41
Results and discussion	42

## Chapter 5

Adsorptive stripping voltammetric behaviour of copper(II) complexes of glycyglycyl-L-histidine at a hanging mercury drop electrode

Introduction	59
Results and discussion	60
Cyclic voltammetric behaviour of copper complexes of GGH	60
Adsorptive differential pulse cathodic stripping voltammetric determination of trace amounts of GGH	81
Conclusion	85

## Chapter 6

Adsorptive differential pulse cathodic stripping voltammetric determination of glycy-L-histidylglycine at a hanging mercury drop electrode using its copper(II) complexes

Introduction	87
Results and discussion	88
Cyclic voltammetric behaviour of copper complexes of GHG	89
Adsorptive differential pulse cathodic stripping voltammetric determination of GHG	101
Conclusion	104

## Chapter 7

Cathodic stripping behaviour of glycyl-L-histidine and L-histidylglycine at a hanging mercury drop electrode in the presence of copper(II) ions

Intoduction	106
Results and discussion	107
Cyclic voltammetric studies	108
Cathodic stripping differential pulse voltammetric studies	119
Conclusion	124

## Chapter 8

Cathodic stripping behaviour of carnosine and thyrotropine releasing factor at a hanging mercury drop electrode in the presence of copper(II) ions

Intoduction	125
Results and discussion	126
Adsorptive stripping cyclic voltammetric behaviour of the Car and TRF complex systems	132
Conclusion	137

## Chapter 9

Solid phase removal of chloride interference in the differential pulse polarographic determination of nitrate using nitration reactions

Intoduction	138
Results and discussion	139



Conclusion	144
Chapter 10	
Conclusion	145
References	147

## SUMMARY

### CATHODIC STRIPPING VOLTAMMETRY OF PEPTIDE COMPLEXES

Small peptides containing the histidine residue are considered as models of the metal binding site of bioactive peptides and proteins. The present study has been concerned with the cathodic stripping voltammetry of the copper complexes of imidazole (the parent molecule), and several histidine containing peptides; glycylglycyl-L-histidine (GGH), glycyl-L-histidylglycine (GHG), L-histidylglycine (HG), glycyl-L-histidine (GH), Carnosine (Car) and thyrotropine releasing factor (TRF). Accumulation and reduction mechanisms were further studied by cyclic voltammetry, and indirect cathodic stripping voltammetric method of determining these peptides has been developed.

In the presence of excess of imidazole copper(II) at pH 8.5 adsorbs at a hanging mercury drop electrode and gives two cathodic stripping voltammetric peaks, at -0.36 and at -0.47 V. The first peak is only present at accumulation potentials more negative than -0.05 V vs Ag/AgCl and appears to be due to the adsorption of polymeric copper(I<sub>m</sub>)<sub>2</sub> or its reduced copper(I) form. The peak at -0.47 V is only present at high imidazole concentrations: the accumulation is uniform from 0 to -0.35 V but is negligible at potentials more negative than -0.45 V. This peak appears to be due to the adsorption of Cu(I<sub>m</sub>)<sub>4</sub><sup>2+</sup>. Copper(II) can be determined using the first peak after accumulation at -0.6 V and the detection limit is about

$2 \times 10^{-9}$  M after 3 min accumulation. This method could not be adapted for determination of imidazole as no adsorption occurred in the excess of copper(II) ions.

A single peak is obtained in the cyclic voltammograms of GGH complex at -0.6 V for accumulation at 0 V and it increases in size by accumulating at various potentials between 0 and -0.6 V and scanning from 0 V to -1.0 V. Another peak appears at -0.4 V between accumulation potentials 0 and -0.3 V. The exact position and heights of these two peaks are depend on both concentrations of GGH and copper(II) ions, potential and time of accumulation, and on the scan rate and direction . On the basis of dc and dp polarographic behaviour of copper(II)-GGH complex, the second peak around -0.6 V can be assigned to the reduction of Cu(II)-GGH complex to Cu(Hg). Cyclic voltammetric studies performed at various deposition potentials and successive cyclic voltammetric studies showed that the species responsible from the first peak is the Cu(I)-GGH complex which is formed on the surface of HMDE from the reaction between the free copper(II) (from the deoxidation of copper amalgam) and Cu(Hg) in the presence of GGH around the drop and stabilized by adsorption. The fact that Cu(I)-GGH complex is more easily reducible than Cu(II)-GGH complex can be explained in terms of different structures of these complexes, copper(I) preferring coordination number two in complexes with monodentate imidazole and derivatives.

In addition to the better understanding of the redox behaviour of this biologically interesting peptide, the copper(I) complex reduction peak can be utilised to determine GGH in nanomolar levels by means of dp cathodic stripping voltammetric stripping preceded by accumulation at -0.2 V in the presence of excess of copper(II) ions.

For copper(II)-GHG system three cathodic stripping peaks were observed when the accumulation was performed at -0.6 V including the reduction of free copper(II) to copper amalgam at more positive potentials. On the basis of dc and dp polarographic behaviour and cyclic voltammetric studies carried out at various accumulation potentials the second cathodic peak around -0.2 V and the third cathodic peak at -0.35 V can be assigned to a stepwise one electron reduction of copper(II)-GHG complex to copper(I)-GHG complex followed by the reduction of copper(I)-GHG complex to copper amalgam. This third peak can be used for very sensitive adsorptive differential pulse cathodic stripping determination of polarographically inactive GHG molecule and a detection limit lower than  $1 \times 10^{-8}$  M level can be achieved.

The voltammetric studies of the copper complexes of GH and HG showed the resemblance in the cyclic voltammetric behaviour in terms of signal obtained after changing the ligand concentration and the accumulation potential. Two reduction peaks were observed related to the complex after accumulation at potentials more negative than -0.2 V and the first peak was found to be more dependent on the

accumulation potential. Additionally, the free copper(II) reduction peak at more positive potentials was observed even after 1:1 concentration ratio and it has disappeared in the excess of ligand solution. The main difference between the behaviour of both dipeptide complexes is that the size of the first peak is bigger for HG complex which continues to increase with more negative accumulation potentials. Like the GHG-copper complexes the complex peaks are caused by stepwise reduction processes. Other compounds studied, Car and TRF, also forming copper complexes, gave a single reduction peak in their voltammetric response which can be utilised for a sensitive method allowing to determine these compounds in submicromolar levels.

Apart from the studies with copper complexes with histidyl peptides and other compounds, a dp polarographic investigation of chloride interference on nitrate determination is described. This part is a complementary study to the polarographic determination of nitrate developed earlier in this laboratory. It has been based on a reaction of nitrate with benzoic acid giving a single product which is reduced at a low negative potential. Chloride was noted to have an interference reducing the nitrate to nitrosyl bromide whilst being oxidised to chlorine in concentrated sulphuric acid solution. Here the interference of chloride on nitration reaction of benzoic acid was shown graphically and the study was repeated with thiophene-2-carboxylic acid which reacts more rapidly than benzoic acid on line might have suffered less

interference. Preliminary studies showed that it is not the case and preseparation is needed to eliminate the interference. Present study shows that Dionex extraction cartridges based on silver(I) can be used effectively for removing chloride prior to the developed method for nitrate determination.

## CHAPTER 1.

### INTRODUCTION TO THE VOLTAMMETRIC METHODS

Voltammetry is a class of electroanalytical techniques in which the potential of the working electrode is varied with time while the current flowing through the electrode is measured. Polarography is a subclass of voltammetry in which the working electrode is a dropping mercury electrode (DME). Since its first discovery in 1922, classical dc polarography has been extended to further techniques. Although it is now rarely used for analysis, the principles of dc polarography are very useful as an introduction to the more recent advanced methods.

The following section gives a brief introduction to voltammetric methods and then the theory and applications of stripping analysis will be discussed. For a more detailed account of the theory and applications readers are referred to several excellent books and reviews on these voltammetric methods<sup>1-6</sup>.

#### 1.1 Direct current Polarography

Direct current (dc) polarography, invented in the 1920's by Heyrovsky, involves the measurement of the current at the DME while a slow linear voltage is applied to the cell. DME has a periodically renewed surface so that long term accumulation of the products of electrolysis at the electrode solution interphase is prevented. The resulting current-voltage curves are S shaped polarograms consisted of a series of oscillations

due to the continuous growing and dislodging of the drop. Further techniques have been developed to improve this form of polarogram and to increase the sensitivity.

A plateau is obtained on the polarogram owing to diffusion being the rate determining process. The current correspond to the plateau is known as the limiting diffusion current ( $i_d$ ). The Ilkovic equation gives the relation between the diffusion controlled limiting current ( $\mu A$ ) and the concentration of the electroactive species in the solution ( $\text{mol/cm}^3$ );

$$i_d = k n C D^{1/2} m^{2/3} t^{1/6}$$

where  $n$  is the number of electrons involved in the redox reaction,  $D$  is the diffusion coefficient of the electroactive species ( $\text{cm}^2/\text{s}$ ),  $m$  is the flow rate of the mercury ( $\text{g/s}$ ) and  $t$  is the drop time of the mercury electrode ( $\text{s}$ ),  $k$  is a constant with a value of 607 for taking mean oscillations into account and 708 for the maximum oscillations. The contributions of the electroactive species of interest to migration and convection currents are eliminated by employing the experimental conditions such as supporting electrolytes and quiescent solutions, so that the observed current arises from the diffusion process. The Ilkovic equation gives only the diffusion controlled faradaic current. The total current also contains the capacitive current due to the formation of a double layer at the electrode surface. This double layer has a finite capacitance and therefore a significant current is required to charge the electrode-solution interphase to the required potential. The sensitivity of dc technique is limited to



ca.  $5 \times 10^{-5}$  M due to the capacitive current. Capacitive current is very large at the start of the drop's lifetime, but decreases with the growth of the drop. Faradaic current, defined in Ilkovic equation, increases during the drop growth.

Most reductions of metal ions and some electrochemical reactions of organic and inorganic molecules are reversible i.e. the rate of electron transfer is fast in comparison to mass transport to the electrode surface. For an  $O + ne = R$  redox system, in which O and R represent the oxidised and reduced species respectively, the current-potential curve is defined as ;

$$E = E^{\circ} + \frac{RT}{nF} \ln \left[ \frac{(i_d - i)}{i} \right] \left( \frac{D_R}{D_O} \right)^{1/2}$$

$$= E_{1/2} + \frac{RT}{nF} \ln \left[ \frac{(i_d - i)}{i} \right]$$

where  $i$  is the current at potential  $E$ ,  $i_d$  is the diffusion limited current,  $E^{\circ}$  is the standard redox potential of the redox couple and  $D_R$  and  $D_O$  are the diffusion coefficients of the reduced and oxidised electroactive species. The half wave potential,  $E_{1/2}$ , is the potential at which the current equals one half of the limiting value ( $i = i_d/2$ ) and this parameter is of particular value in the identification of the organic or inorganic species. For a reversible system the half wave potential is equal to the standard reduction potential.

However many electrochemical reactions of organic molecules are irreversible, i.e. the kinetics of the reaction must be considered as well as the thermodynamics to derive the relationship between current and potential. For an irreversible system, using maximum currents at the end of drop life, it can

be written as;

$$E = E^0 + 0.916 \frac{RT}{\alpha nF} \ln \left[ \frac{(i_d - i)}{i} \right] + \frac{RT}{\alpha nF} \ln 1.359 k_s (t/D)^{1/2}$$

where  $\alpha$  is the transfer coefficient which signifies the fraction of the potential influencing the rate of electroreduction and  $k_s$  is the heterogeneous charge transfer rate constant. This equation simplifies to :

$$E = E_{1/2} + 0.916 \frac{RT}{\alpha nF} \ln \left[ \frac{(i_d - i)}{i} \right]$$

$$\text{where } E_{1/2} = E^0 + \frac{RT}{\alpha nF} \ln 1.359 k_s (t/D)^{1/2}.$$

$E_{1/2}$  is not equal to  $E^0$  in this case. The difference between these values is called the overpotential;

$$\eta = E_{1/2} - E^0$$

which increases with the irreversibility of the system. Reversible and irreversible processes can be characterised upon the wave shape, position and drop time dependence<sup>1</sup>. Hydrogen ions are also involved in many electrode reactions of organic molecules. The half wave potential of the reduction process shifts to more negative potentials according to the equation

$$E_{1/2} = k - 0.059 (m/n) \text{ pH}$$

where  $m$  is the number of protons involved and  $k$  is a constant standard potential.

## 1.2 Pulse polarography

Extensions to the polarographic method were made by the

invention of pulse polarography by Barker and Gardner<sup>1</sup> in the late 1950's. Pulse polarography utilises the differing time dependence of faradaic and charging currents. The normal pulse technique (npp) imposes a series of pulses of increasing amplitude to successive drops at a preselected time near the end of each drop lifetime (Figure.1.1). The initially high charging current decays away very rapidly and the residual faradaic current is sampled during the final part of the 50 to 60 ms potential pulse. Since electrolysis during the waiting time is negligible, the initially uniform character of the concentration distribution in solution is preserved until the pulse is applied. Even though the electrode is approximately spherical, it acts as a planar surface during the short time of the electrolysis, and therefore the sampled faradaic current on the plateau is;

$$i_d = nFA D_0^{1/2} C_0^* / \pi^{1/2} (\tau - \tau')^{1/2}$$

where  $(\tau - \tau')$  is time measured from pulse rise (s) and A is the area of the electrode (cm<sup>2</sup>) and  $C_0^*$  is the bulk concentration of the species. The limit of detection for npp is about 10<sup>-6</sup>-10<sup>-7</sup> M.

For a reversible system ;

$$E = E_{1/2} + RT/nF \ln (i_d - i)/i$$

can be written.

The npp technique is very useful in analytical applications since it can respond to both reversible and irreversible processes and it is far less affected by problems of adsorption than is the dc technique. Although npp gives a marked

improvement in sensitivity over the dc technique, it still gives a sigmoidal-shaped polarogram.

Differential pulse polarography (dpp) is the technique in which a small amplitude (10-100 mV) potential pulse of approximately 60 ms duration are applied to the DME near to the end of the drop lifetime. The current output is sampled at two time intervals (Figure.1.2), immediately on the ramp prior to the imposition of the pulse and then again at the end of the pulse (after 40 ms), when the capacitive current has decayed, and the difference in these two currents is displayed. The resulting i-E curve in dpp has a peak shape in which the greatest increase in the current is reached at the half wave potential. The peak current in dpp, when the pulse amplitude ( $\Delta E_p$ ) is less than  $RT/nF$ , is described as below equation where  $t_p$  is the pulse width<sup>4</sup> ;

$$i_p = (n^2 F^2 A C / 4 R T) \Delta E_p (D / \pi t_p)^{1/2}$$

A wide range of organic and inorganic molecules of environmental significance can be detected by this technique with detection limits in the range  $10^{-7}$  to  $10^{-8}$  M. Although pulse techniques were developed specifically for the DME, they can be employed with other kinds of electrodes such as hanging mercury drop electrode and mercury thin film electrode in stripping analysis.

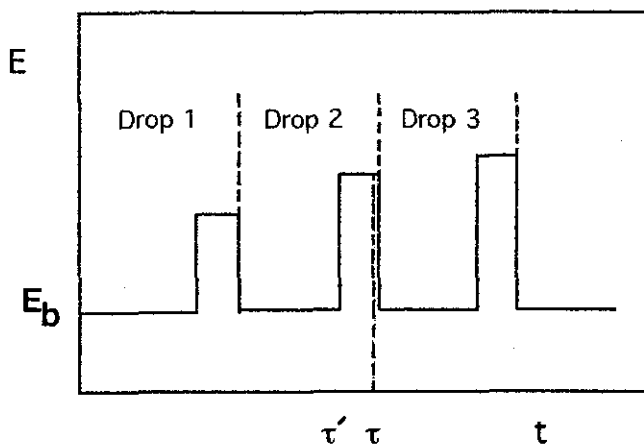


Figure.1.1- Sampling scheme for normal pulse polarography<sup>1</sup>.

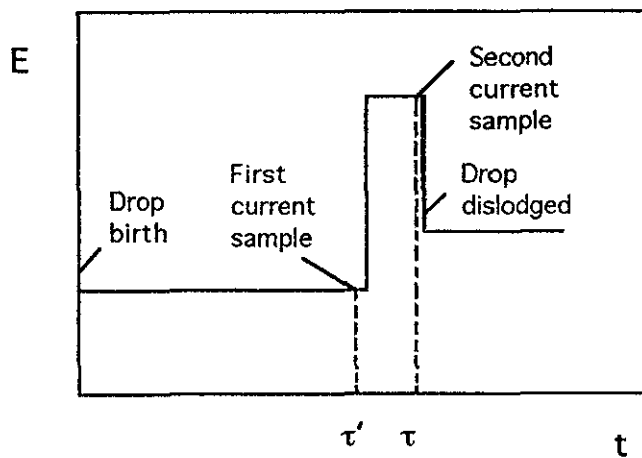


Figure.1.2- Events for a single drop of a differential pulse polarographic experiment<sup>1</sup>.

### 1.3 Other wave forms

Square wave polarography (swp), first proposed by Barker and Jenkins, is faster than dpp as a complete potential scan is accomplished on each mercury drop. In swp, a square wave voltage (typically 30 mV peak-to-peak) is superimposed upon the slow dc scan voltage of classical polarography. In addition to the speed of the technique, concentrations as low as  $5 \times 10^{-8}$  M can be determined.

Another developed technique is the alternating current (ac) technique in which a periodic waveform, generally of low amplitude, is superimposed upon a dc potential applied to an electrochemical cell. The background current and noise caused by capacitance effects can be diminished by phase-sensitive measurement of the in-phase component of the alternating current. This mode is suitable for application of detection limits ( $10^{-6}$ M) lower than dc mode. Furthermore, the possibility of measuring the change in the drop capacity allows to determine adsorbed but nonelectroactive species.

### 1.4 Sweep Techniques

In the area of preliminary mechanistic investigations the sweep techniques, i.e. linear sweep (LSV) and cyclic voltammetry (CV) are very useful<sup>3</sup>. In LSV, the potential of a small, stationary working electrode is changed linearly with time from an initial potential ( $E_1$ ) to the potentials where reduction or oxidation of a determinant occurs ( $E_2$ ). In CV the wave form is initially the same as in LSV, but on reaching the potential  $E_2$  the potential is reversed to  $E_1$  or another value

(E<sub>3</sub>). The sweep rates used generally range from a few mV/s to a few hundred V/s. Resulting voltammogram has a peak shape in which the peak height increases with increasing scan rate. The Randles-Sevcik equation gives the relation between the concentration of determinant and the peak current ( $i_p$ );

$$i_p = 2.69 \times 10^{-5} n^{3/2} C A D^{1/2} v^{1/2}$$

where  $v$  is the scan rate (V/s).

For a reversible system, the reduction and oxidation peaks on both forward and reverse scans have a distance of  $0.059/n$  between the peak potentials. This value is greater for quasi reversible systems and no reverse peak is observed for irreversible processes. Additionally peak potential,  $E_p$ , is independent of scan rate in reversible processes while it is shifting to more negative values for irreversible systems.

### 1.5 Voltammetry with solid electrodes

In a stirred solution and using a stationary electrode S shaped voltammograms can be observed. Limiting current is given by the equation<sup>3</sup> :

$$i_L = nFADC / \delta$$

where  $\delta$  is the Nernst diffusion layer thickness.

The use of solid rotating electrodes increases the sensitivity by about one order of magnitude in many cases, but it is mostly used in mechanistic studies. For quantitative determinations amperometric measurements are very useful in conjunction with chemically modified electrodes. The use of chemical

functionalities on the electrode surface as anchoring groups to attach certain reagents by covalent bonding improves the selectivity of the method and effectively lower the potential required for oxidation or reduction<sup>4</sup>. The detection limit may be down to about  $10^{-8}$  M. The main problems associated with the use of chemically modified electrodes are the possibility of saturation of the surface during the preconcentration step and the difficulty of generation of a new fresh and reproducible surface.

### 1.6 Stripping voltammetry

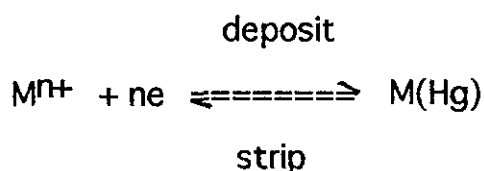
One of the most sensitive analytical techniques is stripping voltammetry consisting of a preconcentration step prior to the measurement step. The solution is stirred during the electrolysis to ensure a more rapid supply of the depolarizer from the bulk of the solution<sup>7</sup>. In addition to its enrichment on the working electrode, this step may serve to isolate the analyte from a complex matrix. After a rest period to allow the solution to become quiescent, the stripping of the deposit is carried out. The resulting polarisation curve gives peak shaped response of current with linearly changing electrode potential and the height (or the area) of the peak is proportional to the concentration of determinant in the solution.

The electrodes used in stripping techniques are mainly mercury and solid electrodes made of metal or graphite<sup>8</sup>. The basic and simplest type of mercury electrode is the stationary mercury drop prepared by hanging (HMDE) or electrolytically



depositing a mercury drop onto an inert metal (i.e. mercury thin film electrode MTFE). Reproducibility of results with mercury electrodes is usually very good and it is more useful for reduction because reduction of aqueous hydrogen ion on mercury has a much higher overvoltage than it does on the noble solid metals. To study at positive potentials, where mercury dissolution occurs, solid micro electrodes made of platinum, silver, gold or graphite are used. Reproducibility of the results depends on the reproducible renewal of the active surface area of the electrode and sensitivity is usually lower than with mercury electrodes.

Applications of stripping methods varies with the nature of the deposit formed. Its most known version is anodic stripping voltammetry (ASV). Metals capable of forming a sufficiently concentrated amalgam with mercury can be preconcentrated on a stationary mercury electrode. The metal formed from the cations during the electroreduction dissolves in the mercury; it is then anodically dissolved from the amalgam and the anodic current is monitored<sup>8</sup>.



Noble metals or metals not forming amalgams can be deposited from their ions on a suitable inert electrode such as noble metal electrodes and graphite electrode. Higher sensitivity is achieved with mercury film electrode (sub ppb) owing to the higher surface area to volume ratio and less metal diffusion inside the electrode results a better resolution with narrower

peaks.

In adsorptive stripping voltammetry (AdSV) the analyte is preconcentrated at the stationary electrode surface by controlled interfacial adsorption<sup>7</sup>. Adsorption on the electrode surface may be of the surface active analyte itself or the product of a reaction of the analyte with an ion or a selected reagent with formation of a complex (it is later defined as adsorptive cathodic stripping voltammetry<sup>9</sup>) or by reaction of the analyte with a reagent previously adsorbed on electrode surface. The voltammetric response of the surface confined species is directly related to its surface concentration, with the adsorption isotherm giving the relationship between the surface and the bulk concentrations. The Langmuir isotherm is the most frequently used isotherm<sup>10</sup> and can be written in terms of the fractional coverage of the surface;

$$\theta = \Gamma / \Gamma_m$$

where  $\Gamma$  is the surface concentration of adsorbate ( $\text{mol}/\text{cm}^2$ ) and  $\Gamma_m$  the surface concentration corresponding to a monolayer at the surface.

$$BC = \theta / 1 - \theta$$

C is the bulk concentration of adsorbate and B is the adsorption coefficient. When  $1 \gg BC$  this equation can be simplified as

$$\Gamma = \Gamma_m BC$$

Hence at very low adsorbate concentrations the surface

concentration is directly proportional to the bulk concentration. This isotherm is very useful corresponding to a physical model in which the maximum surface coverage is that of a complete layer, generally a monolayer, upon the electrode surface. Although it is the most widely used isotherm, it is not applicable when interaction occurs between adsorbed species on the electrode surface. The Frumkin isotherm has an interaction parameter,  $g$ , which depends on the electrode potential.

$$BC = [ \theta / 1-\theta ] \exp. (-2g\theta)$$

When  $g$  is zero this equation reduces to the Langmuir isotherm.

The amount of adsorbate on a fully covered electrode surface (monolayer coverage) is about  $10^{-9}$  to  $10^{-10}$  mol/cm<sup>2</sup> for low molecular-weight adsorbates depending on their size and orientation on the surface. The extent of adsorption is often related to their solubility in the solvent used. Besides the fact that smaller solubilities tend to promote strong adsorption, electrostatic attraction between an ionic adsorbate and a charged electrode, field-dipole interaction between the electrode double layer and functional groups of organic reactants should also be considered.

Preliminary experiments concerning the nature of the adsorption and redox processes are usually performed using techniques such as chronocoulometry or cyclic voltammetry and differential pulse polarography. In the area of preliminary mechanistic investigation the sweep techniques, in particular

cyclic voltammetry, are probably most useful. Ideal Nernstian behaviour of surface confined non interacting species can be seen by symmetrical cyclic voltammetric peaks with peak half widths of  $90.6 / n$  mV. Under these conditions, the faradaic current arising from the presence of  $\Gamma$  mol/cm<sup>2</sup> of an attached analyte is given by

$$i_p = n^2 F^2 \Gamma A v / 4RT$$

where  $v$  is the potential scan rate,  $A$  is the surface area. In the case of interaction between adsorbed molecules, for a reversible surface voltammetric process the current is given by

$$i_p = n^2 F^2 \Gamma_T A v / RT [4 - \Gamma(r_O + r_R)]$$

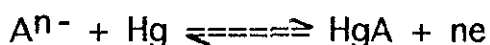
This is without considering the interactions which depend on the electrode potential where  $r_O$  and  $r_R$  are the interaction parameters of oxidised and reduced forms of redox couple respectively and  $\Gamma_T$  is the total amount present on the surface.

In the measurement step of adsorptive stripping experiments differential pulse waveform is widely used since it offers much more discrimination against the background charging current and hence a decreased detection limit. Maximum sensitivity can be achieved utilising the optimum conditions for maximum adsorption. The current obtained with whichever waveform is the measure of the surface concentration of adsorbate, hence the current peak has the form of Langmuir isotherm. At high concentrations of adsorbate deviation from the linearity is observed due to the saturation of the surface

with the analyte. When approaching full surface coverage ( $\theta \rightarrow 1$ ) the current response approaches its maximum value ( $i \rightarrow i_{\max}$ ).

Over the last decade adsorptive stripping voltammetry has been shown to be highly suitable for measuring surface active organic compounds. The interfacial activity of numerous compounds of pharmaceutical, biological and environmental significance has been exploited for their adsorptive stripping measurements at trace levels. Table-1 shows a list of organic substances determined by AdSV technique. Adsorption process of organic molecules depends on their solubility and the change in the solution pH. Biomacromolecules almost always possess surface activity, but their adsorption and redox processes are more complex than those of small molecules. Nonelectroactive organic compounds can also be determined using tensammetric procedures or following an appropriate derivatization reaction.

Another common version of stripping analysis is cathodic stripping voltammetry (CSV). The most important difference is that in ASV the deposited metal dissolves in the mercury electrode and forms an amalgam, whereas in CSV an insoluble film with the ions of the electrode material (in connection with a faradaic process) or with an added reagent. A wide range of organic and inorganic compounds can be concentrated on the electrode at a potential corresponding to the oxidation of the electrode material or appropriate to the formation of the sparingly soluble compound, then cathodic dissolution of the film is monitored.



This type of cathodic stripping voltammetric method has been applied to the determination of a range of anionic species such as  $Cl^-$ ,  $Br^-$ ,  $I^-$ ,  $CrO_4^-$ ,  $MoO_4^-$ ,  $VO_3^-$ ,  $WO_4^-$ , etc<sup>2</sup>.

Another type of the technique includes the formation of an appropriate metal chelate followed by its controlled interfacial accumulation on the electrode surface and also called as adsorptive cathodic stripping voltammetry (AdCSV)<sup>9</sup>. This method has been applied to both metal and organic compound determinations. Two main advantages related to adsorptive deposition were reported; first, any oxidation state can be collected rather than only the metallic state and secondly the material is collected as a monomolecular layer on the electrode surface, so all the material is accessible to reduction. Therefore, the reduction current is independent of diffusion of the electroactive species and larger currents can be obtained employing fast potential scanning techniques.

Analytical conditions for the direct determination of trace elements in aqueous solutions using AdCSV employing the reduction of the element in the adsorbed complex are summarised in Table-2. Catechol and oxine were used as complexation agents by van den Berg's group for the determination of various trace metals in sea water<sup>9</sup>. Direct measurements in sea water were performed after pH adjustment by addition of PIPES/NaOH buffer. The detection limits lie at the  $10^{-10}$  M level for these metal ions.

Table.1.1- Adsorptive stripping voltammetry of selected organic compounds<sup>11</sup>.

Molecule	Indicator electrode	Supporting electrolyte	Detection limit (M)
Dopamine	Pt	EtOH	$5 \times 10^{-8}$
Bilirubin	Static Hg drop	CH <sub>3</sub> COONa	$5 \times 10^{-10}$
Heme	HMDE	60 % EtOH/H <sub>2</sub> O	$1 \times 10^{-9}$
Riboflavin	Static Hg drop	$10^{-3}$ M NaOH	$2.5 \times 10^{-11}$
Chlorpromazine and other phenothiazines	Impregnated graphite, carbon paste	Phosphate buffer	$5 \times 10^{-9}$
Adriamycin	Carbon paste	Acetate buffer	$10^{-8}$
Codeine, cocaine and papaverine	Static Hg drop	NaOH	$10^{-8}$
Diazepam and nitrazepam	Static Hg drop	Acetate buffer	$5 \times 10^{-9}$
Cimetidine	Static Hg drop	0.1 M HCl	$4 \times 10^{-9}$
Digoxin and digitoxin	Static Hg drop	$5 \times 10^{-3}$ M NaOH	$2 \times 10^{-10}$
Progesterone and testosterone	Static Hg drop	$5 \times 10^{-3}$ M NaOH	$2 \times 10^{-10}$
Nitro containing pesticides	Static Hg drop	BR buffer	$5 \times 10^{-10}$
Thiourea	Static Hg drop	0.1 M NaClO <sub>4</sub>	$2 \times 10^{-11}$

Table.1.2- Some applications of AdCSV to element analysis<sup>9</sup>

Metal	Reagent*	pH range	Supporting electrolyte	Detection limit(60s)	Scan wave
As	Copper		1 M HCl	3	dp
Cd	Quinolin-8-ol	7.5-8.5	HEPES	0.1	dp
Co	DMG	7.5-10	NH <sub>4</sub> <sup>+</sup>	0.1	dp
Co	DMG	7.5-9.0	TEA-NH <sub>4</sub> <sup>+</sup>	0.1	sw
Co	DMG	7.4-8.9	TEA-NH <sub>4</sub> <sup>+</sup>	1	dp
Co	Nioxime	7.6	HEPES	0.1	dp
Cu	Quinolin-8-ol	6-9	Borate	0.2	dp
Cu	Catechol	6-9	Borate	0.3	dp
Cu	Tropolone	6-9	Borate	0.4	dp
Fe	Catechol	6.8-8.0	PIPES	2	dp
Fe	1-Nitroso-2-naphthol	6.8	PIPES	2	LS
Ge	Catechol	Acidic	0.1 M H <sub>2</sub> SO <sub>4</sub>	10	dp
I	Copper	2-5	Acetate	3	dp
I	Mercury(I)	8	Natural pH	0.6	sw
Mo	Quinolin-8-ol	2.5-3.0	-	1	dp
Mo	Tropolone	2	-	0.1	dp
Ni	DMG	7-10	NH <sub>4</sub> <sup>+</sup>	0.1	dp
Ni	Bipyridine	9	NH <sub>4</sub> <sup>+</sup>	200	dp
Pb	Quinolin-8-ol	7.0-8.5	HEPES	0.3	dp
Pd	DMG	5.15	Acetate	2	dp
Sb	Catechol	5.8-6.8	MES	0.6	dp
Se	Copper	4.5	NH <sub>4</sub> SO <sub>4</sub>	3	dp
Se	Copper	1.6		0.1	dp
Sn	Tropolone	4.5	Acetate	2	dp
Sn	Tropolone	1.5-2.7		0.05	dp
Tc	Thiocyanate	2	H <sub>2</sub> SO <sub>4</sub>	5	dp
Te	Copper	4.5	NH <sub>4</sub> SO <sub>4</sub>	10	dp
Ti	Mandelic acid	2.8-4.2	-	0.3	dp
Ti	Cupferron	1-1.5		5	dp
U	Quinolin-8-ol	6.5-7.1	PIPES	0.2	dp
U	Catechol	6.3-7.2	PIPES	0.7	dp
U	2-TTA-TBP	3.6		1	LS
V	Catechol	6.6-7.2	PIPES	0.6	LS
Zn	APDC	6.2-8.5	BES	0.3	dp

\*APDC : ammonium pyrrolidinedithiocarbamate, BES : N,N-bis (2-hydroxyethyl) -2-amino- ethanesulphonic acid, DMG : dimethylglyoxime, HEPES : N-hydroxyethylpiperazine-N'-2-ethanesulphonic acid, MES : 2-(N-morpholino) ethanesulphonic acid, PIPES : piperazine-N,N'-bis-2-ethanesulphonic acid, TBP : tributyl phosphate, TEA ; triethyl-amine, 2-TTA : 2-thenoyltrifluoroacetone.



Reduction of the metal is preferable to ligand reduction as the reduction potential is specific to the metal minimising the interference by other metals. In the measurements based on ligand reduction the sensitivity tends to be lowered by adsorption of the ligand. However, reduction of the ligand is convenient if the metal is reduced only at very negative potentials as in the case of some rare earth metals<sup>9</sup>.

Complex formation with a ligand capable of binding only a few metals can increase the selectivity of the analysis. Pihlar et al<sup>12</sup> developed highly sensitive and reliable AdSV procedure for trace amounts of nickel using dimethylglyoxime (DMG) reagent. However the complexes of other reagents are usually not formed selectively. Interferences from other reducible complexes with similar peak potentials should be minimised, for example by addition of EDTA to eliminate copper and lead interference in measurements of iron<sup>9</sup>.

The competitive adsorption of surface active organic compounds is one of the main interferences in AdCSV<sup>9</sup>. The actual interfering effect varies depends on the metal being determined and the ligand used, but generally the natural level of surfactants in fresh and estuarine waters is sufficiently high to diminish the sensitivity of ACSV. On the other hand, organic complexing materials present in natural waters may cause an interference due to complexation with trace metals. This interference by dissolved organic material is easily eliminated by UV irradiation of the sample prior to the determination.

The use of catalysis was also shown to amplify the reduction current<sup>9</sup>. The detection limits were lowered to pM levels for several elements utilising the catalytic effects. The catalytic effect of formazone complex with platinum on the development of hydrogen was used to detect platinum in fresh and sea water<sup>13,14</sup>. The catalytic evolution of hydrogen was attributed to the decrease in the hydrogen overpotential on platinum active centres formed on the mercury surface<sup>13</sup>. The controlled interfacial accumulation of the catalyst leads an ultrasensitive method for measuring traces of platinum. The scope of the method can be extended to voltammetric quantitation of large biomolecules since the widespread occurrence of the catalytic hydrogen process for these species.

The AdCSV has also been successfully exploited to determination of organic compounds which accumulates on the electrode surface as metal complexes. For several analytes it has been shown that accumulation on the mercury drop surface in the form of copper complexes shifts the location of the stripping peaks towards more negative potentials than the stripping peaks of the corresponding mercury complexes. This effect was observed with the hanging copper amalgam electrode<sup>15</sup> and HMDE in the presence of copper(II) ions<sup>15,16</sup>. Forsman<sup>16</sup> has studied the CSV behaviour of various penicillins in the presence and the absence of copper(II) ions for comparison. The mercury complex peak was reported to disappear in the presence of copper(II) and the compounds were determined extremely sensitively by measuring the stripping peak of their copper complex. Similarly, the biologically

important compounds which do not possess any electroactive groups can be determined voltammetrically as their copper complexes.

The analysis of histidyl peptides and compounds containing histidine residue are of great importance in biological fields and reliable analytical methods are essential for their determination. The copper complex formation of these compounds and utilisation of the AdCSV measurements for their determination will be discussed in the following chapter.

## CHAPTER 2.

### COPPER INTERACTION WITH IMIDAZOLE CONTAINING PEPTIDES

#### 2.1. introduction

The biological action of copper usually takes place in association with certain proteins, referred to as copper proteins. These proteins are involved in many metabolic functions such as electron transfer reactions, transport of oxygen and the transport and storage of copper ions. The participation of copper proteins in electron transfer reactions is greatly favoured by the low oxidation potential of the copper(I) ion<sup>17</sup>. In aqueous solutions of many low-molecular-weight copper(I) compounds, univalent copper is almost instantaneously oxidised into copper(II) by molecular oxygen.

It is known that an enzyme provides not only the particular structure that constitutes the active site but that it also provides the environment necessary for catalysis<sup>17</sup>. Although a small molecule containing only the active site of the protein, may have a low catalytic activity, the interpretation of the data obtained from a low-molecular-weight system is less ambiguous than that obtained from a large protein, especially in the presence of metal ion. Very accurate data can be obtained. Thus a low-molecular-weight complex may yield important information regarding the geometry of the metal binding site for such metal ion-protein interaction. There are a few reviews dealing with certain aspects of low-molecular-weight models for copper proteins in solution and crystalline

phase<sup>17-19</sup>. Additional accurate data on model systems are needed to gain a detailed understanding of the interactions with copper ions.

## 2.2. Copper(II) complexes of imidazole and imidazole containing ligands

The imidazole group plays an important role in biochemistry because of its presence in histamine and histidine. The structural features associated with the imidazole ring has been reported<sup>18</sup>. Imidazole (1,3 -diazole) is amphoteric being a moderately strong organic base capable of accepting a hydrogen ion at the pyridine-like nitrogen ( $pK_a = 7.1$ ) as well as a very weak acid capable of loss of hydrogen ion from the pyrrole-like nitrogen ( $pK_a = 14.3$ ). Imidazole is generally regarded as being aromatic in which the  $\pi$  electrons of N-1 completes the aromatic sextet.

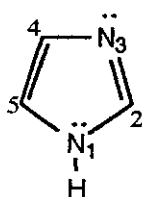


Figure 2.1-Imidazole

In near neutral solutions the unprotonated imidazole molecule usually functions as a ligand using the unshared pair of electrons on N-3 (Figure 2.1). Bonding of a metal ion at N-1 is expected to be unfavourable since the aromaticity of the ring is thereby compromised.

A pH metric study of the complex showed that the coordination number of copper is four in the copper(II)-imidazole system

and the pK values of the complex were given as 4.20, 3.42, 2.88 and 2.1, respectively<sup>18</sup>. In sufficiently basic media the conjugate base of imidazole,  $\text{Im}^-$ , is formed and its complexes with dipositive metal ions are considered to have a stoichiometry of  $\text{M}(\text{Im})_2$ . These complexes are generally insoluble and are considered to be polymeric.

The histidine molecule (Figure 2.2) presents three potential coordination sites in aqueous solution. The carboxyl group, the imidazole nitrogen and the amino nitrogen become available for complexation as pH increases<sup>18</sup>. The logarithms of the stabilisation constants of the copper(II) complex were reported as 10.1 and 8.0.

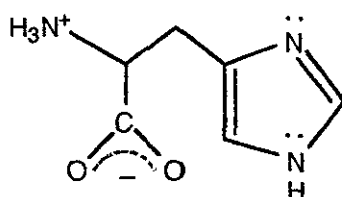


Figure.2.2- The structure of histidine.

Peptides containing a histidine residue are of interest as models of bioactive polypeptides and proteins. Sarkar and coworkers<sup>20-22</sup> studied the design of a peptide molecule mimicking the specific copper(II)-transport site of human serum albumin to investigate the nature of the coordination equilibria existing in approximated physiological conditions. Glycylglycyl-L-histidine (GGH) is of particular interest because it provides the same copper(II)-binding geometry and specificity as that of albumin involving the  $\alpha$ -amino nitrogen,

an imidazole nitrogen, and two intervening peptide nitrogens as the ligating sites around the square-planar copper(II) ion (Figure.2.3). However, the copper(II)-binding affinity of this peptide was found to be lower than that for albumin<sup>20</sup>.

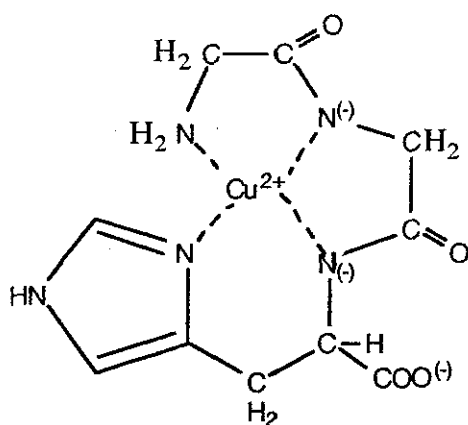


Figure 2.3- The structure of copper(II) complex of GGH18.

Since the imidazole nitrogen atoms of the histidine residues provide one of the primary means by which metal ions may be bound to proteins, the stability of copper(II) complexes with these peptides is considerably enhanced by the presence of this residue and their complex formation is affected by its relative position in the oligopeptide molecule. Similarly, the peptide molecules having the histidyl residue in different position are also important as a model for further studies involving the basic understanding of interaction between peptides and copper ions. The complexing ability of these peptides towards copper(II) has been studied mainly by means of pH titrimetry<sup>20-26</sup>. The acid dissociation and the complex formation stability constants of some of the histidyl peptides are listed in Table.2.1 and Table.2.2, respectively.

Table.2.1- Acid dissociation constants of histidine and some of the histidyl peptides.

Compound	pK <sub>1</sub>	pK <sub>2</sub>	pK <sub>3</sub>	Reference
His	1.9	6.1	9.1	18
GGH	2.84	6.99	8.23	23
GHG	3.19	6.63	8.17	23
	3.03	6.36	7.68	22
GH	2.75	6.85	8.33	23
	2.66	6.61	7.97	22
HG	2.94	6.01	7.87	23
	2.32	5.39	7.15	22
Car	2.64	6.58	9.04	22

Table.2.2- The equilibrium constants of the copper(II) complexes of histidyl peptides (LH)<sup>24</sup>.

Equilibrium	GGH	GHG	GH	HG	Car
$\text{Cu}^{2+} + \text{L}^- \rightleftharpoons \text{CuL}^+$	7.04 <sup>25</sup>	8.52	8.68	8.02	8.14
$\text{Cu}^{2+} + 2 \text{L}^- \rightleftharpoons \text{CuL}_2$		15.78	15.41	14.15	14.39
$\text{Cu(L-H)} + \text{H}^+ \rightleftharpoons \text{CuL}^+$		3.20	4.14	6.30	6.24
$\text{Cu}^{2+} + 2\text{L}^- + \text{H}^+ \rightleftharpoons \text{CuHL}_2^+$			12.48	11.48	11.21
$\text{Cu}^{2+} + 2\text{L}^- \rightleftharpoons \text{CuL(L-H)}^- + \text{H}^+$	8.70 <sup>25</sup>	8.41	7.68		
$\text{Cu}^{2+} + \text{HL} \rightleftharpoons \text{CuHL}_2^+$	5.33 <sup>26</sup>	4.94 <sup>26</sup>	5.08 <sup>26</sup>		3.98
$\text{Cu(L-2H)}^- + \text{H}^+ \rightleftharpoons \text{Cu(L-H)}$		9.01	9.48	9.76	
$\text{CuL(L-H)}^- + \text{H}^+ \rightleftharpoons \text{CuL}_2$		7.37	7.73	8.49	8.69
$\text{Cu}_2(\text{L-H})_2 + 2 \text{H}^+ \rightleftharpoons 2 \text{CuL}^+$				9.15	8.32



Complexes of copper(II) with glycyl-L-histidylglycine (GHG) have been studied in solution<sup>24,26</sup> and in the crystalline phase<sup>27</sup>. GHG forms a complex with copper(II) via its amino, peptide and imidazole nitrogens. Coordination about copper(II) is completed by an oxygen from the carboxylate group of another ligand and a water molecule (Figure.2.4). A study of pH static titration with glass and copper amalgam electrodes has indicated that highly polynuclear species are formed in equilibrium solutions of the complex<sup>28</sup>.  $\text{CuL}^+$  (where GHG = LH) was detected in a very limited pH range (about pH 4.5) since it has a great tendency to polymerise. Another indication of the study is that the binuclear copper coordination found in the crystalline state also appears to exist in the solution.

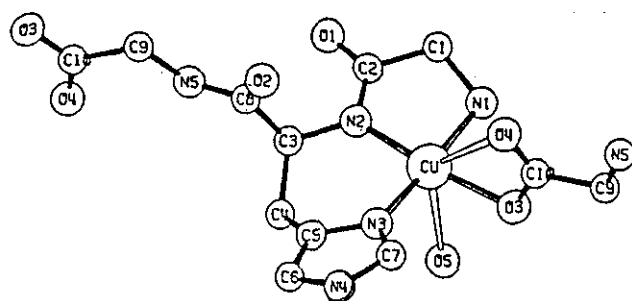


Figure.2.4- The crystal structure of copper(II) complex of GHG

The  $pK_a$  values of glycy-L-histidine (GH) are assigned as for GHG and the similar metal binding in their complexes with copper was suggested to explain the high stability constants of the mono and bis complexes<sup>24,26,29</sup>. The log K values of the above three peptides for the formation of  $[CuHL]^{2+}$  decrease in the order GGH, GH and GHG, which agrees with that of the basicity of the imidazole group (see Table.2.1) confirming the imidazole interaction with copper(II) in the complex formation. In strongly basic medium GH and GHG form polymer complexes in which the imidazole residue acts as a bridge to connect copper atoms<sup>26</sup>.

L-Histidyl glycine (HG) having the histidyl residue in a different position was reported to form 1:1 complexes via amino and imidazole nitrogens as hydroxo-bridged species<sup>29</sup>. In basic solutions polymer formation was reported similar to the GH and GHG complexes<sup>25</sup>. In neutral solutions a dimer formation was observed, in which four coordination positions of copper(II) are occupied by two nitrogen atoms of deprotonated amide and amino group, one oxygen atom of carboxyl or carbonyl group in one molecule and one nitrogen atom of imidazole group of another peptide molecule. Each peptide is thus bonded to two different copper atoms. Similar dimer formation was later suggested for the Carnosine (Car) complex from the crystallographic<sup>30</sup> and pH metric<sup>31</sup> studies. Car ( $\beta$ -alanyl-L-histidine) is found in vertebrate muscle<sup>18</sup> and its function is uncertain. Because of the  $\beta$ -alanyl residue (Figure.2.5), the dipeptide is not a fragment of proteins which contain only alpha-amino acid residues.

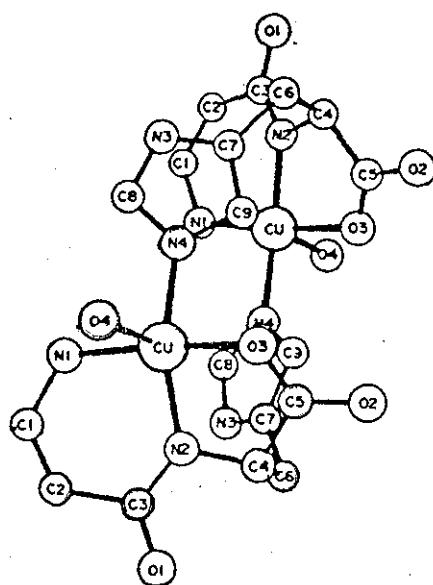


Figure 2.5- The crystal structure of copper(II) complex of carnosine.

Tyrotropin-releasing factor (TRF), L-pyroglutamyl-L-histidylprolinamide, also contains an acylated histidine residue. The combined evidence from pH metric titration and visible absorption spectra suggest that at pH 8.5 TRF chelates copper(II) via imidazole nitrogen, and histidyl and pyroglutamyl deprotonated amide nitrogens (Figure.2.6)<sup>18</sup>. Its interaction with copper(II) was investigated by Farkas et al<sup>32</sup> by pHmetric and spectrophotometric methods. spectrophotometric methods and the logarithm of stability constant for  $[CuL]^+$  species was reported as 3.64. The smaller pK values for copper(II) complexes of TRF can be explained by the weaker electron repulsion of the side chain. The predominant species was found as  $[CuLH_2]^+$  and the coordination in this complex structure via three nitrogen donor

atoms means that copper(II) ion has a free coordination site. As for GH and GHG this provides a possibility for the formation of bis complexes. However, this possibility was excluded on the basis of both calorimetric and spectroscopic measurements<sup>32</sup>.

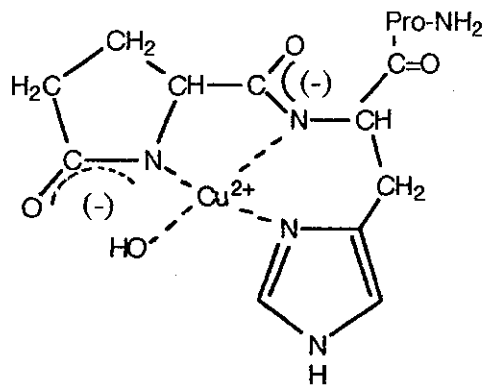


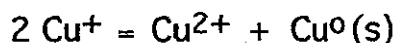
Figure 2.6- The structure of copper(II) - TRF complex.

Although the co-ordination structures of the copper complexes of histidyl peptides are well established, there are few reports on their electrochemical behaviour<sup>33-38</sup>. Only one predominant cathodic peak which corresponds to the reduction of Cu(II) complex to Cu(Hg) has been reported for complexes with glycylglycylglycine<sup>33</sup>, glycyl-L-histidyl-L-lysine and glycyl-L-histidylglycine<sup>35</sup> and glycylglycyl-L-histidine<sup>36</sup>. This is in agreement with the well known fact<sup>33</sup> that the electrochemical reduction of copper(II) preferentially occurs by two electrons to form Cu(Hg). However, complexation stabilising copper(I) can give rise to a one-electron reduction of copper(II) resulting in two successive and distinct

monoelectronic steps as reported for copper(II) complexes of histidine<sup>37</sup> and imidazole<sup>38</sup>.

### 2.3. Copper(I) Complexes

Besides the fact that the copper(I) state is important in electron transfer reactions, in which some copper proteins are known to participate, a little attention was paid to the univalent copper complexes of peptides and amino acids. The reason for the limited amount of information available is that copper(I) is thermodynamically unstable in aqueous solutions and disproportionates almost instantaneously. The equilibrium constant for the reaction ;



has the value<sup>39</sup> of  $1.6 \times 10^6 \text{ M}^{-1}$ . This instability of copper(I) ion is partly due to the relatively strong dissolution of copper(II) ions in aqueous solution. Thus, the stability of copper(I) ions can be increased by using solvents other than water in which copper(II) ions are less hydrated.

On the other hand, the disproportionation reaction of copper(I) ion in aqueous solutions can be altered by introducing a ligand which forms much stronger complexes with copper(I) than with copper(II) ions. The examples are acetonitrile and some halides and sulphur and nitrogen containing ligand systems<sup>17</sup>. The stability order for copper(I) complexes with the ligand systems was given as  $\text{RS}^- > \text{RNH}_2 > \text{OH}^- \gg \text{H}_2\text{O}$ . The low affinity of copper(I) ions for water molecules is consistent

with the fact that the binding sites of univalent copper in proteins are the sites having hydrophobic environments.

Another way to introduce the univalent copper ion into aqueous solutions is to generate copper(I) ions in the presence of these stabilising complexing reagents, by using either a metallic copper<sup>40,41</sup> or a copper amalgam electrode<sup>15</sup>. The use of hanging copper amalgam drop electrode (HCADE) has lowered the detection limit for determinations of purine<sup>15</sup> and thiocyanate<sup>42</sup> widening the possibilities of the CSV technique.

The appearance of copper(I) complexes in the voltammetric studies with estuarine waters are largely affected by the presence of chloride ions<sup>43</sup> forming cuprous chloride complexes. This species is shown to be the most important copper moiety adsorbed on the HMDE which forms from the anodic dissolution of amalgam. The adsorption is enhanced by addition of organic films (gelatine and glycine) which acts as an anchoring medium for the  $\text{CuCl}_2^-$  intermediate. From the above and the other studies with a copper rod<sup>41</sup> and with a mercury thin film electrode<sup>44</sup>, the dissolution reaction in chloride media was proposed as



The copper(I) complexes of nitrogen containing ligands are known to be more stable than the corresponding copper(II) complexes<sup>17</sup> as listed in Table-2.3. Imidazole groups are the most important binding site for the copper(I) ion among the nitrogen containing ligands. Hawkins and Perrin<sup>40</sup> studied the stability constants of copper(I) and copper(II) complexes of

imidazole and derivatives in aqueous solutions. Solutions of the copper(I) complexes were prepared by anodic electrolysis of metallic copper in the presence of ligand solution. It was suggested that all monodentate amines preferentially stabilise copper(I) in 1:1 or 1:2 complexes presumably with linear structures. The complex was also prepared in aqueous solutions<sup>45</sup> stabilising the copper(I) with acetonitrile. Copper(I) reacts with imidazole forming  $\text{Cu}(\text{Im})_2^+$  which at  $\text{pH} > 6.5$  polymerizes. In this case imidazole acts upon copper(I) as a bidentate ligand forming polynuclear chains as shown in Figure.2.7.

In the presence of a complexing reagent, the copper(II)/copper(Hg) couple splits into copper(II)/copper(I) and copper(I)/copper(Hg) couples which form two well separated reduction peaks. Histidine and purine compounds can be determined in this manner by producing the copper(I) complexes. The copper(I)-purine complex adsorbs on the electrode surface and can be deposited by electro-oxidation at a hanging copper amalgam drop electrode<sup>15</sup> or electro-reduction of HMDE<sup>15,46</sup> in the presence of copper(II) ions. Similarly, the reduction mechanism of copper complexes of histidine and Carnosine complexes were studied in the excess of ligand solution<sup>37</sup>.

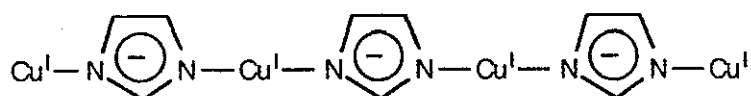


Figure 2.7-The structure of polymeric copper(I) complex of imidazole.

Table-2.3 Stability constants of copper complexes of nitrogen containing ligands<sup>17</sup>.

Ligand	Copper(II)		Copper(I)	
	$\log\beta_1$	$\log\beta_2$	$\log\beta_1$	$\log\beta_2$
Ammonia	4.31	7.98	5.93	10.86
Pyridine	2.65	4.86	3.17	6.64
Imidazole	4.26	7.87	5.78	10.98
Benzimidazole	3.56	6.34	4.47	9.73
Glycine	8.2	15.2		
Triglycine	5.66	10.17	6.2	



For the histidine complex, a two-electron reduction through two consecutive steps was observed with an intermediate copper(I) complex stabilised by adsorption at the mercury surface. On the other hand, the copper(I) complex is obtained chemically when concentrated copper(II) and histidine solutions are kept in contact with copper amalgam. The formation of copper(I) was tested upon interruption of the controlled potential oxidation at -0.5 V and addition of cuproin in dichloromethane. The color of organic phase changed to pink confirming the formation of copper(I)-cuproin complex. These results are in agreement with the studies of Thomas and Zackarias<sup>47</sup> who proved the generation of copper(I) by measuring the peak separation potential which is about 60 mV. These values also suggested that the electron transfer is nearly reversible.

Consequently, the redox behaviour of copper complexes of these biologically interesting compounds on the HMDE can reveal some useful information and the mercury electrode may be treated as a hydrophobic substrate-model of a physiological redox site, in the presence of both copper(II) and copper(I) states. Besides the further understanding of the reduction mechanisms of these complexes, CSV can be exploited for the determination of these compounds. The previous work in this laboratory has shown that histidine can be determined in nanomolar levels by using the reduction peak at -0.27 V vs. Ag/AgCl reference electrode by means of differential pulse adsorptive-cathodic stripping voltammetry<sup>48</sup>.

In this study, CSV behaviour of the copper complexes of histidyl peptides were investigated as useful models for biologically important molecules and developing a sensitive method for determining these substances was also aimed.

## CHAPTER 3

### EXPERIMENTAL

#### Apparatus and reagents

Cathodic stripping voltammetry was carried out with a Metrohm 626 Polarecord with a 663 VA-stand, or with a Metrohm 646/647 VA Processor, using a multimode electrode in the HMDE mode. The three electrode system was completed by means of a glassy carbon auxiliary electrode and an Ag/AgCl (3 M KCl) reference electrode. All potentials given are relative to this Ag/AgCl electrode.

The cyclic voltammetric experiments were carried out by connecting the electrodes on the Metrohm 663 stand to a Princeton Applied Research 174A polarographic analyser; the multimode-electrode (HMDE) was still activated by means of the Metrohm 626 Polarecord. The pH measurements were made with a Corning combined pH/reference electrode and a Radiometer PHM 64 pH meter.

Supporting electrolytes and buffers were prepared using analytical grade reagents supplied by BDH. A  $1 \times 10^{-2}$  M solution of GGH was prepared by dissolving precisely weighed amount of pure substance supplied by Sigma in a 5 ml of deionized water using sonication. Standard solution ( $1 \times 10^{-2}$  M) of GHG was prepared by dissolving precisely weighed amount of pure substances supplied by Sigma in a 5 ml of 0.2 M HCl using sonication. Ligand solutions were kept in a refrigerator and prepared freshly each day.

Imidazole (UV spectroscopic grade, specially prepared for use in UV spectrophotometric beta-lactam assays) was obtained from B.D.H. Ltd. and the other chemicals were from the Sigma Chemical Company. All were used without further purification.

A 0.2 M solution of imidazole was prepared by dissolving 0.1361 g of imidazole in water acidified with 6 drops of a 6 M HCl solution in a 10 ml calibrated flask .

Standard solution of copper(II) was prepared by diluting Spectrosol atomic absorption standard solution. Stock solution of copper(I) was prepared by dissolving copper(I) chloride in hydrochloric acid according to Svehla<sup>48</sup>. A 0.1 M sodium hydrogen carbonate solution was used for voltammetric studies at pH 8.3.

For the study of the interference of chloride on the determination of nitrate, benzoic acid and thiophene-2-carboxylic acid were prepared by dissolving the appropriate amounts of the reagent in concentrated sulphuric acid to give 0.01 M solutions. Dionex OnGuard-Ag cartridges with a 1.8-2.0 meq/cartridge loading capacity were used for preseparation. Cartridges were washed with deionized water before use and initial 2 ml of the sample was discarded.

### Procedures

The general procedure used to obtain adsorptive stripping voltammograms was as follows: A 20 ml aliquot of 0.1 M

buffer solution (usually hydrogen carbonate solution) was placed in a voltammetric cell and the required amounts of standard ligand and copper(II) solutions were added. The stirrer was switched on and the solution was purged with nitrogen for 5 min. After forming a new HMDE, accumulation was effected for the required time at the appropriate potential while stirring the solution. Maximum drop size and stirrer speed were used throughout with 663 VA-stand and medium drop size was used with the 647 VA stand. At the end of the accumulation period the stirrer was switched off and after 20 s had elapsed to allow the solution become quiescent, negative potential scan was initiated between the accumulation potential and -0.8 V. If the adsorptive accumulation was carried out at more negative potentials, immediately after accumulation step, the potential was changed to -0.1 V from where a negative potential step was initiated.

Cyclic voltammetry was carried out either immediately after forming a new HMDE or after preceding accumulation at different potentials for different times while stirring the solution. Either negative or positive scan was initiated after accumulation in dependence on the potential of accumulation.

Sampled direct current sampled polarography was performed using the static mercury drop electrode (SMDE) with a drop time of 1 s and scan rate 5 mV/s.

The procedure used in the study of interference of chloride on nitrate determination is as follows : Sample solution (1 ml) was pipetted into 3 ml of the reagent solution (0.01 M benzoic acid or thiophene-2-carboxylic acid in concentrated sulphuric acid) placed in a test tube and the combined solution was vortex-mixed for 60 s. The solution was then made up to 25 ml with a suitable cooling and transferred into a polarographic cell, deoxygenated for six min with nitrogen gas and then polarographed. The SMDE with a forced drop time of 1 s was used with a pulse amplitude of -100 mV and a 2 mV/s scan rate.

## CHAPTER 4

### ADSORPTIVE STRIPPING VOLTAMMETRIC BEHAVIOUR OF COPPER(II) AT A HANGING MERCURY DROP ELECTRODE IN THE PRESENCE OF EXCESS OF IMIDAZOLE

#### Introduction

The imidazole ring, as a histidine moiety, functions as a ligand toward transition metal ions in a variety of biologically important molecules including the iron-haem system, vitamin B<sub>12</sub> and its derivatives, and several metalloproteins<sup>50</sup>. The relationship between the structural property of the imidazole ring and the complexation properties with copper(II) has been reviewed<sup>18</sup> (see chapter 2 ).

The polarographic behaviour of the copper(II) complex of imidazole, formed at high concentrations of ligand, has been investigated in water-ethanol mixtures<sup>38</sup> and this study showed that the complex is reduced in two steps giving two waves of approximately equal height, the first at -0.19 V and the second at -0.57 V vs SCE. Both waves have been considered to be due to one electron reductions. In this study the highest copper(II) and copper(I) complexes were found to be  $\text{Cu}(\text{Im})_4^{2+}$  and  $\text{Cu}(\text{Im})_2^+$  respectively. Similar results were obtained with the copper(I)-imidazole complex system<sup>51</sup>. The complex was prepared from the chloride salt in acetonitrile containing buffer to stabilise the copper(I) against disproportionation. Again a two step wave results due to the

ability of imidazole to strongly complex copper(I) as well as copper(II).

Previous work in this laboratory has indicated that copper(II) can be accumulated rapidly and selectively at a HMDE modified by adsorption of a poly-L-histidine film<sup>52</sup>. In view of the importance of compounds containing the imidazole ring, and the affinity of this ring for co-ordinating copper ions, a study has been made of the adsorptive stripping voltammetric behaviour of copper(II) in the presence of excess of the parent imidazole molecule. Copper(II) can be determined by this means.

#### Results and discussion

The shapes of the differential pulse stripping voltammograms and of the cyclic voltammograms obtained after accumulation in a  $1.0 \times 10^{-7}$  M solutions of copper(II) in the presence of excess of imidazole were found to be dependent on the pH, accumulation potential, accumulation time, copper(II) and imidazole concentrations. The influence of the pH on the adsorptive stripping differential pulse stripping peak current of a  $2.0 \times 10^{-7}$  M solution of copper(II) in the presence of  $1.0 \times 10^{-3}$  M imidazole was summarised in Table 4.1.

At pH 4.5 (0.1 M acetate buffer) no significant adsorption of the complex at the electrode surface was observed. In basic media two different peaks, at -0.36 and -0.46 V vs Ag/AgCl, were observed and the heights of both peaks decreased with increasing pH above 8.5. This effect can be attributed to the formation of hydroxo complexes with copper(II). As the



highest currents were obtained in 0.1 M bicarbonate solution (pH 8.5), this electrolyte solution was chosen for use in further studies. A very small shift (only a few mV) was observed in the peak potentials when the pH was varied in basic media showing that there is no loss or gain of protons in the reduction process.

The influence of the accumulation potential on the voltammetric behaviour of a  $3 \times 10^{-7}$  M solution of copper(II) in various imidazole concentrations is shown in Figure 4.1. The cyclic voltammograms obtained when accumulation was carried out at 0 V for 120 s (Figure.4.1a), in the presence of  $1 \times 10^{-3}$  M of imidazole gave a single peak at -0.42 V in the cathodic scan. Two small broad peaks at -0.40 and -0.35 V were observed in the subsequent anodic sweep. No peak was observed when the imidazole concentration was significantly lower.

When accumulation was performed at -0.6 V, a single peak at -0.17 V was observed in the presence of  $1 \times 10^{-6}$  M of imidazole (Figure.4.1b). As the imidazole concentration was increased to  $1 \times 10^{-3}$  M the peaks are increased in height and shifted to negative values. The difference in the peak potentials of the cathodic and the anodic waves was found to be 60 mV.

Table 4.1 - Effect of pH on the peak current at -0.46 V obtained for the dp AdSV of the copper-imidazole complex recorded after accumulation at -0.1 V for 120 s. Initial concentrations : [Copper(II)] =  $2 \times 10^{-7}$  M; [Imidazole] =  $1 \times 10^{-3}$  M.

pH	4.5	7.0	8.5	9.5	10.5
Peak current (nA)	0	12.2	29.2	9.0	5.0

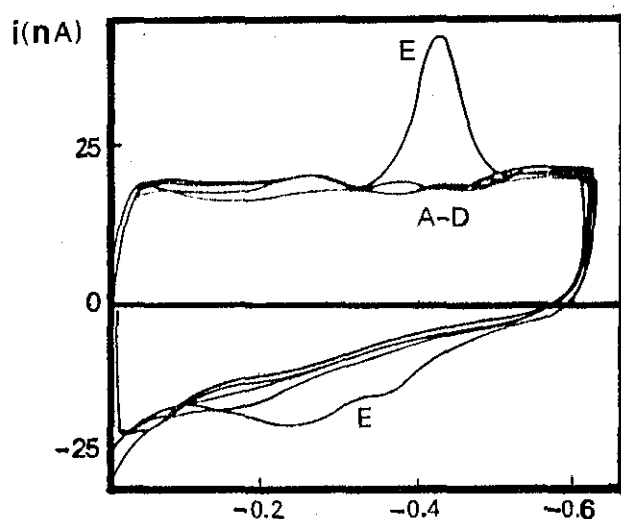


Figure.4.1- Effect of the imidazole concentrations and the accumulation potential on the cyclic voltammograms at an HMDE of a  $3 \times 10^{-7}$  M solution of copper(II) at pH 8.5. Accumulation was performed at a) 0; b) -0.6 and c) -0.1 V for 120 s. [Im] : A)0; B) $1 \times 10^{-6}$ ; C) $1 \times 10^{-5}$ ; D) $1 \times 10^{-4}$  and E) $1 \times 10^{-3}$  M for (a) and (b). For (c) : A) $1 \times 10^{-4}$ ; B) $3 \times 10^{-4}$ ; C) $5 \times 10^{-4}$ ; D) $7 \times 10^{-4}$ ; E) $1 \times 10^{-3}$  and F) $1.5 \times 10^{-3}$  M.

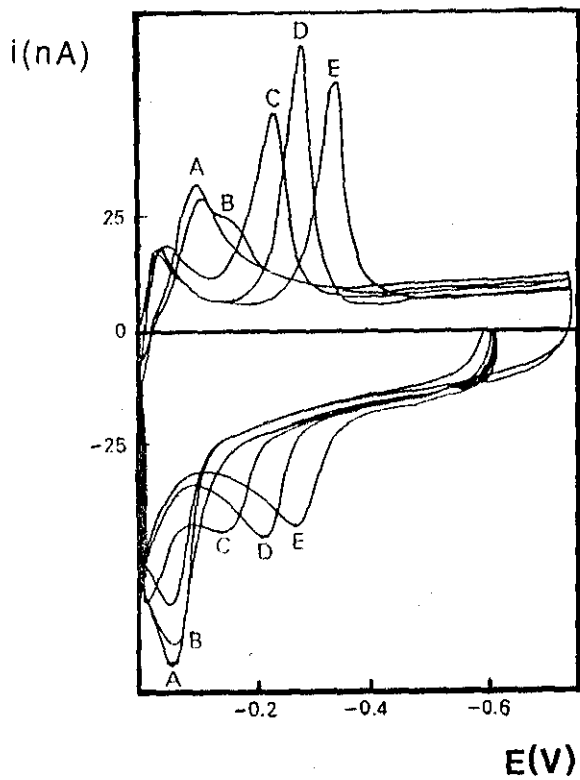


Figure.4.1b

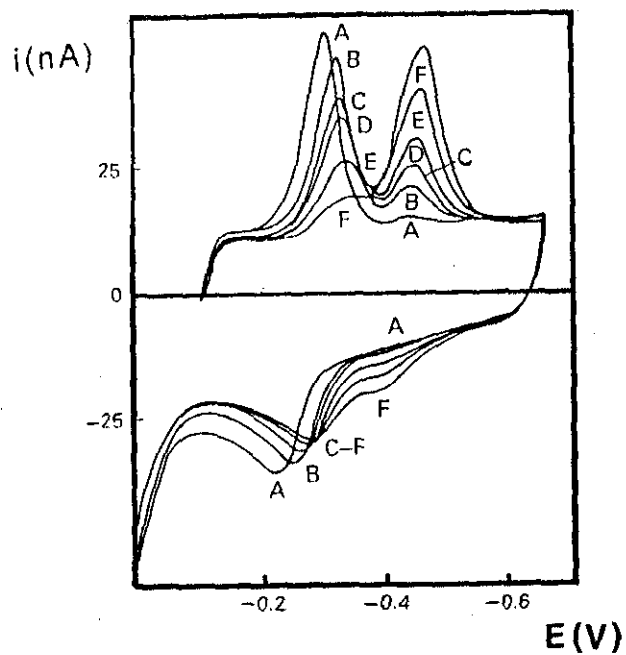


Figure.4.1c

At imidazole concentrations between  $1 \times 10^{-4}$  and  $1 \times 10^{-3}$  M (Figure 4.1c), two peaks were observed in the cathodic scans: the first at about -0.36 V and the second at -0.46 V. Associated with them, the peaks at -0.40 and -0.30 V were observed in the anodic scan. The peak potential of the first peak and related anodic peak shifted to negative values by addition of imidazole. Decreases in the height of the peak at -0.35 V and increases in the height of the peak at -0.46 V were observed with increasing imidazole concentration. At a concentration of  $2 \times 10^{-3}$  M only the peak at -0.46 V was present in the cyclic voltammogram. The influence of the accumulation potential on the peak currents of the complex in the presence of a  $1 \times 10^{-3}$  M imidazole is shown in Table 4.2.

The peak at less negative potential was shifted significantly in the cathodic direction with an increase in the imidazole concentration, as expected for complex formation (see Table 4.3).

Cyclic voltammograms of a  $3 \times 10^{-7}$  M solution of copper(II) in the presence of  $1 \times 10^{-3}$  M of imidazole obtained by successive scans at the same drop are shown in Figure.4.2. Initial accumulation was performed for 2 min. No further accumulation was carried out between the scans. When accumulation was performed at -0.1 V (Figure.4.2a) the two cathodic peaks at -0.37 V and at -0.46 V and associated with them two anodic peaks at -0.40 and at -0.30 V were observed. A decrease in the height of the peak at -0.46 V and a simultaneous increase in the height of the peak at -0.37 were observed with increasing scan number.

An isosbestic point was obtained at  $-0.41$  V. The presence of two cathodic peaks appears to be due to accumulation of two different copper complexes of imidazole at the electrode surface. The subsequent predominance of the peak at  $-0.36$  V must be caused by the complex which is reduced at  $-0.46$  V being converted into that responsible for the peak at  $-0.36$  V. Only the cathodic peak at  $-0.36$  V and the anodic peak at  $-0.30$  V were observed in the voltammograms when accumulating at  $-0.6$  V (Figure.4.2b). A small increase in the peak current with successive scans suggests film formation on the electrode surface.

Table 4.2 - Influence of the accumulation potential on the peak currents of a dp adsorptive stripping voltammogram of a  $3 \times 10^{-7} \text{ M}$  of copper(II) in the presence of  $1 \times 10^{-3} \text{ M}$  of imidazole at pH 8.5. Accumulation time: 120s.

$E_{\text{acc}}$ (V)	$i_p$ at -0.36 V (nA)	$i_p$ at -0.46 V (nA)
0	-	37.5
-0.05	5.0	37.5
-0.10	26.0	42.5
-0.15	37.0	44.0
-0.20	35.5	41.0
-0.30*	35.5	40.0
-0.33*	37.0	39.0
-0.37*	42.5	33.5
-0.40*	61.5	19.0
-0.42*	72.5	12.0
-0.45*	84.0	-
-0.50*	89.0	-

\* Potential scanned from -0.20 V.

Table 4.3- Effect of the imidazole concentration on the cathodic peak potential of the copper(II) complex at pH 8.5.  $[Cu^{2+}] = 3 \times 10^{-7}$  M accumulated at -0.6 V for 120 s.

[Im] (M)	$1 \times 10^{-6}$	$1 \times 10^{-5}$	$1 \times 10^{-4}$	$1 \times 10^{-3}$
$E_p$ (V)	-0.18	-0.22	-0.27	-0.36

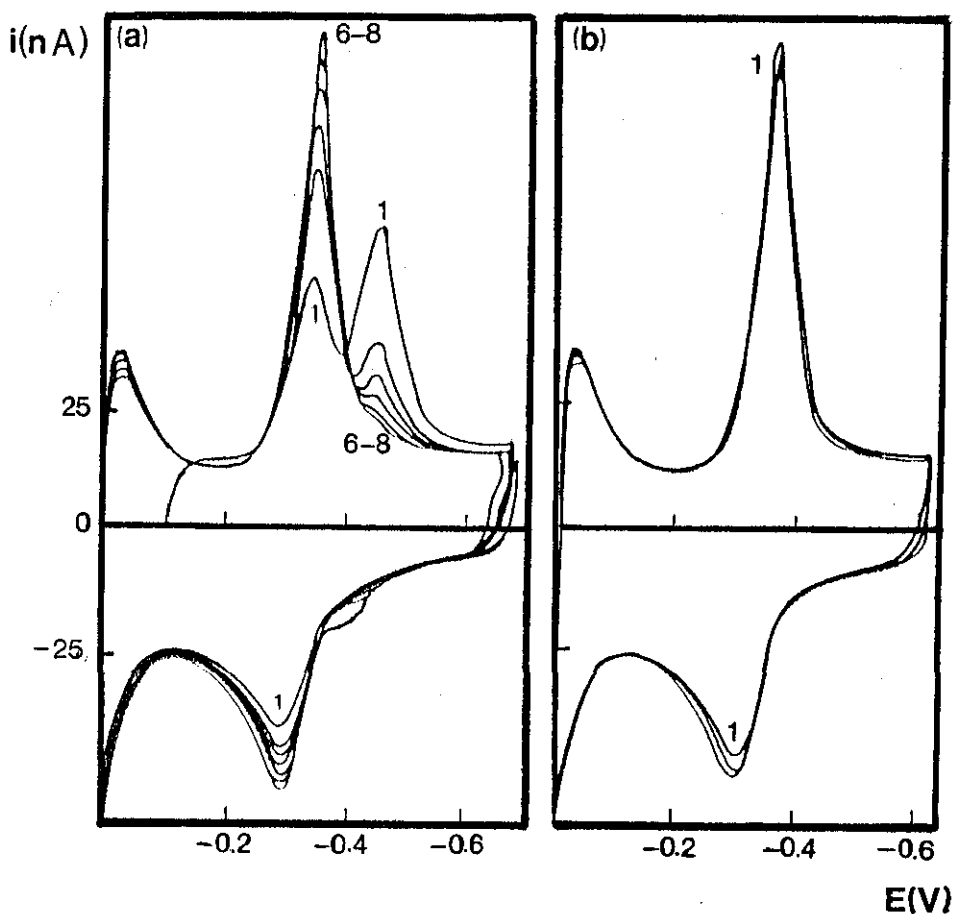


Figure.4.2 - Effect of the successive scans on the cyclic voltammograms of a  $3 \times 10^{-7}$  M of copper(II) solution in the presence of  $1 \times 10^{-3}$  M of imidazole at pH 8.5. Accumulation potentials are a) -0.1V and b) -0.6 V.

The influence of the addition of copper(II) on the cyclic voltammograms obtained for a  $1 \times 10^{-3}$  M solution of imidazole in 0.1M hydrogencarbonate solution pH 8.5 is shown in Figure.4.3. Accumulating at -0.1 V (Figure.4.3a), a single peak at about -0.42 V was observed at copper(II) concentrations lower than  $1 \times 10^{-7}$  M. The height of this peak increased with increasing copper(II) concentration. At copper(II) concentrations higher than  $1 \times 10^{-7}$  M, a second peak was observed at -0.36 V. The height of this peak increased with further increase in the copper(II) concentration. When this peak was present in the voltammogram, only a small increase in the height of the peak at -0.42 V was observed with increasing copper(II) concentration. A similar behaviour was observed in the anodic scans and, in this case a peak at -0.30 V, associated with the cathodic peak at -0.37 V, predominated. These results agree with those obtained by increasing the imidazole concentration and suggest that the complexes responsible for the two peaks are strongly dependent on the [Cu(II)] : [imidazole] ratio.

The influence of accumulation time at -0.1 V on the complex peak heights is shown in Figure.4.4. After 2 min accumulation time the peak current gives a slight decrease indicating a saturation on the electrode surface.



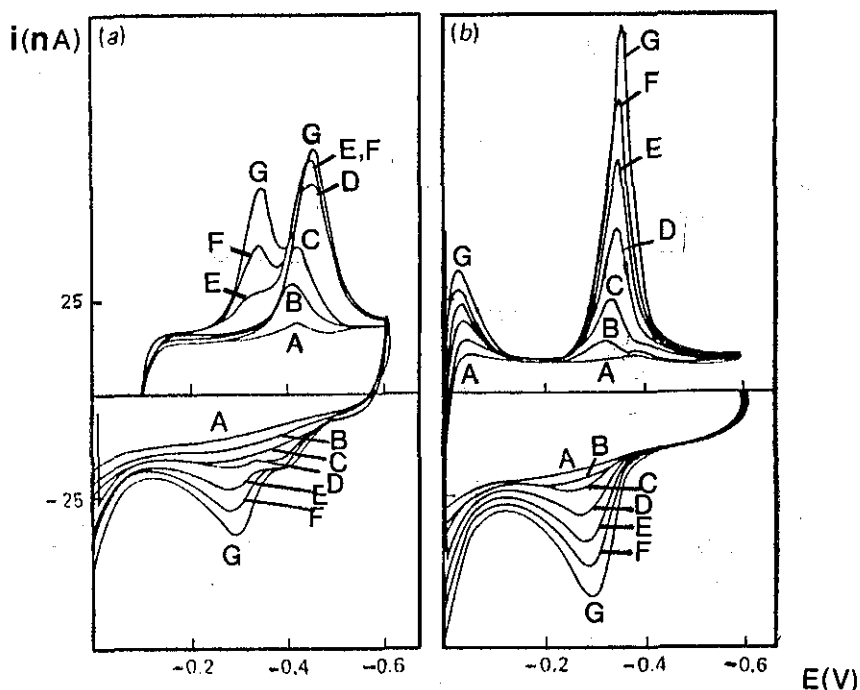


Figure.4.3- Effect of the copper(II) concentration on the cyclic voltammograms at an HMDE, for a  $1 \times 10^{-3}$  M imidazole solution at pH 8.5. Accumulation at (a) -0.1 V and (b) -0.6 V for 120 s.  $[Cu^{2+}]$ : (A) 0 ; (B)  $5 \times 10^{-8}$ ; (C-G)  $1-5 \times 10^{-7}$ .

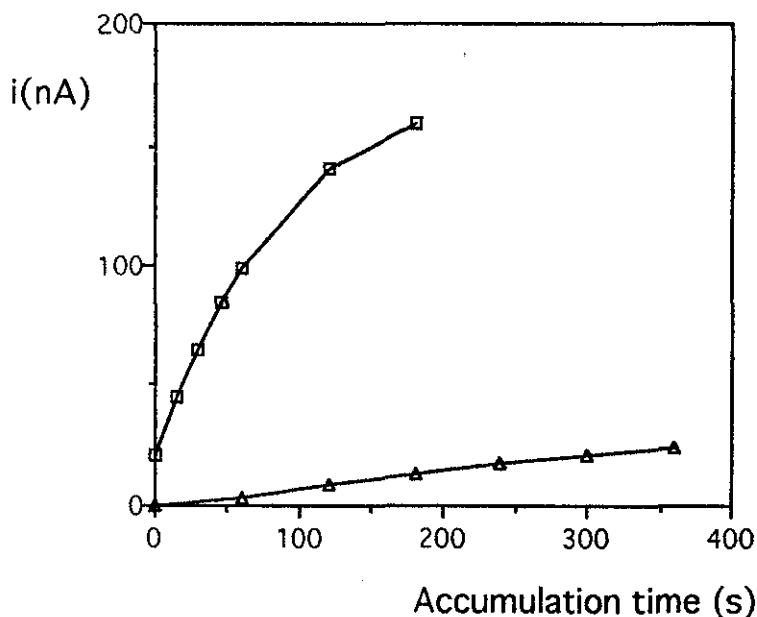


Figure.4.4- Effect of accumulation time on the stripping peaks of the complex in the presence of  $1 \times 10^{-3}$  M imidazole containing (-□-)  $5 \times 10^{-7}$  M and (-Δ-)  $6 \times 10^{-8}$  M copper(II) solution accumulated at -0.1 V and -0.6 V, respectively.

In the explanation of the nature of these peaks two mechanisms can be considered. One hypothesis for the cyclic voltammograms obtained is: both peaks could be due to the reduction of two different forms of copper(II) which can be interconverted. In fact, Nozaki et al<sup>53</sup> observed four different copper(II) complexes in the copper(II)-4-methylimidazole system, the zone of predominance of each depending on the 4-methylimidazole concentration. However, the dependence of the peak currents on the accumulation potential in the present study could not be explained on the basis of this mechanism.

Although usually a direct two electron reduction to copper(I) would be proposed to explain the reduction mechanism of each of the two peaks assigned as above, the formation of copper(I) complexes have also been reported by other workers for the imidazole system (see Chapter 2).

The occurrence of two reduction peaks in cyclic voltammograms obtained in the present study suggests the possibility that the reduction of the copper(II)-imidazole complex occurs via two one electron steps. In fact this stepwise reduction was reported for the polarographic behaviour of imidazole complexes prepared in water-ethanol mixture<sup>38</sup>. However, this reduction mechanism is not consistent with the present study of dp polarography of the complex as only one peak was observed for different metal ion to ligand ratio in pH 8.4 sodium hydrogencarbonate solution (Figure.4.5).

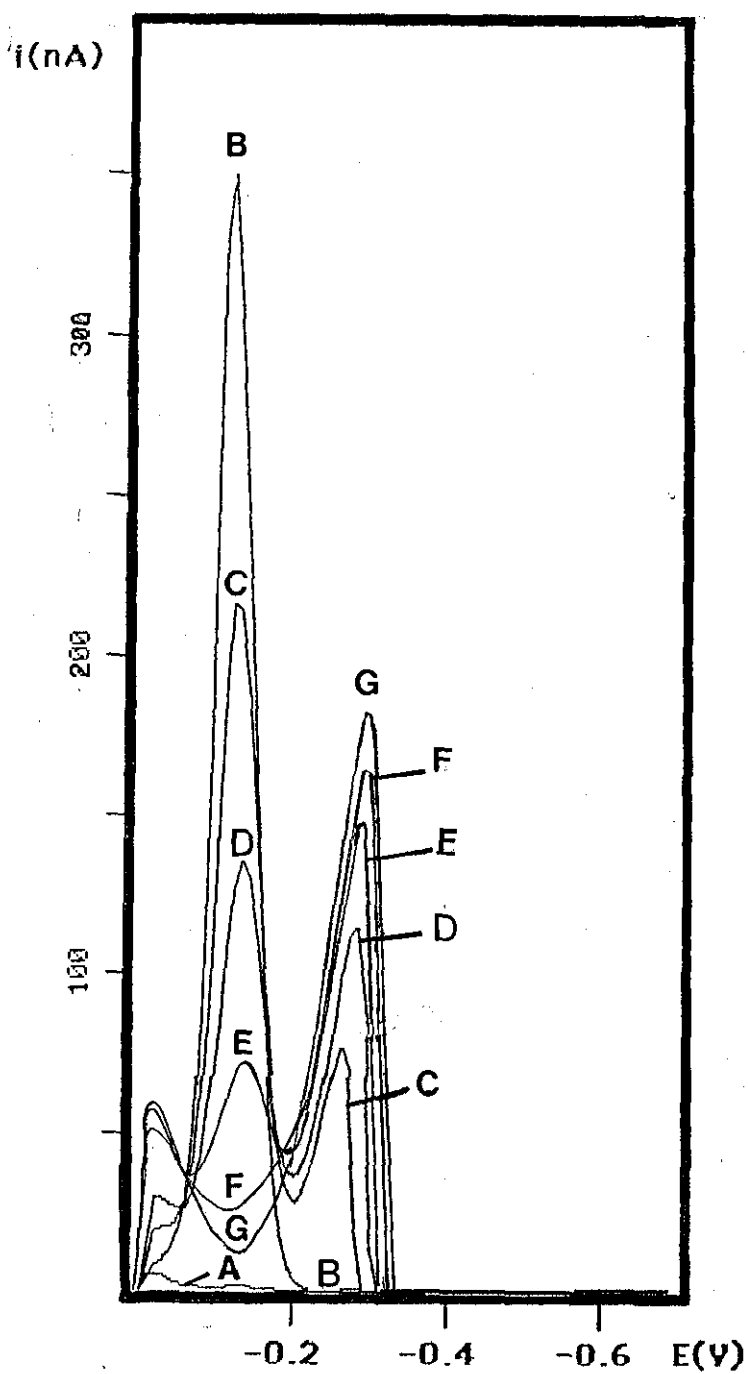


Figure.4.5- The dp polarographic behaviour of  $5 \times 10^{-5}$  M copper(II) at pH 8.3 in the presence of (B) 0; (C)-(G)  $1-5 \times 10^{-5}$  M imidazole. (A) 0.1 M sodium hydrogencarbonate solution only.

The reduction peak of uncomplexed copper(II) ion at  $-0.12$  V disappeared at 1:1 ratio. The complex peak currents increase while the peak potentials are shifting to more negative values with increasing imidazole concentrations. For 1:20 concentration ratio the peak potential is  $-0.42$  which would correspond to the second peak of the cyclic voltammogram obtained for  $-0.1$  V accumulation potential.

On the other hand, the cyclic voltammetry behaviour is not completely consistent with the assumed consecutive reduction steps. Increases in the second peak when the conditions are changed occur with decreases in the first peak. This behaviour would not be expected if the peaks were due to the copper(II) to copper(I) and copper(I) to copper(Hg) reduction respectively. The appearance of the first peak depending on the accumulation potential or scanning to the potentials more negative than  $-0.1$  V suggests that the formation of the species responsible for this peak is highly dependent on the electrode potential and the metal ion to ligand ratio. The cyclic voltammetry suggests that this species is more stable and more easily formed and is adsorbed at the electrode surface.

Another hypothesis which assumes the formation of a copper(I) species is that the peaks at  $-0.36$  (reduction) and  $-0.30$  V (oxidation) are due to the reduction or oxidation of copper(I) in the polymeric film formed at the surface, whereas the copper(II) to copper(I) reduction peak takes place at a more positive potential. This reduction via two consecutive steps can clearly be seen in Figure.4.1b where the free copper(II) reduction peak at  $-0.12$  V is split on addition of excess of

imidazole into two peaks. The dependence of the formation of the copper(I) species on the accumulation potential suggests that the copper(Hg) formed at sufficiently negative potentials is reoxidised to copper(I) species in the presence of excess of imidazole by switching the electrode potential to more positive values. Copper(I) is therefore generated at the electrode surface when the potential is held at potentials more negative than -0.1 V and then forms complexes with imidazole prior to the adsorption on the electrode surface. The copper(I) species was also shown to form chemically when concentrated copper(II) is kept in contact with copper amalgam in the presence of stabilising complexing reagent<sup>37</sup>.

On the basis of the polarographic studies and the dependence of the peak shape on the imidazole concentration the second peak at -0.46 V can be attributed to the reduction of the higher order complex of copper(II) present in the solution, possibly  $\text{Cu}(\text{Im})_4^{++}$ , to copper(Hg). The decrease of the peak height of the second peak with accumulation potentials more negative than -0.3 V suggests that the species responsible for the second peak does not strongly adsorb on the mercury surface as does the copper(I) complex.

The peak current obtained when accumulation was performed at -0.6 V and the scan was started at 0 V increased rectilinearly with the square root of the scan rate. This relation suggests diffusional behaviour probably caused by multimolecular film formation. A shift in the cathodic peak potential from -0.32 to -0.36 V was observed when the scan rate was varied from 10 to 100 mV/s. A shift from -0.30 to

-0.26 V was observed for the anodic peak under the same conditions. Similar results were obtained for both peaks (i.e. those at -0.36 and -0.42 V) when accumulation was carried out at -0.1 V. These results indicate a small degree of irreversibility of the system.

From the above results it is apparent that copper(II) can be determined using an excess of imidazole as an accumulation reagent. When the accumulation was performed at -0.6 V, the height of the copper(II)-imidazole peak at -0.36 V obtained using a solution containing  $6 \times 10^{-8}$  M of copper(II) and  $10^{-3}$  M of imidazole showed a rectilinear relation ( $r = 0.998$ ) with the accumulation time up to 6 min (see Figure.4.4). Rectilinear calibration curves were obtained for copper(II) in the presence of  $1.0 \times 10^{-3}$  M of imidazole when accumulation was carried out at 0 or at -0.6 V for 3 minutes (Figure.4.6).

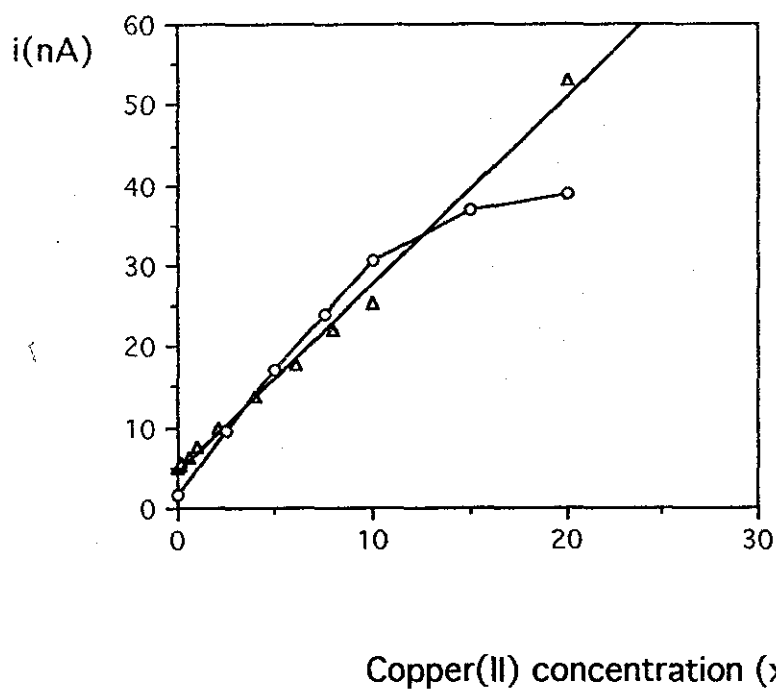


Figure.4.6- Plots of stripping peak heights against concentration of copper(II) added. Imidazole concentration is  $1 \times 10^{-3}$  M in 0.1 M  $\text{NaHCO}_3$ . Accumulation potential : (-o-) 0 V; (- $\Delta$ -) -0.6 V.

When accumulation was performed at 0 V for 3 minutes, a rectilinear calibration curve was obtained from  $2.5 \times 10^{-8}$  to  $1 \times 10^{-7}$  M ( $r = 0.999$ ) with slope of  $2.84 \times 10^8$  nA/mol. At copper(II) concentrations higher than  $1 \times 10^{-7}$  M a deviation from linearity was observed probably due to the saturation of the electrode surface. Better sensitivity ( $5.4 \times 10^8$  nA/M) in a wider range ( $1 \times 10^{-9}$  to  $2 \times 10^{-7}$  M) were obtained when accumulation was performed at -0.6 V (Figure.4.6). The limit of detection was  $2 \times 10^{-9}$  M for accumulation at -0.6 V for 3 minutes.

Several reagents have been suggested for the differential pulse adsorptive stripping voltammetric determination of copper(II)<sup>54,55</sup>. The limits of detection for determinations with catechol and 8-hydroxyquinoline are given as  $3 \times 10^{-10}$  and  $1 \times 10^{-10}$  M respectively<sup>56</sup> based on an accumulation time of 1 min from a stirred solution: the use of catechol has the disadvantage that its solutions are readily oxidised by air and the reagent must be freshly prepared. The detection limit using imidazole does not appear to be as good. This method could not be adapted for determination of imidazole as no adsorption occurred in the presence of excess of copper(II) ions.



## CHAPTER 5

### ADSORPTIVE STRIPPING VOLTAMMETRIC BEHAVIOUR OF COPPER(II) COMPLEXES OF GLYCYLGLYCYL-L-HISTIDINE AT A HANGING MERCURY DROP ELECTRODE

#### Introduction

Tripeptides containing the histidyl residue are of interest as models of bioactive polypeptides and proteins. GGH was shown to simulate the native copper(II) binding characteristics of serum albumin and it serves as a suitable model for many important studies of the interaction between copper(II) and albumin. Although the coordination structures of the copper complex of GGH are well established (see Chapter 2), there are few reports on its electrochemical behaviour. Takehara and Ide<sup>36</sup> have reported anomalous current fluctuations in the reduction process of copper(II) complex of GGH in equimolar solutions. No attempts to investigate the adsorptive stripping voltammetric behaviour of copper(II)-GGH complexes and use them for the determination of trace amounts of either copper or the tripeptide have so far been reported. Therefore a detailed study of adsorptive stripping voltammetric behaviour of Cu(II)-GGH complexes was carried out. In addition to the better understanding of the redox behaviour of these biologically interesting complexes on the surface of mercury drop, the possibility of developing a sensitive method for voltammetric determination of trace amounts of polarographically inactive GGH was kept in mind.

## Results and discussion

GGH was shown to be electrochemically inactive over the pH and potential ranges studied. The dc polarograms of the copper(II)-GGH complex obtained in the presence of excess GGH showed a single polarographic wave of constant height over the pH range from 6.0 to 11.8, in which range the 1:1 complex is known to be formed<sup>18,20</sup>. The 1:1 complex formation at pH 8.3 was confirmed by the fact that the height of the wave of  $1 \times 10^{-5}$  M solution of uncomplexed copper(II) solution decreased to one half after addition of GGH corresponding to  $5 \times 10^{-6}$  M and to zero when the GGH concentration was increased to  $1 \times 10^{-5}$  M. The differential pulse polarographic peak potential varied linearly with pH as shown in Table 5.1. The polarographic maximum observed was readily removed by means of Triton X-100.

### Cyclic Voltammetric Behaviour of copper complexes of GGH

Stripping cyclic voltammograms obtained at HMDE with  $5 \times 10^{-7}$  copper(II) and  $1 \times 10^{-5}$  M GGH in a pH 8.3 hydrogen carbonate solution are shown in Figure 5.1. Figures 5.1a and 5.1b show multiple scans between 0 and -0.8 V after holding the potential initially at 0 V and -0.7 V, respectively, for 2 min. Two reduction peaks are observed, around -0.4 V and -0.6 V, the exact position of which slightly depends on both GGH and copper(II) concentration. Moreover, the height of these two peaks was found to be dependent on the concentration of GGH and copper(II), potential and time of accumulation, and on the

scan rate, direction and switching potentials of subsequent cyclic voltammetric scans.

On the basis of dc and dp polarographic behaviour of copper(II)-GGH complex, the second peak around -0.6 V can be assigned to the reduction of copper(II)-GGH complex to copper(Hg). This assumption is supported by the fact that copper(Hg) is accumulated when the potential is held at -0.7 V which is clear from the appearance of the anodic peak at -0.07 V corresponding to the reoxidation of copper(Hg) to free copper(II) and the free copper(II) reduction at -0.12 V in subsequent cathodic scan (see Figure 5.1b). The first peak around -0.4 V is not present during the first scan after holding the potential at 0.0 V (see scan 1 in Figure 5.1a). In subsequent scans, however, the first peak increases continuously in size, as does the second peak.

The morphology of these two peaks and their dependence on the scan rate suggest that they correspond to the reduction of adsorbed species. A single reoxidation peak is observed on the reverse scan at -0.25 V; the shape of this peak indicates diffusion controlled process. The nature of this anodic peak was established using 1 min accumulation at -0.8 V in the solution containing  $1 \times 10^{-7}$  M copper(II) without GGH. In the anodic scan after this accumulation, a single anodic peak at -0.07 V was observed, which corresponds to the reoxidation of copper(Hg) formed during accumulation step.

Table 5.1- Polarographic data of solutions containing  $1 \times 10^{-4}$  M copper(II) and  $1 \times 10^{-3}$  M GGH in different pH media in phosphate, borate buffers and NaOH solution

pH	6.0	7.0	8.0	9.0	10.0	11.8
$E_{1/2}$ (V)	-0.39	-0.42	-0.53	-0.61	-0.68	-0.69

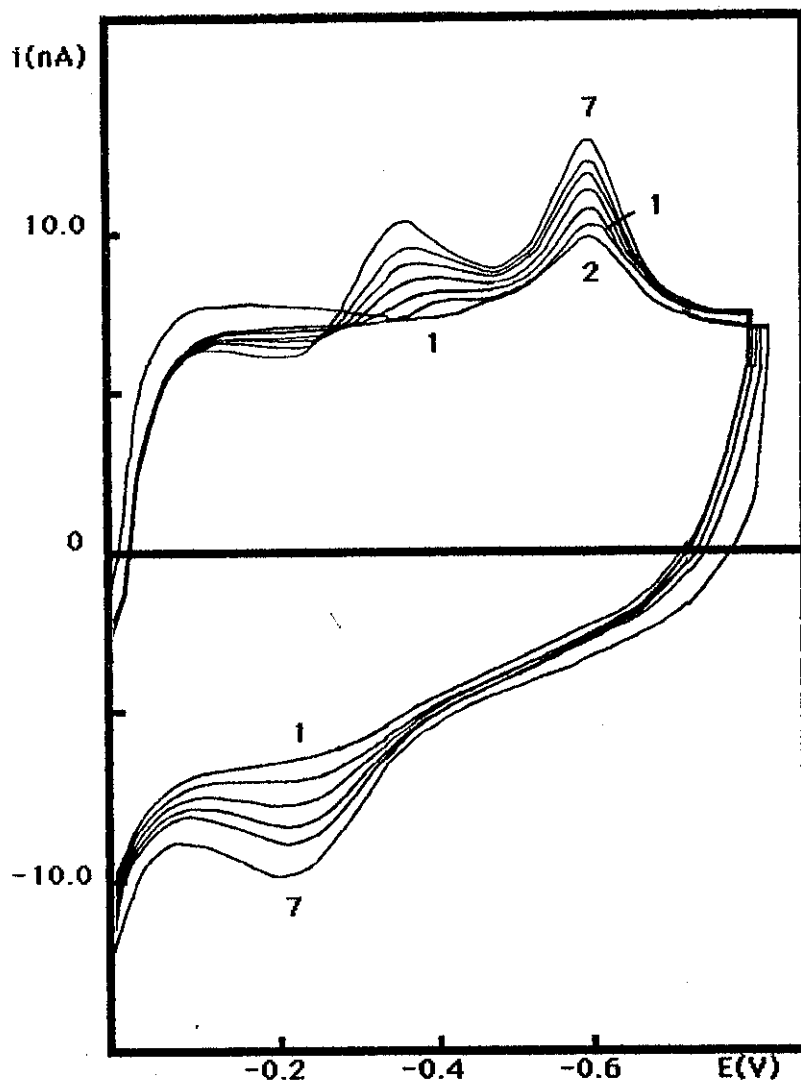


Figure 5.1- Multiple scan cyclic voltammograms of the complex solution at pH 8.3. Initial concentrations : copper(II) :  $5 \times 10^{-7}$  M; GGH :  $1 \times 10^{-5}$  M. Scan rate 50 mV/s; accumulation time 2 min in stirred solution; the scan number is indicated on the plot. Accumulation potential : (a) 0 V, (b) -0.7 V. Cycling was made between 0 V and -0.8 V.

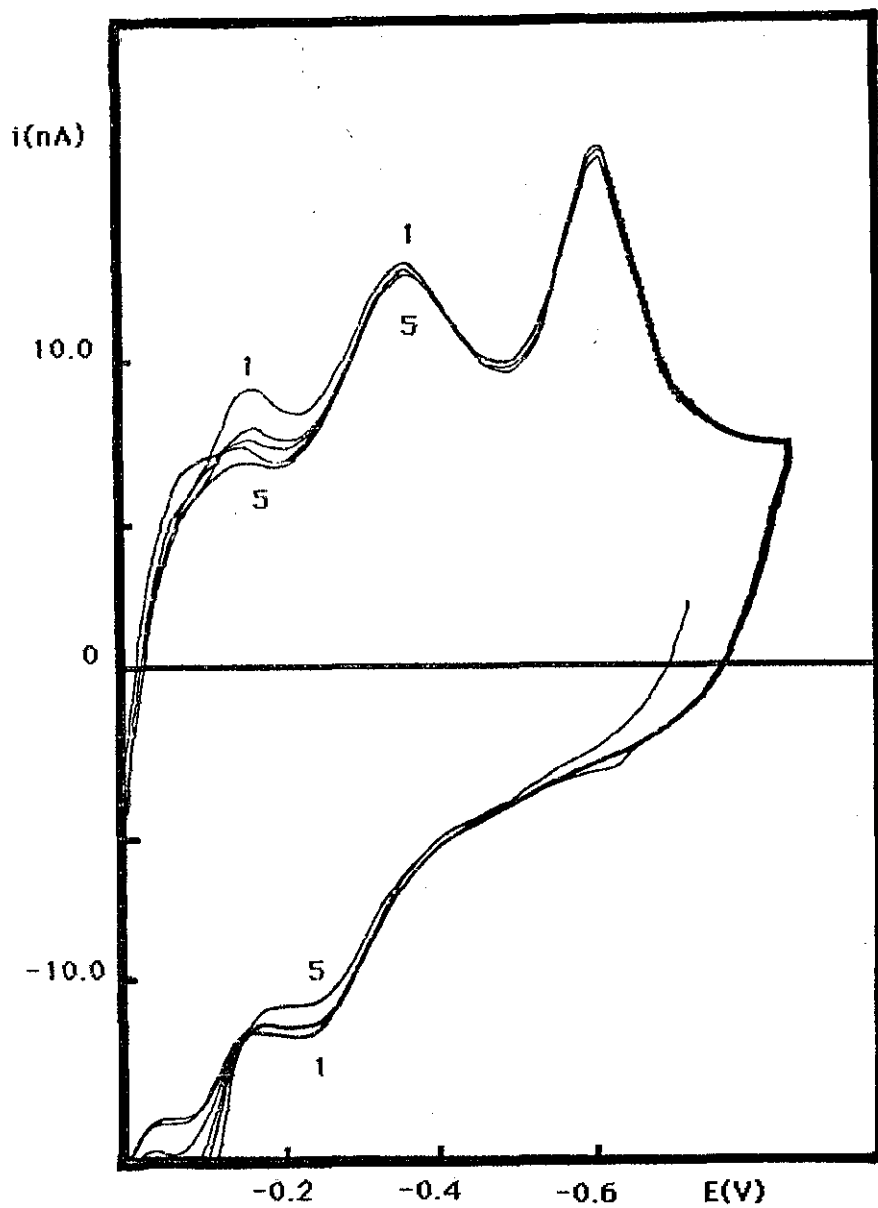


Figure.5.1b

However, when after the same accumulation step GGH was added so that total concentration was equal to  $1 \times 10^{-4}$  M, a single anodic peak at -0.22 V was observed, the shape of which suggested diffusion controlled process. No cathodic peak around -0.4 V was observed in the subsequent cathodic scan with switching potential to -0.15 V. Thus the possibility that the peak at -0.22 V corresponds to the reoxidation of copper(Hg) to the species responsible for the cathodic peak at -0.4 V can be excluded. However, the second cathodic peak around -0.6 V can clearly be seen in the subsequent cathodic scan. Therefore, we can assume that anodic peak at -0.22 V corresponds to the reoxidation of copper(Hg) to copper(II)-GGH complex. No experimental findings support the assumption of Takehara<sup>36</sup> that oxidation of copper(Hg)-GGH complex to copper(II)-GGH complex is involved under these conditions. Nevertheless, in accordance with Takehara's findings, it can be assumed that at potentials more negative than -0.6 V GGH is desorbed because of its negative charge at pH 8.3 and strong repulsion force caused by highly negative charge of HMDE. It explains why reoxidation of copper(Hg) to copper(II)-GGH complex is a diffusion controlled process in contrast to the adsorption controlled process corresponding to the cathodic peaks around -0.4 and -0.6 V. (However, re-adsorption of GGH can occur during subsequent anodic or cathodic scans at potentials closer to electrocapillary zero).

The copper(Hg) formed at sufficiently negative potentials is reoxidised to copper(II) on cycling to 0 V and the two cathodic

peaks around -0.4 and -0.6 V remain of constant height during the first and subsequent scans. The free copper(II) cathodic peak at -0.12 V which is observed clearly for the first scan gradually disappears during the subsequent scans. This indicates whereas the species responsible for the peaks around -0.4 and -0.6 V are adsorbed at the electrode surface, the uncomplexed copper(II) diffuses away from the surface.

When experiment illustrated in Figure 5.1b was repeated using  $1 \times 10^{-7}$  and  $3 \times 10^{-7}$  M copper(II), the two peaks were again obtained of constant height on cycling, but became proportionately smaller as the copper(II) concentration was decreased. However, when the copper(II) concentration was only  $5 \times 10^{-8}$  M, the peak around -0.4 V was not present and the capacitance background current was higher than in Fig.5.1a.

Cycling the potential between 0 and -0.4 V produced no peak around -0.4 V (see Figure 5.2a), but holding the potential at -0.5 V and subsequent cycling between 0 and -0.5 V did (see Figure 5.2b). The formation of both peaks on scanning to -0.7 V is also shown in Figure 5.2b for comparison. When accumulation was effected at -0.7 V and the potential was then held at 0 V for 1 or 2 min before cycling between 0 and -0.9 V, the peak around -0.4 V disappeared and the peak around -0.6 V was reduced in height (see Figure 5.2c). Obviously, the dissolution of copper(Hg) (which is formed during accumulation at -0.7 V) at a potential value of 0 V results in the desorption of species responsible for cathodic stripping peaks.

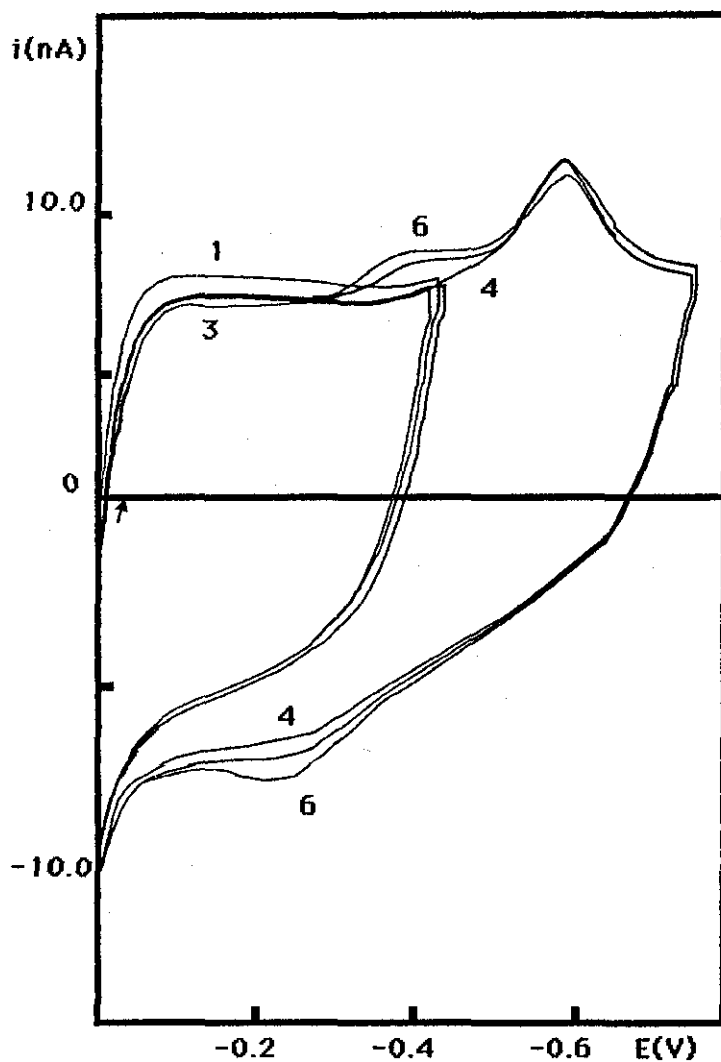


Figure 5.2- Multiple scan cyclic voltammograms of the complex at an HMDE. Initial concentrations :  $1 \times 10^{-5}$  M GGH;  $5 \times 10^{-7}$  M Cu(II); pH 8.3; scan rate 50 mV/s; accumulation time 2 min in stirred solution; (a) Accumulation at 0 V, cycles 1-3 between 0 V and -0.4 V, cycles 4-6 between 0 V and -0.7 V; (b) Accumulation potential -0.5 V, cycling between -0.5 V and 0 V; (c) Accumulation potential -0.7 V, scan to 0 V, cycles 1-2 between 0 V and -0.9 V, scan 3 and 4 held at 0 V for 1 and 2 min, respectively, before scanning.



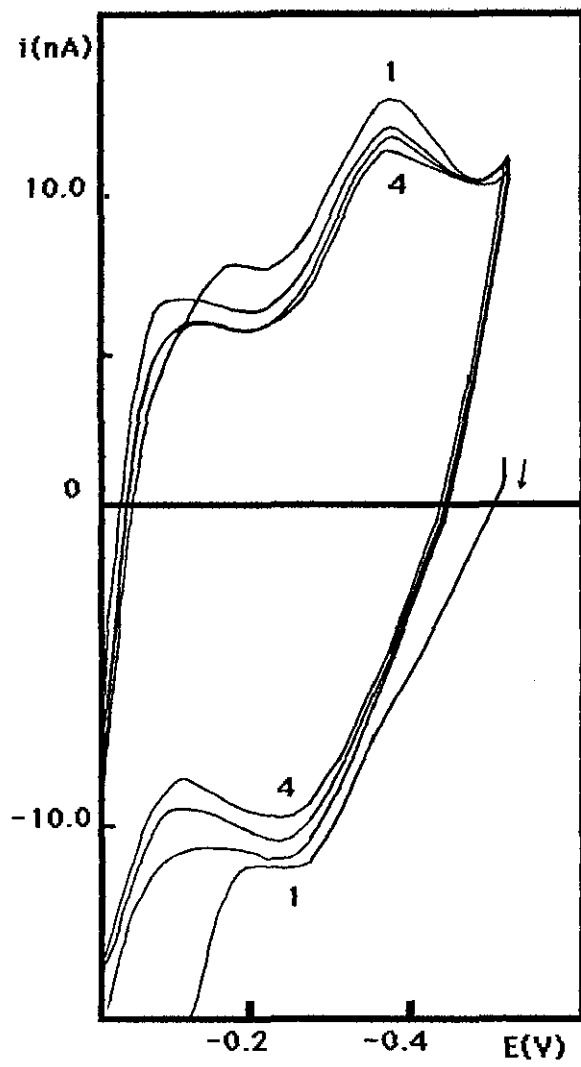


Figure.5.2b

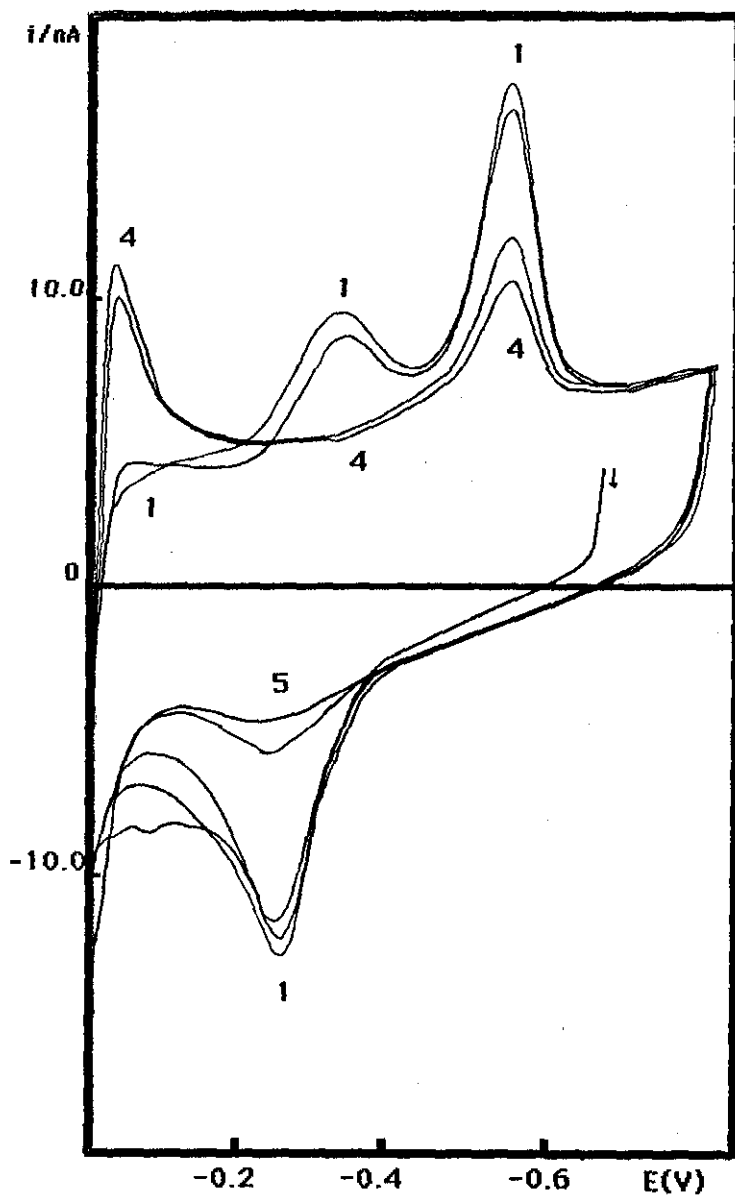


Figure.5.2c

The species responsible for the cathodic peak around -0.6 V was barely or only weakly accumulated under these conditions (i.e. excess of GGH) using the accumulation potential 0 or -0.4 V (see Figure.5.3a and 5.3b). However, with  $1 \times 10^{-7}$  M copper(II) and equal concentration of GGH, the second peak, whose potential was shifted to -0.54 V, has increased with longer accumulation times at -0.1 or -0.2 V. Practically no accumulation could be seen at 0 V. Moreover, no accumulation was observed for the second peak at higher concentrations ( $1 \times 10^{-6}$  M) of both copper(II) and GGH. This can be explained by the preferred accumulation of GGH rather than its copper(II) complex under these conditions.

The cyclic voltammograms at Figure 5.3b were obtained by accumulating at -0.4 V and then cycling the potential to -0.8 V and then through 0 V and back to -0.4 V. With no accumulation at -0.4 V, neither reduction peak were obtained. As little as 15 s accumulation, however, fully formed the small second peak at -0.6 V for the first part of the scan to -0.8 V; this peak was slightly smaller with accumulation times of 1 and 2 min. These longer accumulation times, however, caused the first peak at -0.4 V to increase significantly in size. It seems probable that both copper(Hg) and GGH are accumulated at -0.4 V; the reoxidation, on the positive going scan, is largely reoxidation of copper(Hg) to free copper(II) are only seen after 2 min accumulation.

Figure.5.4 shows the voltammograms obtained by accumulating at various potentials between 0 and -0.6 V, before

immediately changing the potential to 0 V and scanning from 0 to -1.0 V. the peak around -0.6 V increases in size gradually between accumulation potentials 0 and -0.3 V, and then, from -0.4 to -0.6 V the peak around -0.4 V appears at an appreciable fixed height as does the second peak around -0.6 V. The progressive increase in the height of the second peak, while the first peak is still being established, at lower accumulation potentials indicates a need for greater accumulation of copper(Hg) -and the resulting greater concentration of free copper(II) at the electrode surface on cycling to 0 V- for formation of the species responsible for the peak around -0.4 V. This is confirmed by the voltammograms shown in Figure 5.5. These voltammograms were obtained at increasing accumulation times at -0.4 V, and scanning immediately from 0 to -0.8 V. One minute accumulation gave full formation of both peaks for accumulation at -0.4 V and more negative potentials (compare with Figure 5.4). In the voltammograms in Figure 5.5, the more rapid increase of the second peak at the lower accumulation times is clear.

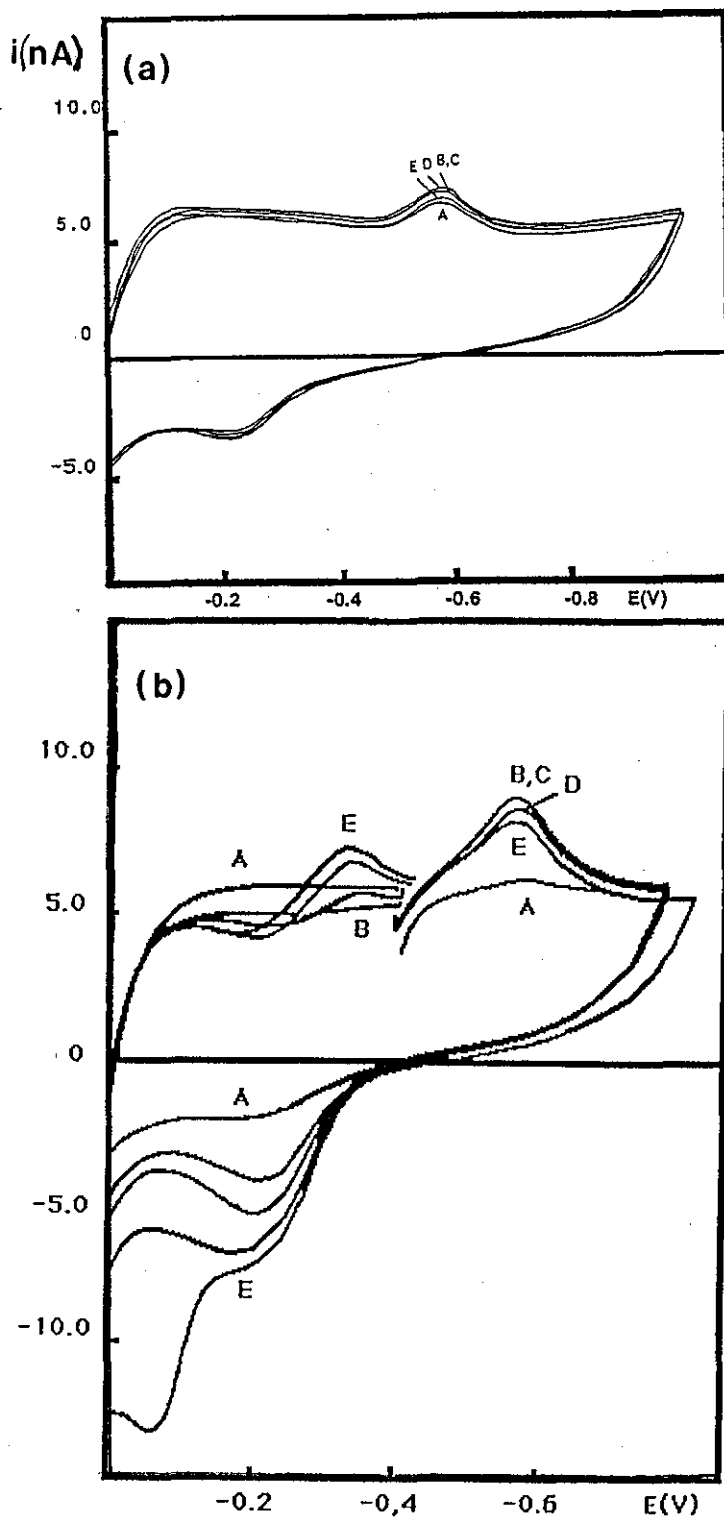


Figure 5.3- Effect of accumulation times at various potentials. Initial concentrations :  $5 \times 10^{-7}$  M Cu(II) and  $1 \times 10^{-5}$  M GGH; pH 8.3; scan rate 50 mV/s; accumulation time : (A) 0 s; (B) 15 s; (C) 30 s; (D) 1 min; (E) 2 min. Accumulation potential : (a) 0 V, scanning between 0 V and -1.0 V; (b) -0.4 V, scanning from -0.4 V to -0.8 V and to 0 V and then back to -0.4 V.

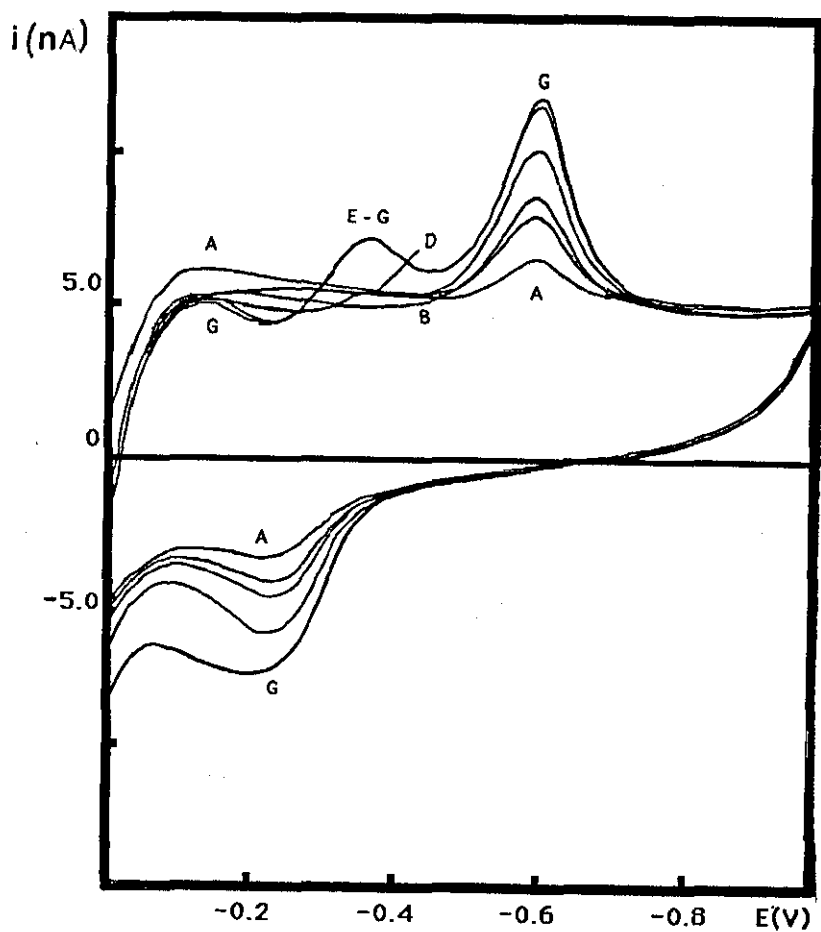


Figure 5.4- Effect of accumulation potential. The initial concentrations :  $5 \times 10^{-7}$  M Cu(II);  $1 \times 10^{-5}$  M GGH, pH 8.3; accumulation time : 1 min in stirred solution; after accumulation all scans were made immediately from 0 V at scan rate 50 mV/s; accumulation potential : (A) 0; (B) -0.1; (C) -0.2; (D) -0.3; (E) -0.4; (F) -0.5; (G) -0.6 V.

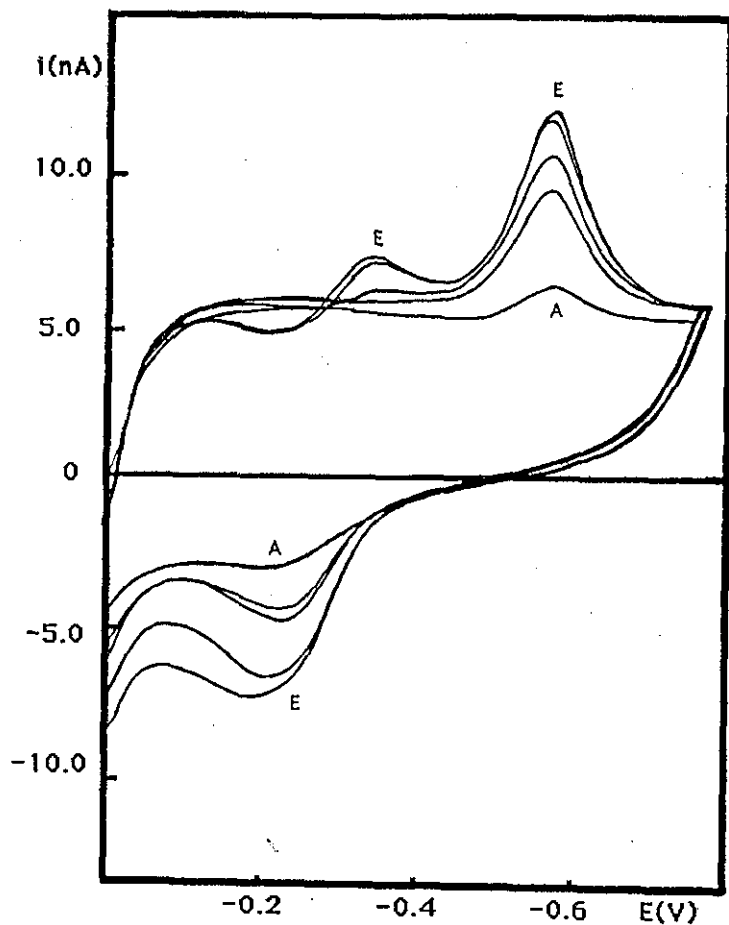


Figure 5.5- Effect of accumulation time at -0.4 V on the cyclic voltammograms of the complex. Scan was made from 0 V at a rate of 50 mV/s. Initial concentrations :  $5 \times 10^{-7}$  M copper(II);  $1 \times 10^{-5}$  M GGH, pH 8.3; accumulation time : (A) 0; (B) 15; (C) 30; (D) 60; (E) 120 s.

In Figure 5.6 the effect of accumulating copper(Hg) at -0.4 V in the absence of GGH, which was then added whilst the cell was on open circuit before scanning from 0 V to more negative potentials, is shown; this is compared with the voltammogram obtained similarly without addition of GGH. Clearly the first and second peak can be formed, using these bulk concentrations of copper(II) and GGH, from accumulated copper(Hg) (subsequently reoxidised), without the need to accumulate GGH.

The effect of gradually increasing the GGH concentration with accumulation at -0.8 V is shown in Figure.5.7. The peak around -0.4 V is clearly seen for a ten and twenty fold ratio of GGH to copper(II) in the bulk solution, but at higher ratios still the first peak disappears whilst the second peak continues to increase in size. Note that the GGH to copper(II) ratio at the electrode surface during scan from 0 to -0.4 V will be considerably less than in the bulk solution owing to the formation of copper(Hg) at -0.8 V and its subsequent reoxidation to free copper(II) at the beginning of the scan from 0 V.

Nevertheless, at a sufficiently high GGH to copper(II) ratio in the bulk of the solution, the ratio at the electrode surface even after the above mentioned accumulation and subsequent reoxidation of copper(II) is evidently too high for the first peak to be formed. Note also that the suppression of the peak around -0.4 V coincides with the loss of the oxidation peak at -0.07 V on the anodic scan then the species responsible for the cathodic peak around -0.4 V is not formed and accumulated.



Therefore, it can be assumed that this species is a copper(I)-GGH complex which is formed on the surface of HMDE from the free copper(II) and copper(Hg). The fact that copper(I)-GGH complex is more easily reducible than copper(II)-GGH complex can be explained in terms of different structures of these complexes, copper(I) preferring coordination number two in complexes with monodentate imidazole<sup>57</sup> and some histidine derivatives<sup>58</sup>. To prove the assumption that copper(I)-GGH complex is responsible for the cathodic peak around -0.4 V, an attempt was made to prepare solution of copper(I)-GGH complex and investigate its polarographic and voltammetric behaviour. However, after addition of 20  $\mu$ l of  $1 \times 10^{-3}$  M copper(I) chloride solution to 20 ml of  $1 \times 10^{-4}$  M GGH in 0.1 M NaHCO<sub>3</sub>, only the cathodic peak around -0.6 V was observed. It means that the disproportionation of copper(I) into copper(0) and copper(II) is faster than the formation of copper(I)-GGH complex. Therefore, we have used 0.1 M NaHCO<sub>3</sub> solution in 1 M KCl, since it is well known that chloride ions stabilise copper(I). In this medium,  $5 \times 10^{-5}$  M copper(II) gives two waves with current sampled dc polarography. The first one, which coalesces with the dissolution of the mercury, corresponds to copper(II) to copper(I) reduction, while the second one, with a half wave potential around -0.2 V, corresponds to the reduction of copper(I)-chloride complex to copper(Hg). When a required amount of copper(I) solution is added to give  $5 \times 10^{-5}$  M solution just one wave around -0.2 V was observed corresponding to copper(I) to copper(Hg) reduction.

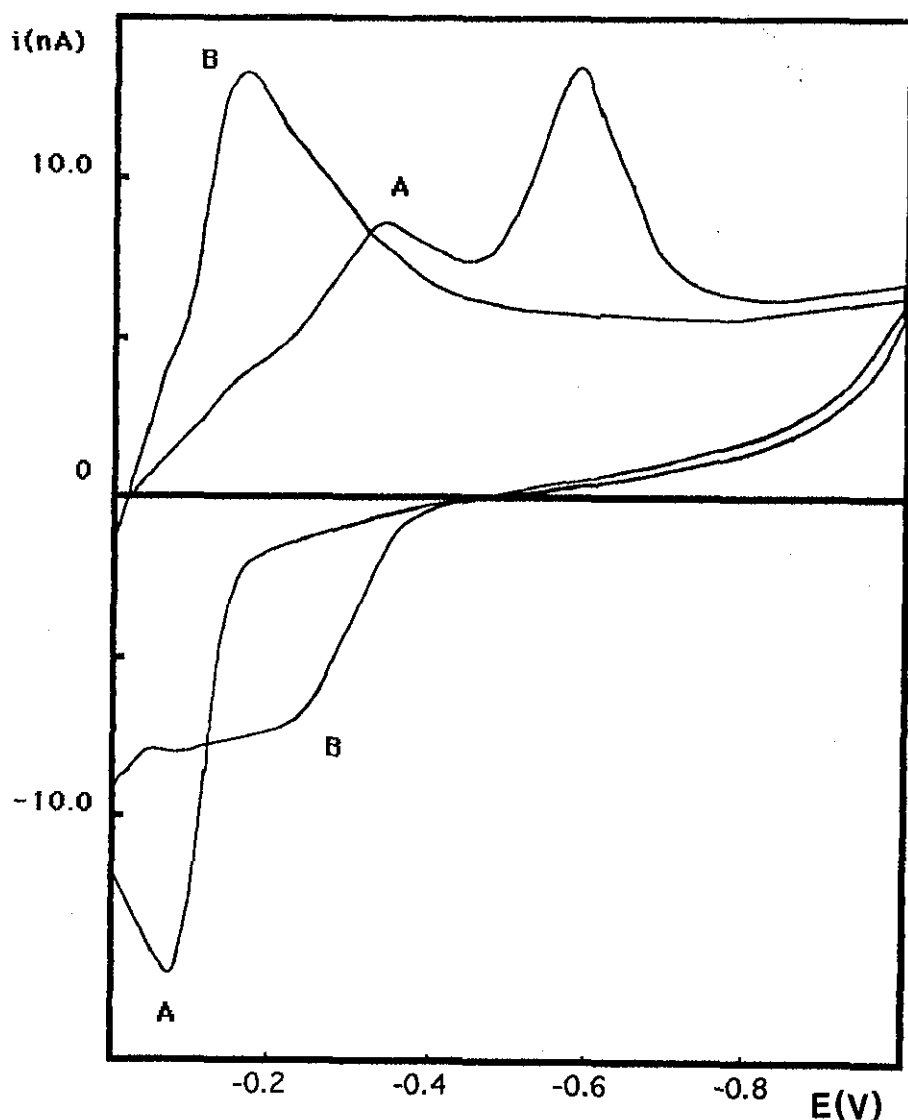


Figure 5.6- Effect of accumulating copper(II) in the absence of GGH. (A) Accumulation of  $5 \times 10^{-7}$  M copper(II) ions in the absence of GGH at -0.4 V for 2 min before going to open circuit, addition of  $1 \times 10^{-5}$  M GGH and then the potential was scanned from 0 V to -1.0 V at a scan rate of 50 mV/s. (B) The same but without addition of GGH.

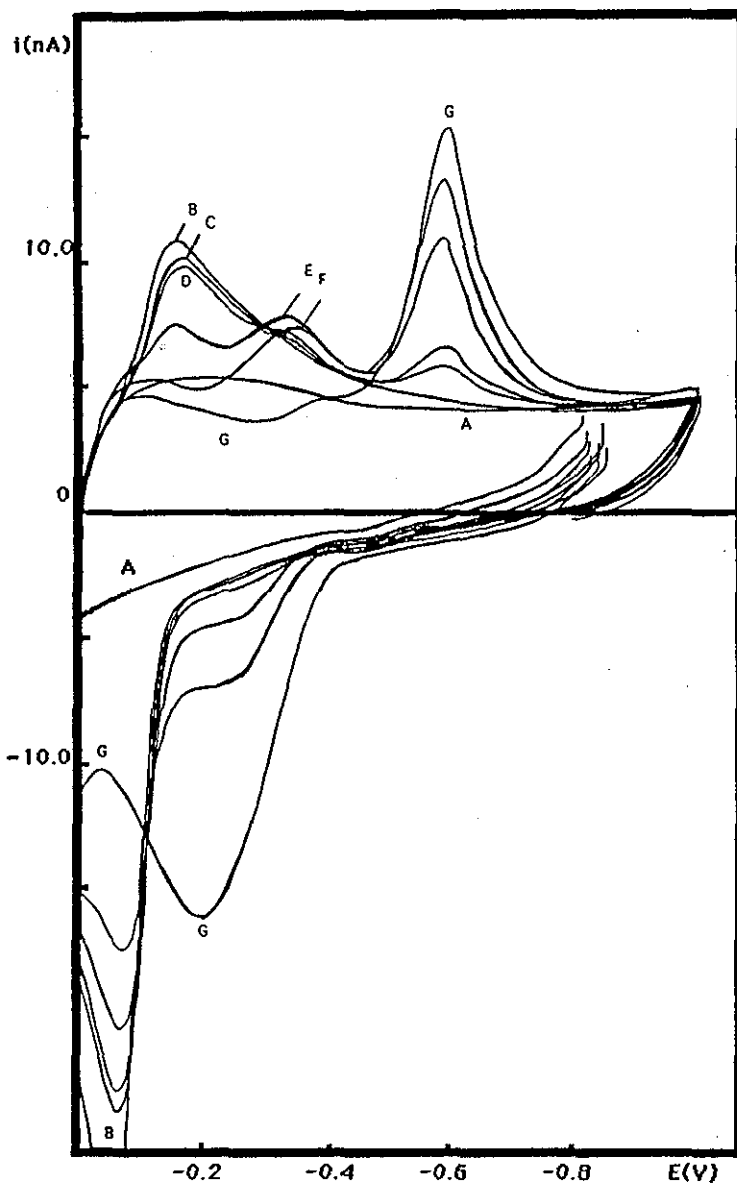


Figure 5.7- Effect of GGH concentration on the cyclic voltammograms of the complex system. Accumulation was performed at -0.8 V for 2 min before scanning to 0 V and back to -1.0 V. (A) Hydrogencarbonate solution only, (B-G)  $5 \times 10^{-7}$  M copper(II); GGH concentration : (B) 0; (C)  $5 \times 10^{-7}$ ; (D)  $1 \times 10^{-6}$ ; (E)  $5 \times 10^{-6}$ ; (F)  $1 \times 10^{-5}$ ; (G)  $5 \times 10^{-5}$  M.

Figure.5.8 shows that the half wave potential of this wave shifts towards more negative values by addition of GGH ( $E_{1/2} = -0.21, -0.23, -0.26$  and  $-0.30$  V in  $1 \times 10^{-5}, 2 \times 10^{-5}, 5 \times 10^{-5}$  and  $1 \times 10^{-4}$  M GGH respectively) and the wave height decreases as the result of lower diffusion coefficient of copper(I)-GGH complex as compared to that of free copper(I).

Cyclic voltammetry of  $1 \times 10^{-5}$  M copper(I) in 0.1 M  $\text{NaHCO}_3$  and 1 M KCl provided just one peak at  $-0.22$  V which obviously corresponds to copper(I) chloride complex reduction to copper(Hg) (Figure.5.9). After addition of GGH, a new cathodic peak around  $-0.3$  V was formed which obviously corresponds to the reduction of copper(I)-GGH complex to copper(Hg). Simultaneously, a cathodic peak around  $-0.5$  V corresponding to the reduction of copper(II)-GGH complex to copper(Hg) was observed, probably as the result of partial disproportionation of copper(I) to copper(0) and copper(II). The peaks around  $-0.2$  V and  $-0.3$  V are diffusion controlled as confirmed by the linear dependence of their height on the square root of the scan rate. On the contrary, the peak around  $-0.5$  V is adsorption controlled its height being proportional to the scan rate. After exposing the investigated solution to air oxygen, the height of the peak around  $-0.3$  V markedly decreased which confirms that this peak corresponds to easily oxidisable copper(I)-GGH complex. The fact that the adsorptive stripping voltammetric peaks of this complex are shifted towards more negative potentials as compared with cyclic voltammetric peaks confirms its strong adsorption on the surface of HMDE.

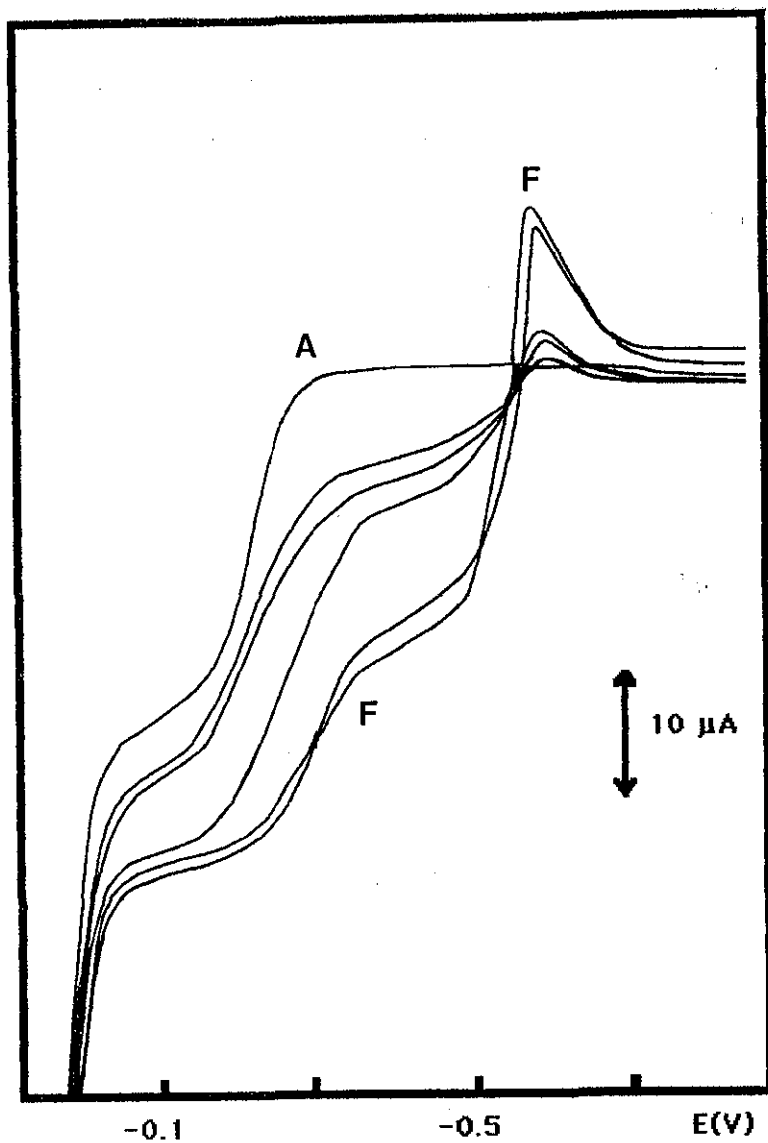


Figure 5.8 The influence of GGH addition to the polarographic behaviour of  $1 \times 10^{-5}$  M copper(I) in 0.1 M  $\text{NaHCO}_3$  containing 1 M KCl. (A) 0; (B-F)  $1-5 \times 10^{-5}$  M GGH.

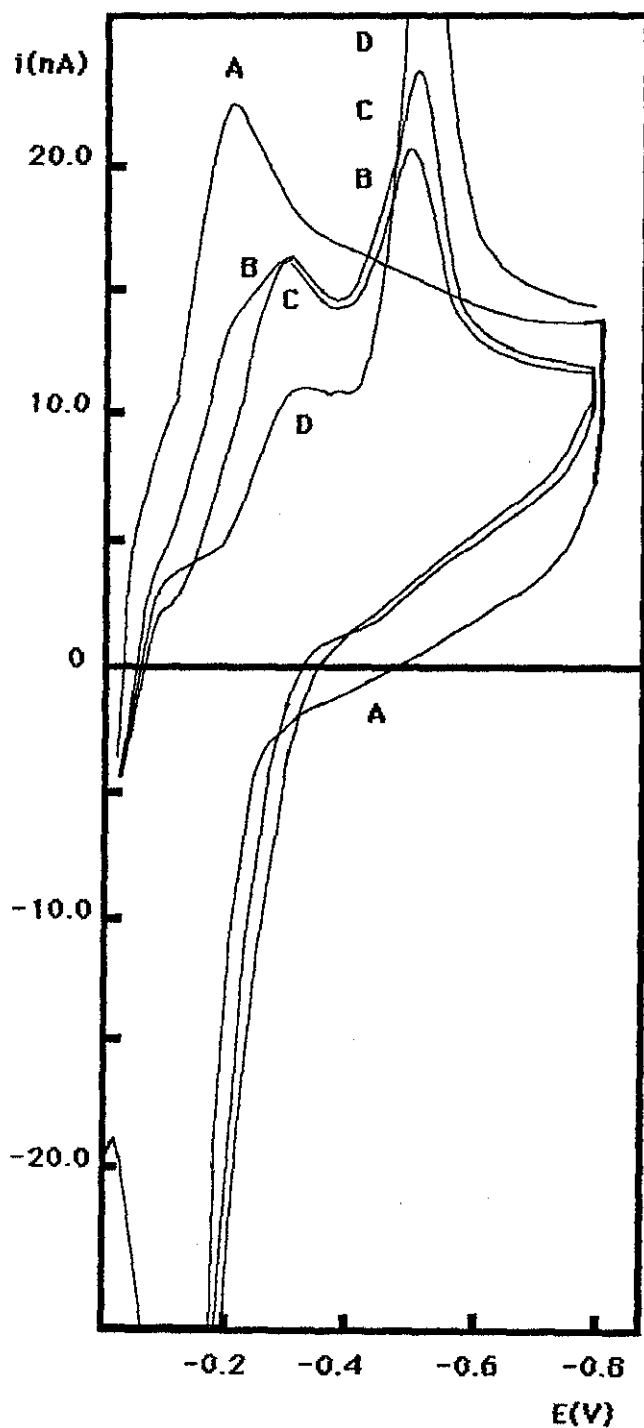


Figure.5.9- The influence of GGH concentration on the cyclic voltammogram of  $1 \times 10^{-5}$  M copper(I) in 0.1 M  $\text{NaHCO}_3$  containing 1 M KCl. (A) 0; (B)  $1 \times 10^{-5}$  M GGH; (C,D)  $2 \times 10^{-5}$  M GGH. (D) was recorded after exposing the solution to air oxygen for 5 min. Scan rate : 20 mV/s.

Adsorptive differential pulse cathodic stripping voltammetric determination of trace amounts of GGH

From the above data it follows that the copper(I)-GGH complex responsible for the peak around -0.4 V is only formed in the presence of excess of copper(II) ions. These are the conditions required for the adsorptive cathodic stripping determination of trace levels of GGH using adsorptive accumulation of the copper(I)-GGH complex at an HMDE. Some accumulation at 0 V of copper(I)-GGH complex was observed using these conditions, but significantly increased accumulation of the species responsible for the peak around -0.4 V was obtained using accumulation potentials very slightly more positive than its reduction potential. Note that differential pulse voltammetric peaks are shifted towards more positive potentials ( $E_p = -0.32$  V) as compared with cyclic voltammetric peaks in agreement with the theory<sup>1</sup>.

On the basis of preliminary investigations involving the influence of the accumulation time on the peak height, the following optimum conditions have been found for the determination of GGH in the concentration region  $(1-10) \times 10^{-8}$  M: 0.1 M  $\text{NaHCO}_3$  (pH 8.3) as a base electrolyte; concentration of copper(II)  $1 \times 10^{-6}$  M; accumulation potential -0.2 V; accumulation time 2 min in stirred solution. Figure 5.10 shows the adsorptive cathodic stripping voltammograms of GGH in  $1 \times 10^{-6}$  M copper(II) solution at pH 8.3. Thus obtained calibration curve is rectilinear with the slope 0.415 A/M and intercept 0.5 nA.

The effect of accumulation time on the peak height under the accumulation conditions is illustrated by the voltammograms in Figure.5.11; saturation of mercury drop is clearly approaching after 1 min accumulation at  $5 \times 10^{-8}$  M GGH concentration.

For the determination of GGH at even lower concentration, it was necessary to prolong the accumulation time to 3 min in stirred solutions keeping all other conditions as given above. The calibration curve thus obtained was again rectilinear in the concentration range of  $2-10 \times 10^{-9}$  M GGH with a slope of 1.40 A/M and the blank signal was 2.7 nA (Figure.5.12). The limit of detection calculated as three times the standard deviation of the determination of GGH at  $4 \times 10^{-9}$  M concentration was about  $3 \times 10^{-9}$  M. Coefficients of variation at the  $1 \times 10^{-8}$  M level are typically < 2% (5 determinations).



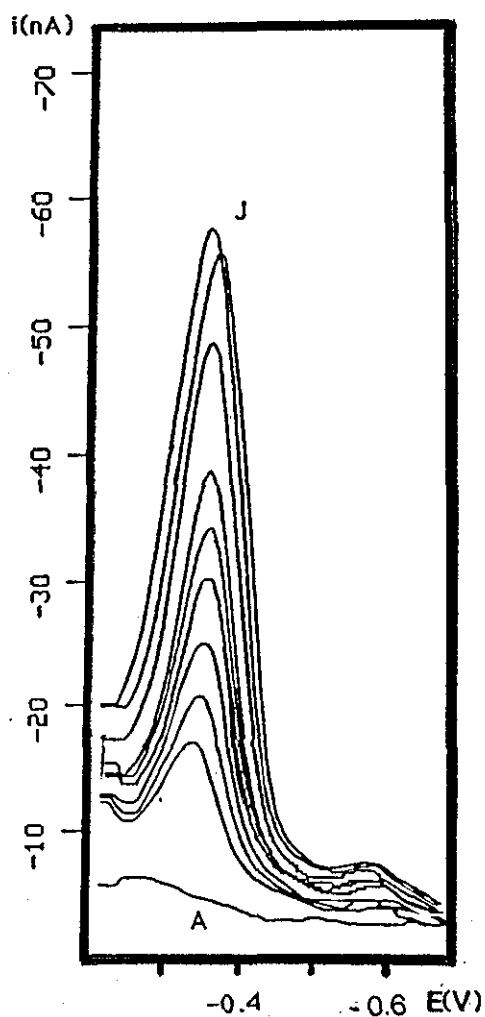


Figure.5.10- Voltammograms for obtaining a calibration graph for the determination of GGH. Accumulation was performed at  $-0.2$  V for 2 min; (A) Blank;  $0.1$  M  $\text{NaHCO}_3$  (pH 8.3) ; (B) 0; (C) 1; (D) 2; (E) 3; (F) 4; (G) 5; (H) 7; (I) 9; (J)  $10 \times 10^{-8}$  M GGH in the presence of  $1 \times 10^{-6}$  M copper(II).

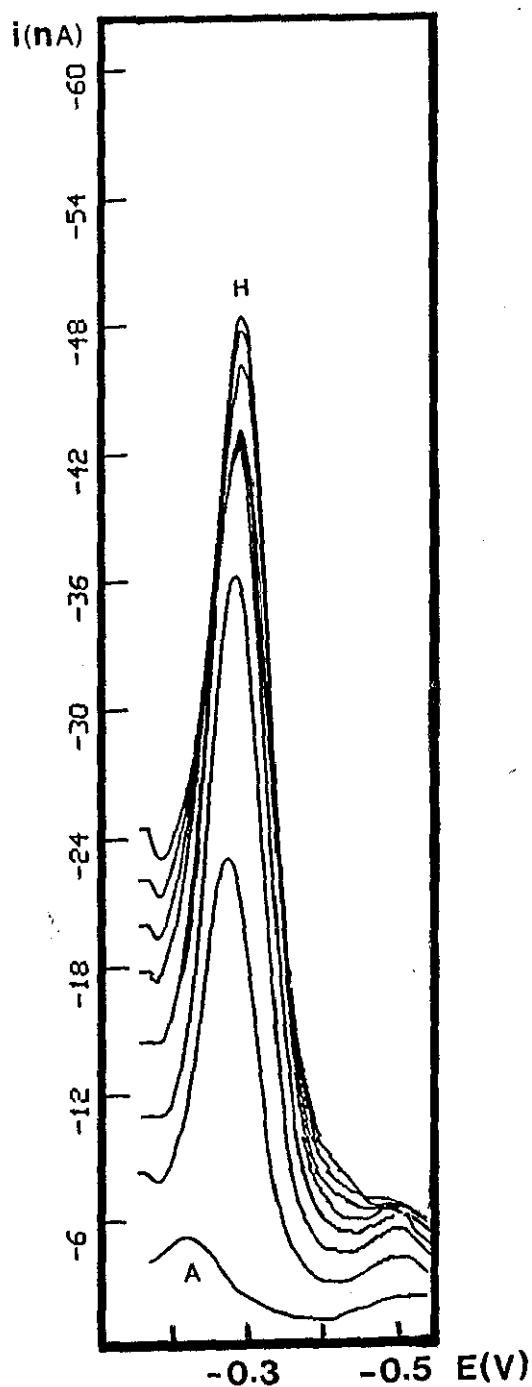


Figure.5.11- Effect of accumulation time under the conditions of GGH determination. Accumulation potential : -0.2 V; Initial concentrations : [Copper(II)] =  $1 \times 10^{-6}$  M, [GGH] =  $5 \times 10^{-8}$  M. Accumulation time : (A) 0; (B) 30; (C) 60; (D) 90; (E) 120; (F) 150; (G) 180 and (H) 210 s.

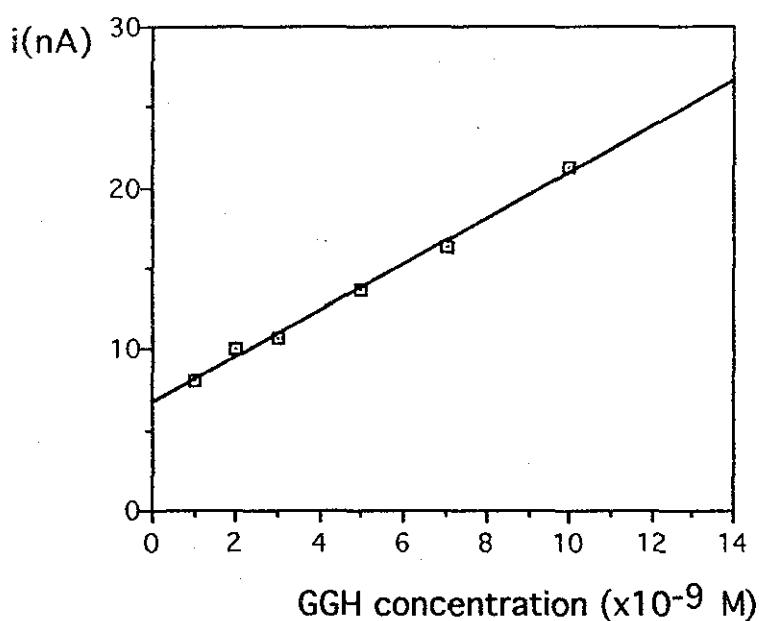


Figure.5.12- Calibration graph for the determination of GGH in the presence of  $1 \times 10^{-6}$  M copper(II). Accumulation was performed at -0.2 V for 3 min.

### Conclusion

Using adsorptive differential pulse cathodic stripping voltammetry, low levels of GGH down to  $3 \times 10^{-9}$  M were determined as copper(I)-GGH complex formed at the HMDE surface. Electroactive substances that are reduced at potentials around -0.4 V vs. Ag/AgCl reference electrode would interfere. Surface active agents interfere by inhibiting adsorption of copper(I)-GGH complex. Zinc and some other bivalent metals would interfere by competing with copper(I) for GGH<sup>18,19</sup> and some amino acids could interfere owing to

the adsorption of its copper(II) complexes<sup>47</sup>. This lack of selectivity inherent in most voltammetric techniques would require a preliminary separation step in the analysis of practical samples. However, the high sensitivity of the proposed method can be successfully exploited for the determination of low concentration of GGH in simple matrices which can be the case in many biologically relevant model studies involving this important tripeptide.

## CHAPTER 6

### ADSORPTIVE DIFFERENTIAL PULSE CATHODIC STRIPPING VOLTAMMETRIC DETERMINATION OF GLYCYL-L-HISTIDYL- GLYCINE AT A HANGING MERCURY DROP ELECTRODE USING ITS COPPER COMPLEXES

#### Introduction

The stability of copper(II) complexes with oligopeptides is considerably enhanced by the presence of histidyl residues in position three<sup>18,20</sup> because of a very strong tetradentate chelate formed. Similarly, the histidyl residue in the second position may lead to a strong tridentate chelate formation as demonstrated on glycyl-L-histidylglycine<sup>28</sup>. This tripeptide, because of its histidyl residue within the chain, is also important as a model for further studies involving the basic understanding of interaction between proteins and copper ions. For this reason, Cu(II)-GHG complexes were investigated as useful models for copper-protein interaction both in solution<sup>24,26,28,59,60</sup> and in a solid phase<sup>27</sup> (see chapter 2).

Therefore, it is quite clear that the position of histidyl residue in the oligopeptide molecule may cause remarkable differences in both the modes of their complex formation and their polarographic and voltammetric behaviour.

There are relatively few papers on the electrochemical behaviour of copper(II) complex of GHG. Takehara and Ide<sup>35</sup> reported a single predominant cathodic peak which corresponds to the reduction of copper(II) complex to copper amalgam for

complexes with glycyl-L-histidyl-L-lysine and glycyl-L-histidylglycine<sup>35</sup>. This is in agreement with the well known fact<sup>34</sup> that the electrochemical reduction of copper(II) preferentially occurs by two electrons to form copper amalgam. When complexation stabilises copper(I), however, this can give rise to a one-electron reduction of copper(II), occurring more readily than the two-electrons reduction. This results in two successive and distinct single electron transfer steps being obtained, as has been reported for copper(II) complexes of histidine and  $\beta$ -alanyl-L-histidine<sup>37</sup>.

So far, no detailed study of the adsorptive stripping behaviour of copper(II) complexes with GHG has been reported. For this reason the present study was carried out and its results are reported with the aim of increasing the understanding of the electrochemical behaviour of these biologically interesting systems and of developing a sensitive method for the cathodic stripping voltammetric determination of GHG which is itself polarographically inactive.

## Results and discussion

GHG was found to be electroinactive over the pH range of 5-12 in which range the 1:1 complex is known to be formed. Sampled dc polarograms of a solution containing  $1 \times 10^{-4}$  M copper(II) and five fold of GHG gives two waves which are not well separated at higher pH. Two main peaks were observed on differential pulse polarograms for the same solution. The peak potentials were shifting with pH from -0.15 to -0.20 V and from -0.36 to -0.47 V which corresponds to the half wave

potentials of the above mentioned dc polarographic waves. At a lower pH, the peak at -0.07 V corresponding to uncomplexed copper(II) was also observed. A polarographic maximum appeared around neutral pH which was easily removed by the addition of Triton X-100. The best developed and highest peaks were observed at pH around 8. Therefore, further studies were carried out using 0.1 M hydrogencarbonate solution (pH 8.3). The 1:1 copper(II) : GHG complex formation at pH 8.3 was confirmed by the fact that the height of the polarographic wave of  $1 \times 10^{-4}$  M solution of uncomplexed copper(II) decreased to one half in the presence of  $5 \times 10^{-5}$  M GHG and the uncomplexed copper(II) wave disappeared completely in the presence of equal amount of GHG (Figure.6.1).

#### Cyclic Voltammetric Behaviour of Copper Complexes of GHG

Stripping cyclic voltammograms obtained in a pH 8.3 hydrogen carbonate solution in the presence of various amounts of GHG are shown in Figure.6.2. Three cathodic peaks and three anodic peaks are observed, the exact position and height of which depend on both GHG and copper(II) concentration, potential and time of accumulation, and on the scan rate, direction and switching potentials of subsequent cyclic voltammetric scans. The reduction peak of free copper(II) (in the absence of GHG) appears at -0.12 V on cathodic scan and the most positive anodic reoxidation peak at -0.07 V can be assigned to reoxidation of copper amalgam back to free copper(II).

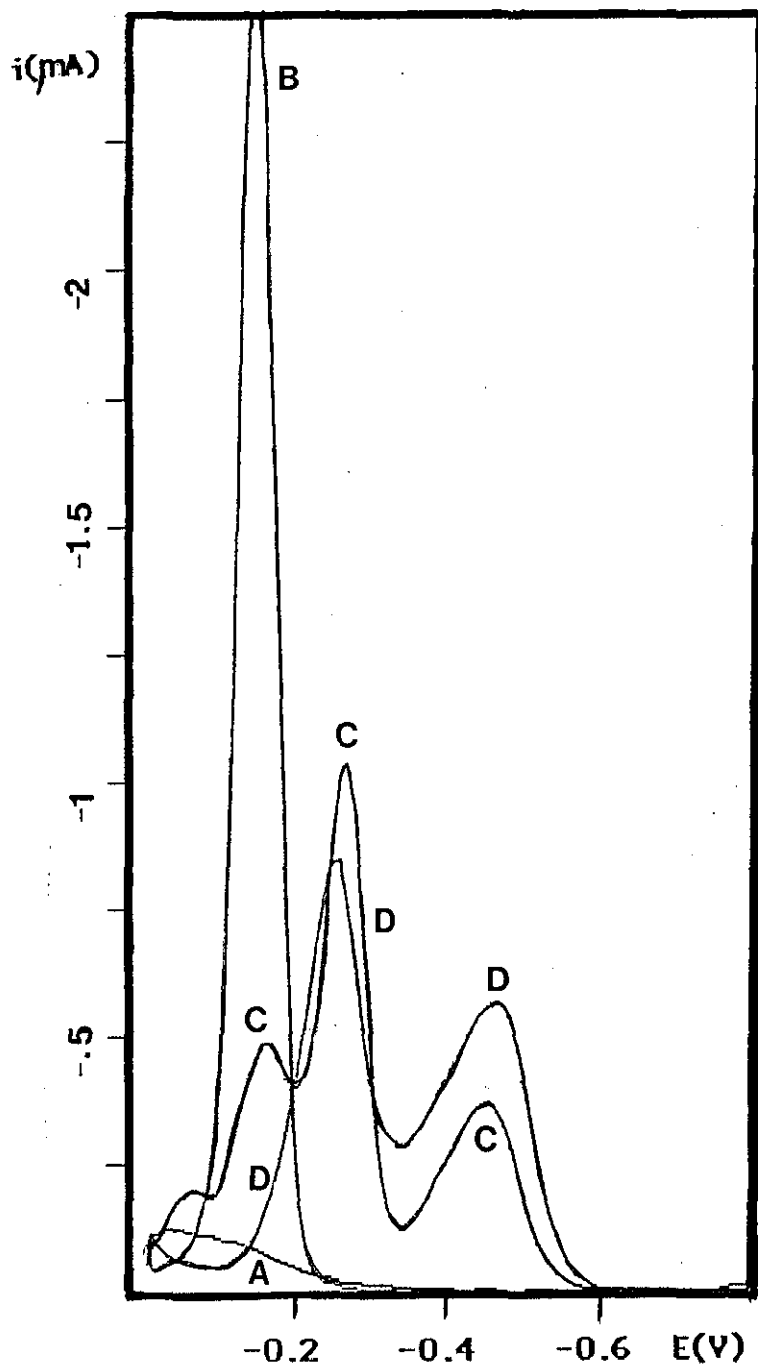


Figure.6.1- The dp polarographic behaviour of  $1 \times 10^{-4}$  M copper(II) (B-D) at an SMDE in the presence of (B) 0; (C)  $5 \times 10^{-5}$  M; (D)  $1 \times 10^{-4}$  M GHG. (A) : 0.1 M  $\text{NaHCO}_3$  only (pH 8.3).



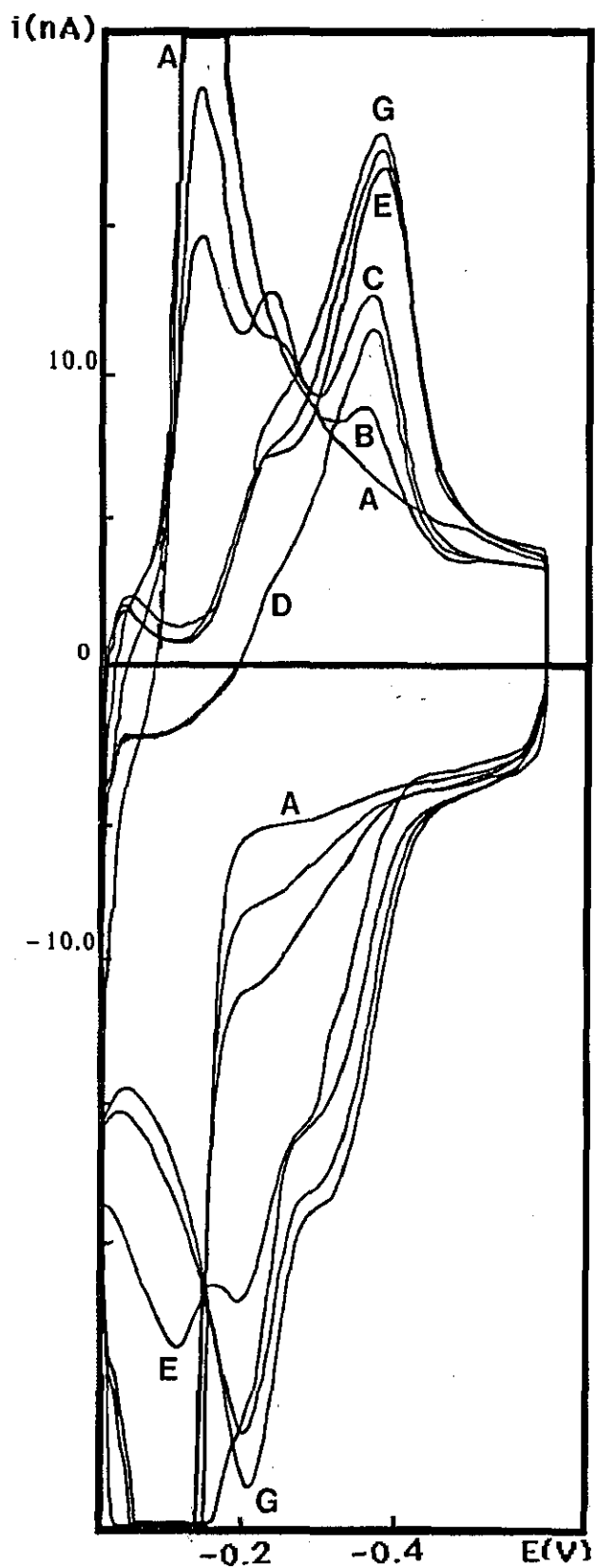


Figure.6.2- Effect of GHG concentration on the cyclic voltammograms of  $1 \times 10^{-6}$  M Cu(II) at pH 8.3 in the presence of (A) 0; (B)  $2.5 \times 10^{-6}$  M; (C)  $5 \times 10^{-6}$  M; (D)  $1 \times 10^{-5}$  M; (E)  $2 \times 10^{-5}$  M; (F)  $3 \times 10^{-5}$  M and (G)  $4 \times 10^{-5}$  M GHG. Scan rate 50 mV/s; Accumulation was performed at -0.6 V; for 2 min.

On the basis of dc and dp polarographic behaviour of copper(II)-GHG complex, the second peak around  $-0.2$  V and the third cathodic peak around  $-0.35$  V can be assigned to a stepwise one electron reduction of copper(II)-GHG complex to copper(I)-GHG complex (peak around  $-0.2$  V) followed by the reduction of copper(I)-GHG complex to copper amalgam (peak around  $-0.35$  V). The morphology of the observed peaks and their dependence on the scan rate suggest that the first cathodic and the most positive anodic peak correspond to a diffusion controlled process, while the second and third cathodic peak together with the remaining anodic peaks correspond to the reduction and/or oxidation of adsorbed species. This assignment is in agreement with the reported electrochemical evidence for the generation of copper(I) complex as an intermediate in the reduction of Cu(II) complexes with glycine<sup>47</sup> and with histidine and carnosine<sup>37</sup> with described polarographic behaviour of copper(I)-histidine complex<sup>51</sup>.

Effect of accumulation potential shown in Figure.6.3 proves that the third peak around  $-0.35$  V is very small at accumulation potentials more positive than  $-0.3$  V which supports the assumption that it corresponds to a species formed at the electrode surface at potentials between  $-0.2$  V and  $-0.3$  V. Furthermore, it is clear that during accumulation at  $-0.1$  V and  $-0.2$  V no copper amalgam is formed since no anodic peak at  $-0.07$  V during subsequent anodic scan can be seen. Therefore, the product of the reduction of copper(II)-GHG complex at  $-0.2$  V is not copper amalgam which was further proved by an experiment with medium exchange. In this

experiment, after accumulation at  $-0.25$  V in the solution containing  $1 \times 10^{-5}$  M GHG and  $1 \times 10^{-6}$  M Cu(II), the HMDE was transferred to the solution containing only  $0.1$  M  $\text{NaHCO}_3$  solution and anodic scan was initiated. No anodic peak indicating the dissolution of Cu(Hg) could be detected. However, the peak around  $-0.35$  V is clearly seen after accumulation at  $-0.25$  V. It means that the species formed at  $-0.25$  V can be further reduced which supports the assumption that second and third peak correspond to a stepwise one-electron reduction of Cu(II)-GHG complex. To establish the nature of the anodic peaks, a medium exchange experiment was carried out using accumulation potential  $-0.7$  V. After accumulating  $1 \times 10^{-5}$  M copper(II) solution in the presence of excess of GHG ( $1 \times 10^{-4}$  M) and transferring the HMDE into a solution containing only hydrogencarbonate solution, only the peak at  $-0.07$  V corresponding to the reoxidation of copper amalgam was observed during subsequent anodic scan. Therefore, it can be assumed that copper amalgam is formed at  $-0.6$  V while GHG is not adsorbed sufficiently strongly at this potential (a repulsion of negatively charged GHG molecules from the negatively charged HMDE surface can play a role) and is removed during medium exchange. This medium exchange experiment confirms that the third cathodic peak around  $-0.35$  V can be assigned to the reduction of copper(I)-GHG complex to copper amalgam. Figure.6.4 shows the cyclic voltammogram of solution given above with and without medium exchange for comparison.

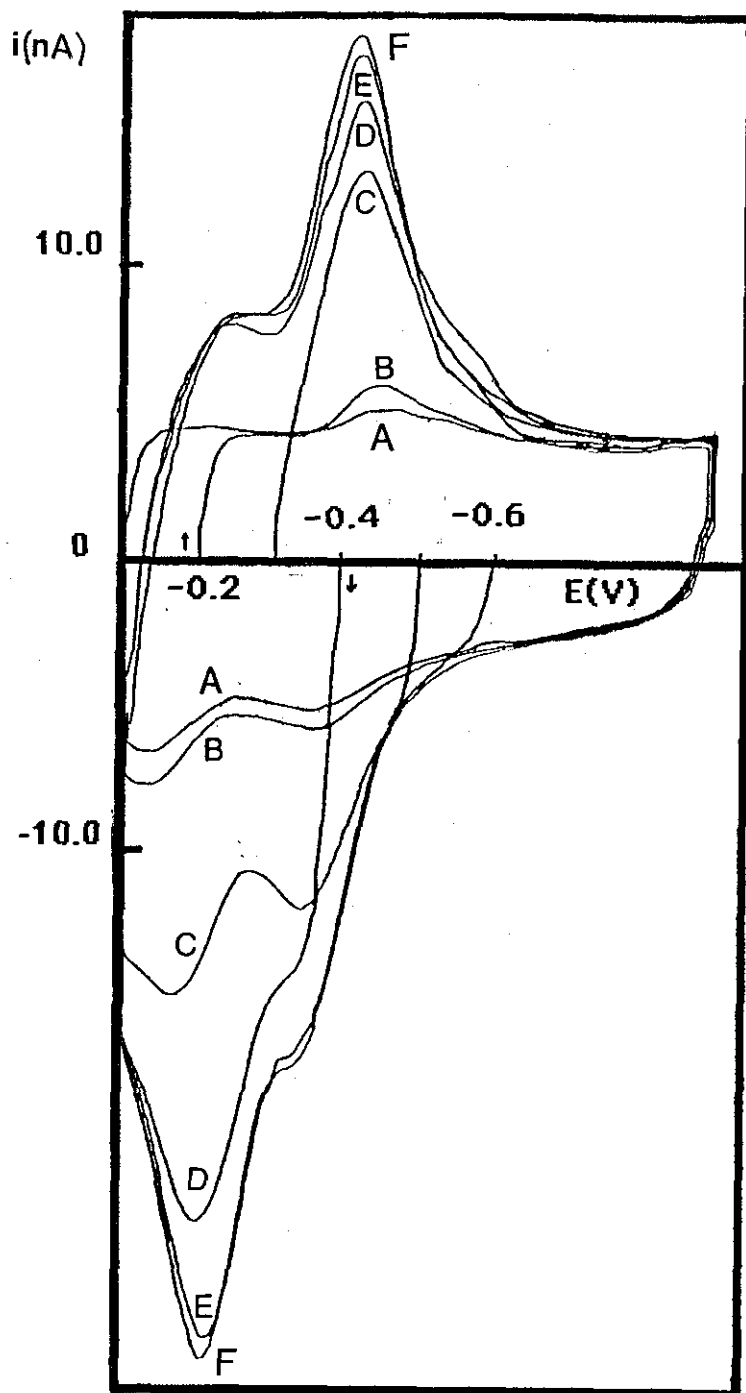


Figure.6.3- Effect of accumulation potential on the cyclic voltammograms of  $1 \times 10^{-6}$  M Cu(II) in the presence of  $1 \times 10^{-5}$  M GHG at pH 8.3. Accumulation time is 2 min at potential: (A) -0.1 V; (B) -0.2 V; (C) -0.3 V; (D) -0.4 V; (E) -0.5 V; (F) -0.6 V. Scan rate is 50 mV/s.

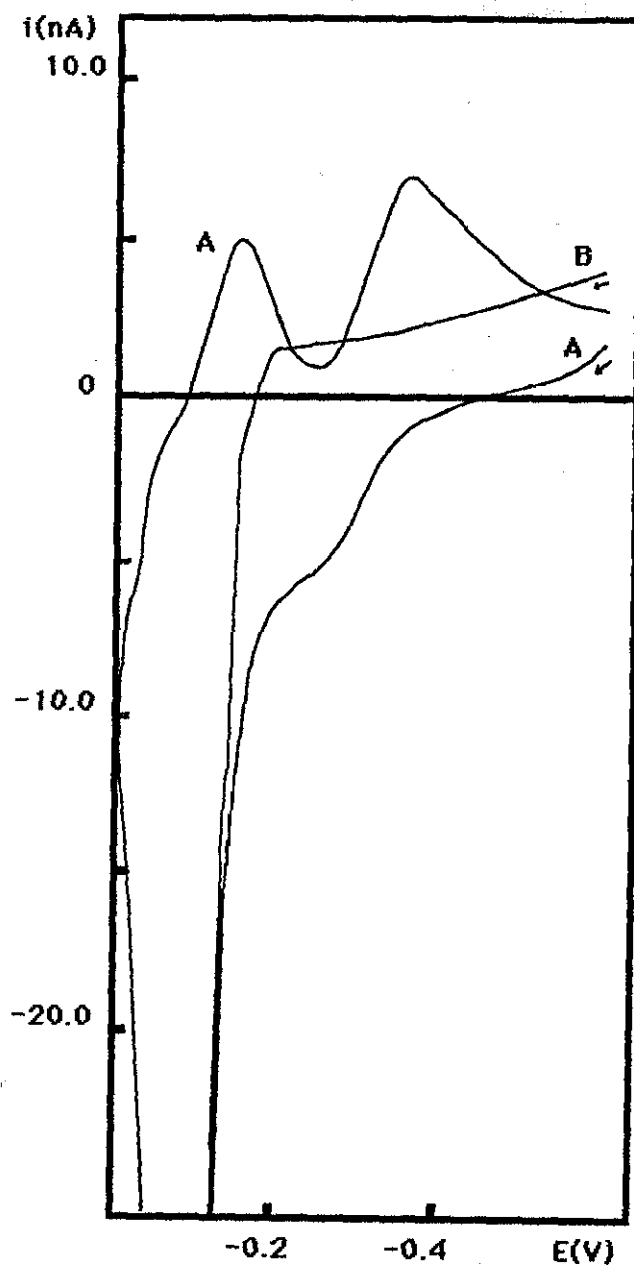


Figure.6.4- Cyclic voltammogram of  $1 \times 10^{-5}$  M copper(II) in the presence of  $1 \times 10^{-4}$  M GHG in 0.1 M  $\text{NaHCO}_3$  solution. Scan was initiated from -0.6 V, where accumulation was performed, to more positive potentials and then to -0.6 V for (A). The HMDE was transferred in 0.1 M  $\text{NaCO}_3$  solution after accumulation step and before the anodic scan for (B).

A similar medium exchange experiment using accumulation of copper amalgam at  $-0.7$  V in the absence of GHG followed by anodic scan after addition of GHG clearly showed that anodic peaks around  $-0.2$  V and  $-0.3$  V can be assigned to a stepwise oxidation of copper amalgam to copper(II)-GHG complex via copper(I)-GHG complex.

The cyclic voltammograms in Figure.6.5 show that the accumulation at  $-0.7$  V in a solution containing 1:10 metal ion to ligand concentration ratio yields two reduction peaks at about  $-0.19$  and  $-0.36$  V developing with collection time in the range of 0-120 s. The relative position of these cathodic and anodic peaks indicate a high degree of irreversibility of both copper(II)-GHG / copper(I)-GHG and copper(I)-GHG / copper (Hg) systems. A small shift in the peak potential of the more positive anodic peak from  $-0.16$  to  $-0.22$  V with increasing accumulation time can be explained by increasing concentration of GHG adsorbed on the HMDE surface. When the accumulation was performed at 0 V, only very small cathodic and anodic peaks were observed. The height of these peaks did not increase with increasing accumulation time thus confirming our assumption on the nature of these peaks.

Multiple scan cyclic voltammograms after accumulation at  $-0.1$  v and  $-0.7$  V are shown in Figure.6.6. After accumulation at  $-0.1$  V, only negligible cathodic peaks were observed during first cathodic scan (see Figure.6.6a). Anodic peaks during first anodic scan were much higher than cathodic peaks thus confirming the assumption that copper amalgam is accumulated during scan at potentials more negative than that

of the cathodic peak around  $-0.35$  V. This assumption is further confirmed by the observed increase of all cathodic and anodic peaks with subsequent scans.

On the other hand, it is possible that copper(I)-GHG complex can be formed at the HMDE surface not only as an intermediate of the reduction of copper(II)-GHG complex to copper amalgam but also via reaction of copper amalgam with copper(II)-GHG complex. The decreasing height of all observed cathodic and anodic peaks with subsequent scans after accumulating at  $-0.7$  V (see Figure.6.6b) can be explained by the desorption of accumulated species at switching potentials which are sufficiently far away from the potential of electrocapillary zero where maximum adsorption of the metal-peptide complexes is expected to occur.

Somewhat different adsorptive stripping voltammetric behaviour of the copper(II)-GHG complexes at pH 10.5 (see Figure.6.7) can be explained by changes in the structure of these complexes with increasing pH<sup>18,24,26,28,59</sup>. Only two peaks at  $-0.29$  V and  $-0.46$  V were observed without accumulation. By increasing the collection time from 30 s to 2 min both peaks were decreased in height and another peak at  $-0.57$  V appeared in addition to the baseline increase at potentials more positive than that of the first peak. This effect can be caused by adsorption of excess of GHG itself on the mercury drop and thickening film formation on the surface by increased collection time reduce the adsorption the complex. Therefore, a hydrogencarbonate solution (pH 8.3) is to be preferred for the analytical applications.

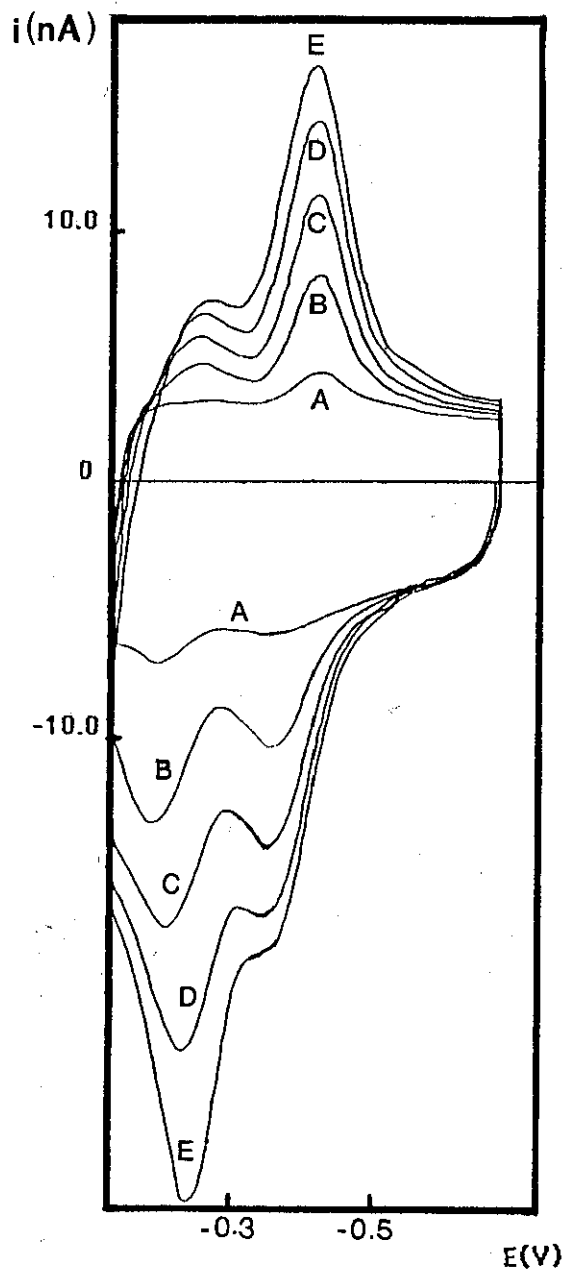


Figure.6.5- Effect of accumulation time on the cyclic voltammograms of  $1 \times 10^{-6}$  M Cu(II) in the presence of  $1 \times 10^{-5}$  M GHG at pH 8.3. Scan rate : 50 mV/s; Accumulation potential: -0.7 V; accumulation time : (A) 0 s; (B) 30 s; (C) 60 s; (D) 90 s; (E) 120 s.



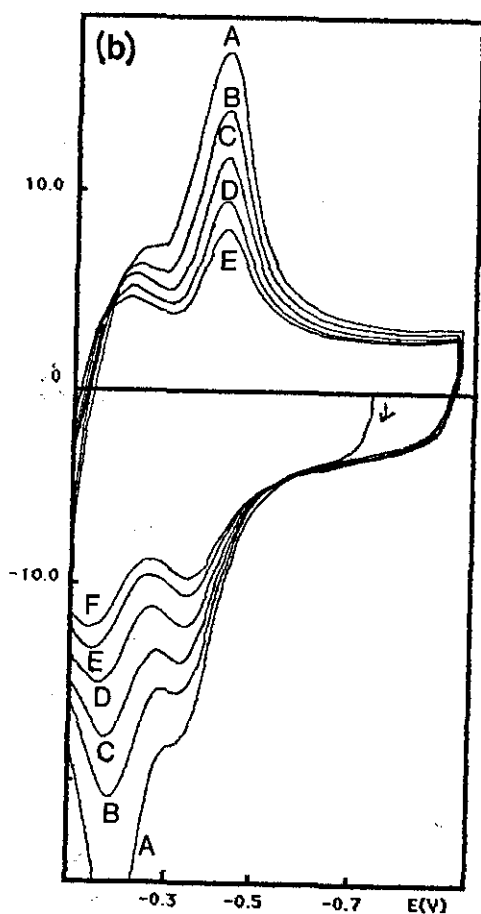
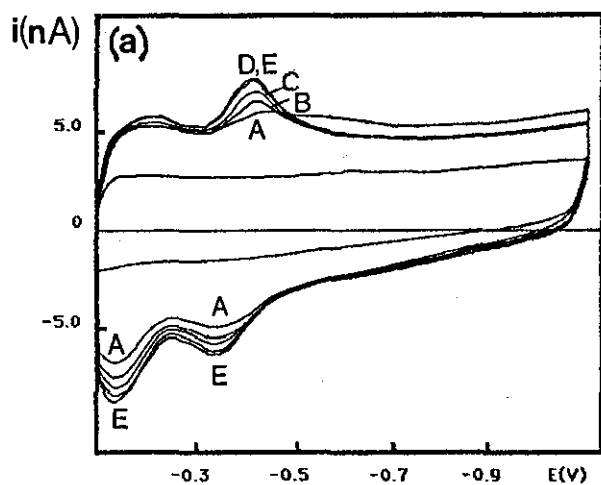


Figure.6.6- Effect of accumulation potential on multiple scan cyclic voltammograms of Cu(II)-GHG complexes.  $1 \times 10^{-6}$  M Cu(II);  $1 \times 10^{-5}$  M GHG; pH 8.3; scan rate 50 mV/s; accumulation time 2 min in stirred solutions; accumulation potential (a) -0.1 V and (b) -0.7 V. The numbers indicate scan numbers.

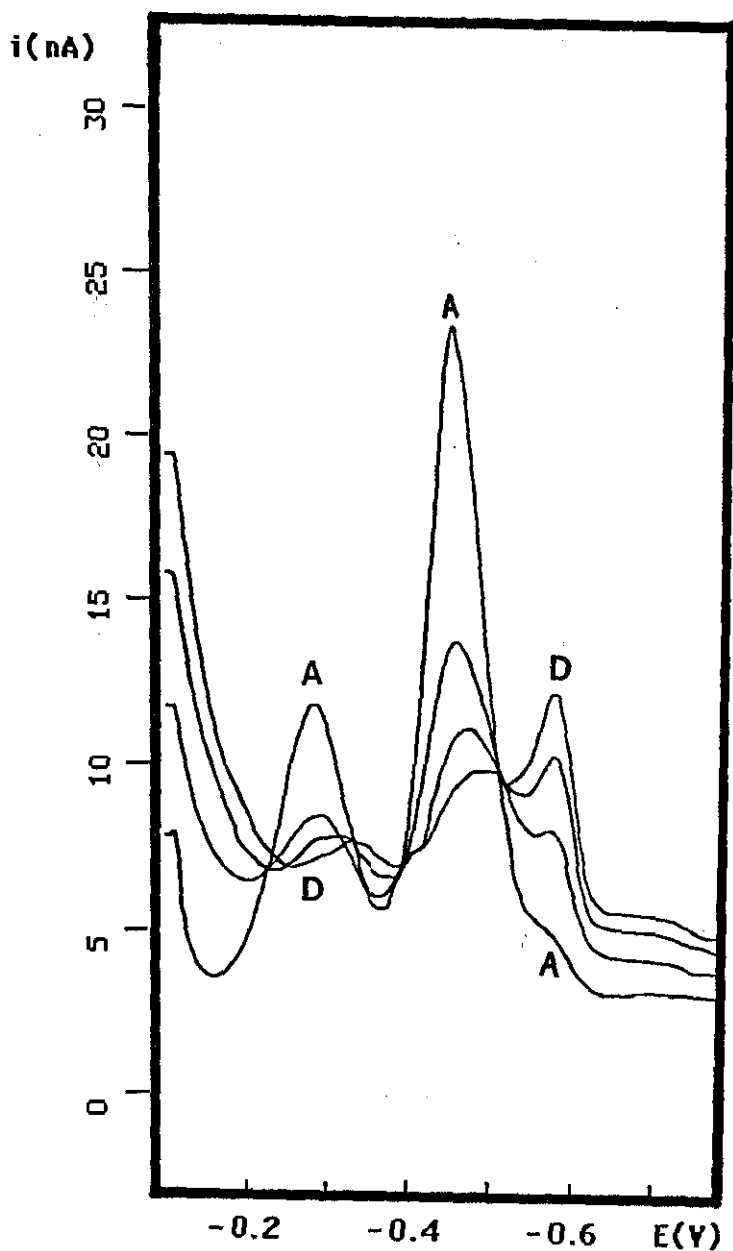


Figure.6.7- Adsorptive differential pulse cathodic stripping voltammograms of  $1 \times 10^{-6}$  M Cu(II) in the presence of  $1 \times 10^{-4}$  M GHG in 0.1 M borate buffer (pH 10.5); scan rate 50 mV/s; modulation amplitude -50 mV; accumulation potential -0.1 V; accumulation time (A) 0; (B) 15 s; (C) 30 s; (D) 60 s.

Adsorptive differential pulse cathodic stripping voltammetric determination of GHG

Hydrogencarbonate solution (pH 8.3) was used for this determination since it gives a smaller background current in the presence of excess of copper(II). In a solution containing  $1 \times 10^{-6}$  M copper(II) and  $1 \times 10^{-7}$  M GHG and using the accumulation potential -0.2 V, the height of the peak around -0.3 V increases rectilinearly with the accumulation time up to 3 min, the peak potential shifting from -0.27 V to -0.31 V with increasing accumulation time.

It should be noted that in the presence of  $1 \times 10^{-6}$  M copper(II) and equal amount of GHG under otherwise identical conditions, the height of the peak around -0.35 V is not a linear function of the accumulation time thus indicating the saturation of the HMDE surface. Under these conditions, the peak potential shifts from -0.24 V to -0.27 V with accumulation time increasing from 15 s to 2 min. note that differential pulse voltammetric peaks are shifted towards more positive potentials as compared with cyclic voltammetric peaks in agreement with the theory<sup>1</sup>.

On the basis of the above results, the optimum conditions have been chosen for the determination of GHG : 0.1 M NaHCO<sub>3</sub> (pH 8.3) as a base electrolyte; concentration of copper(II)  $5 \times 10^{-6}$  M; accumulation potential -0.2 V vs Ag/AgCl reference electrode; accumulation time 2 min in stirred solutions; the height of the peak at -0.37 V was evaluated which corresponds to the reduction of copper(I)-GHG to copper amalgam.

Figure.6.8 shows the voltammetric curves of the GHG complex in the concentration region of  $1-6 \times 10^{-7}$  M. For more sensitive region ( $1-12 \times 10^{-8}$  M) calibration curves were rectilinear with the slope 0.10 A/M and intercept 0.2 nA (Figure.6.9). Coefficients of variation at the  $2 \times 10^{-8}$  M level are typically < 3% (5 determinations). The limit of detection calculated as three times the standard deviation of the determination of GHG at  $2 \times 10^{-8}$  M level was about  $5 \times 10^{-9}$  M.

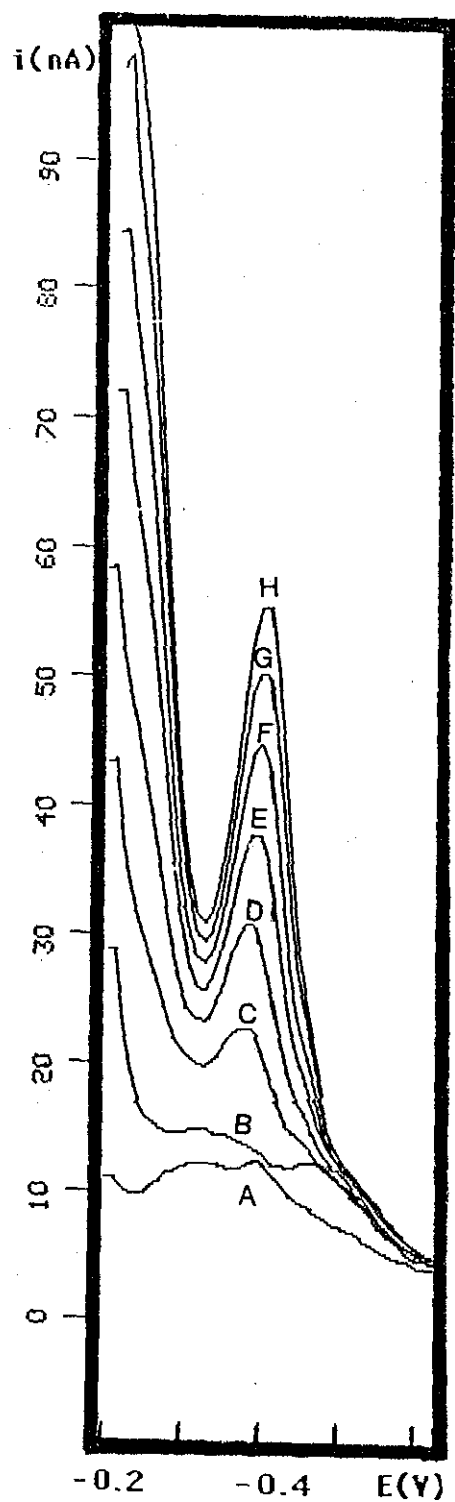


Figure.6.8- AdCS dp voltammetric curves obtained for the determination of GHG. (A) : 0.1 M  $\text{NaHCO}_3$ , (B)-(H)  $5 \times 10^{-6}$  M copper(II) in the presence of (C-H)  $1-6 \times 10^{-7}$  M GHG.

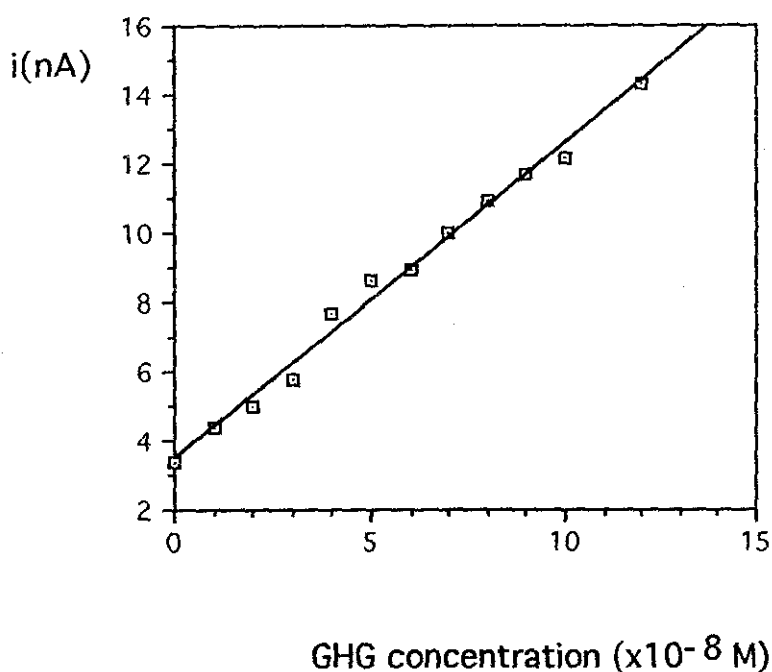


Figure.6.9- Calibration graph for GHG determination in  $5 \times 10^{-6}$  M copper(II) at pH 8.3. Accumulation potential : -0.25 V; accumulation time :2 min.

### Conclusion

Sampled dc polarographic, cyclic voltammetric and adsorptive stripping voltammetric behaviour of the copper(II)-GHG complex described above has some different characteristics from the copper(II)-GGH complex in terms of the peak potentials and the position, number and nature of both reduction and oxidation peaks. Nevertheless, the peak around -0.35 V can be used for very sensitive adsorptive differential pulse cathodic stripping voltammetric determination of

polarographically inactive GHG. The selectivity of this determination is limited by the interference surface active substances which can form complexes either with copper(II) (such as some amino acids<sup>36,47</sup> or peptides<sup>33-35</sup>) or with GHG (such as some other bivalent cations<sup>18,19</sup>). A preliminary separation step would be required in the presence of these interferents. However, in many model biological studies in a simple matrix, the developed method can provide a very sensitive tool for the determination of trace amounts of GHG. Furthermore, it was confirmed by the present study, that adsorptive stripping voltammetry can give us a useful insight into the redox behaviour of biologically interesting complexes of copper with various oligopeptides adsorbed on the electrode surface of the HMDE which can mimic a hydrophobic physiological redox site. It can be expected that further relevant information, clarifying the role of Cu(II)-peptides complexes in redox processes in biological systems, can be obtained in this way.

## CHAPTER 7

### CATHODIC STRIPPING BEHAVIOUR OF GLYCYL-L-HISTIDINE AND L-HISTIDYLGLYCINE AT A HANGING MERCURY DROP ELECTRODE IN THE PRESENCE OF COPPER(II) IONS

#### Introduction

Studies on the copper complexes of histidyl peptides have revealed useful information regarding the geometry of the complexes formed and the coordination by peptides as models of the metal ion binding site of bioactive peptides and proteins. Tripeptides containing histidyl residue have exhibit different electrochemical behaviour as indicated in the previous chapters. Similarly the dipeptides Glycyl-L-histidine (GH) and L-Histidylglycine (HG) having the histidyl residue in different positions may give interesting results. The coordination structures of these dipeptide complexes have been established mainly by means of potentiometric titration<sup>18</sup>. GH was reported to have similar  $pK_a$  values and to bind in a similar manner to GHG through imidazole, peptide and amino nitrogens (see Chapter 2).

There are relatively few reports based on electrochemical behaviour of the copper complexes of these peptides. Takehara and Ide<sup>35</sup> studied the cyclic voltammetric behaviour of the copper(II) complexes of GHL, GHG and GH in aqueous solution by various electrochemical methods. Only one cathodic peak was observed ( at around -0.3 V) for these peptide complexes and



this was assigned to the reduction of the copper(II) complex by loss of the coordinated peptide and amalgam formation.

In this chapter, the cathodic stripping voltammetric behaviour of copper complexes of GH and HG at an HMDE is reported and a very sensitive dp cathodic stripping determination method is described for use in simple matrixes.

## Results and Discussion

GH and HG were found to be electroinactive over the pH and potential range studied. The nature of the copper complexes of these peptides was investigated using polarography and stripping and cyclic voltammetry preceded by accumulation at various potentials.

The differential pulse polarographic behaviour of the copper complexes of these dipeptides was investigated in the pH range 6.0 to 12.0. For the copper complex of HG the first peak appeared in basic medium at -0.35 V while the second one was shifting from -0.41 V to -0.57 V as the pH was increased in the range studied. For both complex systems the free copper(II) reduction peak was observed at more positive potential in neutral solution. The width of the HG complex peaks at half height are about 90 mV indicating a one electron reduction for each peak<sup>6</sup>. However, the pulse height is comparable to the width at the half height.

Two dpp peaks were observed for  $1 \times 10^{-4}$  M copper(II) in the presence of a five fold concentration of GH. Over the pH range the peak potentials changed from -0.18 V to -0.31 V for the

first peak and from -0.28 V to -0.54 V for the second peak. One to one complex formation was confirmed at pH 8.3 hydrogen carbonate solution as the reduction peak of copper(II) at -0.08 V was halved by addition of  $5 \times 10^{-5}$  M GH into a  $1 \times 10^{-4}$  M copper(II) solution and two complex peaks were observed. The free copper(II) reduction peak disappeared completely on adding an equal concentration of ligand.

#### Cyclic voltammetric studies

Cyclic voltammograms recorded at an HMDE for copper(II) ions in solutions containing HG and GH show similarity in behaviour of the complex peaks of these two dipeptides in different pH, accumulation potential and ligand concentration. Figure.7.1 shows the cyclic voltammograms for the HG system at pH 8.3 with an increasing excess of the ligand and illustrates the effect of ligand addition on a solution of  $5 \times 10^{-7}$  M copper(II). The accumulation was effected at -0.4 V for 2 min and the potential was scanned between 0 and -0.7 V. Two reduction peaks were observed at -0.23 V and -0.35 V on the loss of the free copper (II) peak at -0.12 V. Two anodic peaks associated with these cathodic complex peaks are apparent on the reverse scan. An 8:1 ratio of GH to copper(II) is required for the free copper(II) peak to be eliminated.

The effect of accumulation potential on the cyclic voltammetric behaviour of the HG complex is shown in Figure.7.2. The cycle was initiated from the accumulation potential and the potential was scanned first to 0 V and then to the negative values. Only a small second peak can be seen

when the accumulation was made at 0 V. This peak increases in height as the accumulation potential is made more negative, and the first peak begins to appear when accumulation is affected at -0.2 V. The first peak becomes predominant at more negative accumulation potentials. The free copper(II) peak is not apparent in these voltammograms, even with accumulation at potentials where complexed HG is reduced to copper(Hg) : clearly during the initial anodic scan the copper is reoxidised to a complex state. When, after accumulation, the potential is switched directly to 0 V (Figure.7.1) the free copper(II) is more readily formed, particularly at low peptide concentrations.

The effect of accumulation time at -0.4 V, with switching to 0 V, is shown in Figure.7.3. After an initial main increase in the height of the first peak, the second peak begins to increase in size : the second peak approaches a maximum size as the first peak grows. For the same solution system with accumulation and multiple scanning from 0 V, formation and an increase in the second peak is observed with increasing scan number (Figure.7.4) but signs of the first peak -particularly its anodic peak - are apparent at the slower scan speed.

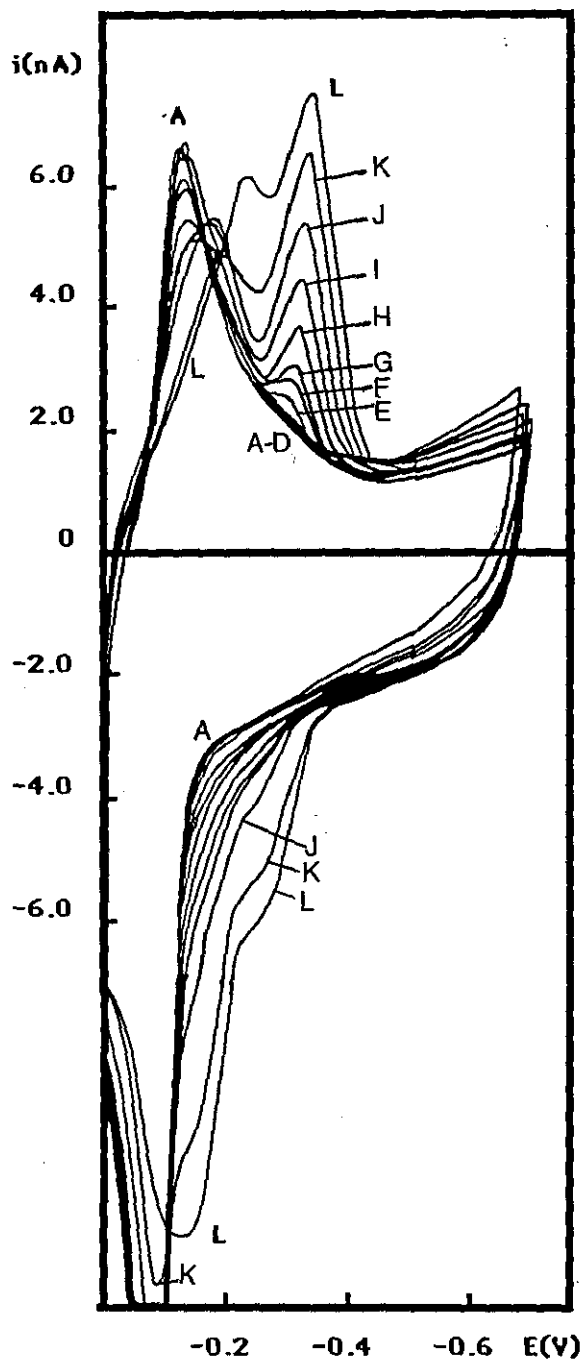


Figure.7.1- The cyclic voltammograms of copper(II)-HG complex system at pH 8.3. Accumulation potential : -0.4 V, accumulation time:120 s. Scan rate: 20 mV/s. (A) copper(II) only ( $5 \times 10^{-7}$  M); HG concentration : (B) 1; (C) 2; (D) 3; (E) 5; (F)  $7 \times 10^{-7}$ ; (G) 1; (H) 1.5; (I) 2; (J) 3; (K) 4 and (L)  $5 \times 10^{-6}$  M.

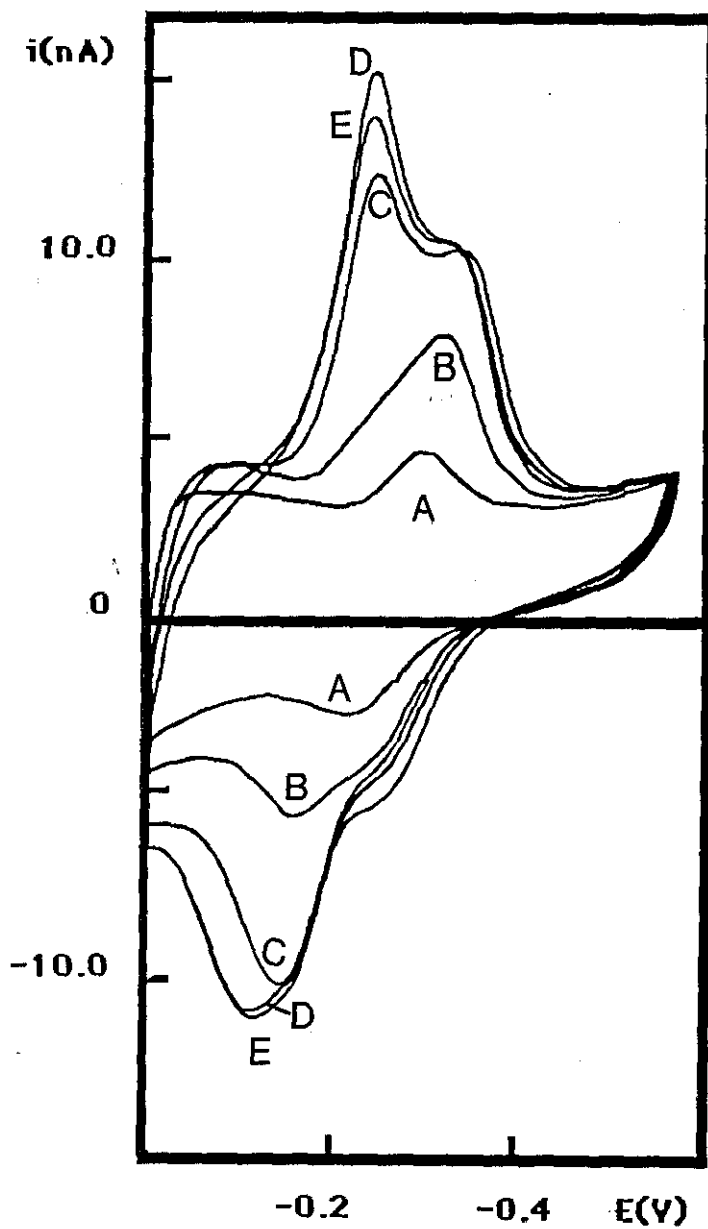


Figure.7.2- The effect of accumulation potential on the cyclic voltammograms of copper complexes of HG at pH 8.3. Initial concentrations : [Copper(II)] =  $5 \times 10^{-7}$  M; [HG] =  $1 \times 10^{-5}$  M. Accumulation was performed for 120 s at potentials : (A) -0.1; (B) -0.2; (C) -0.3; (D) -0.4 and (E) -0.5 V.

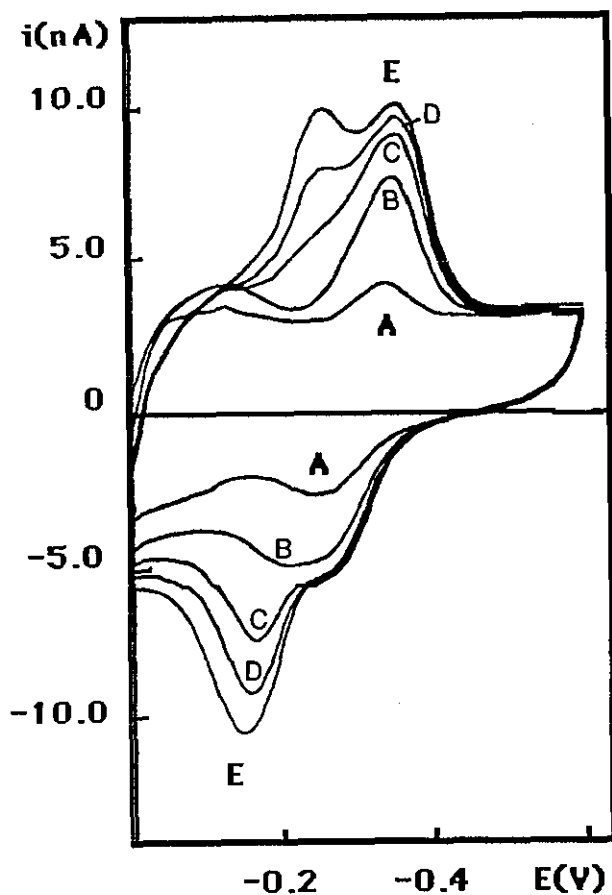


Figure.7.3- The effect of accumulation time on the cyclic voltammograms of  $5 \times 10^{-7}$  M copper(II) in the presence of  $1 \times 10^{-5}$  M HG at pH 8.3. Scan rate 20 mV/s. Accumulation potential : -0.4 V; Accumulation times : (A) 0; (B) 30; (C) 60; (D) 90 and (E) 120 s.

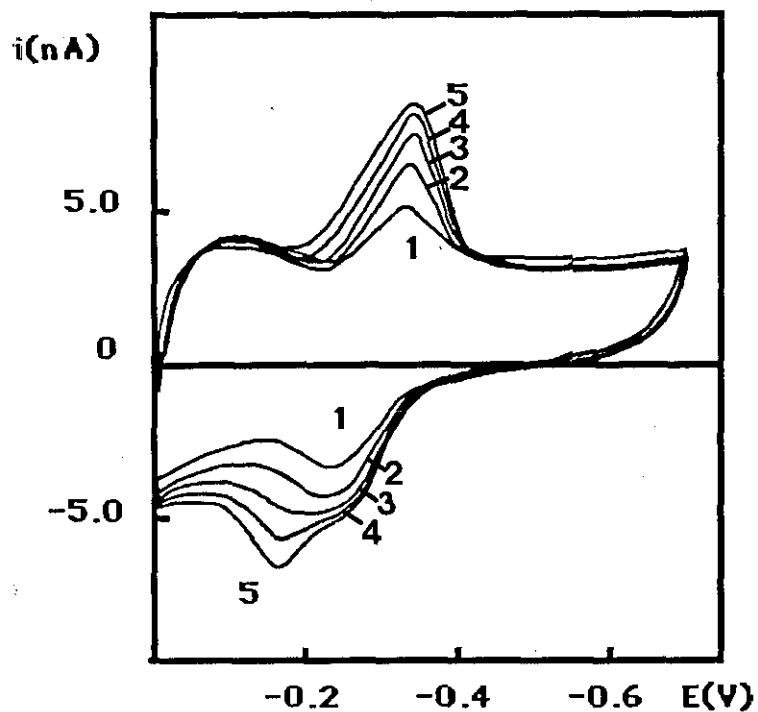


Figure.7.4- Multiple scan cyclic voltammograms of the HG complex system. Accumulation was influenced at 0.0 V for 120 s. Scan rate 20 mV/s. Scan number is indicated on the voltammograms.

Analogous cyclic voltammograms were obtained with GH. The main difference in the cyclic voltammetric behaviour between these dipeptide complexes is that the relative size of the GH complex peaks is smaller than that of the HG complex. Figure.7.5 shows the cyclic voltammograms obtained with increasing excess of GH over copper(II), and accumulating at -0.4 V and scanning from 0 V. The loss of the free copper(II) reduction peak as the two complex peaks are formed is apparent, but the first peak remains as a shoulder on the front of the second peak. A 20 : 1 ratio of GH to copper(II) -higher than HG- is required to eliminate the free copper(II) peak. The effect of accumulating at various potentials , before scanning to 0 V, and then scanning cathodically is shown in Figure.7.6. In contrast to the results obtained with HG, the first peak remains relatively small and never becomes predominant. Figure.7.7 shows the influence of the accumulation potential on the size of the second cathodic peak. The scans were initiated from the accumulation potential to more negative values.

For both complex system a very small peak was observed in their cyclic voltammograms when the accumulation was carried out at 0 V indicating that the accumulation of the complex species strongly depends on the accumulation potential. This influence of the accumulation potential on the height and the number of the stripping peaks indicates that amalgam formation has a strong effect on the type of the collected species.



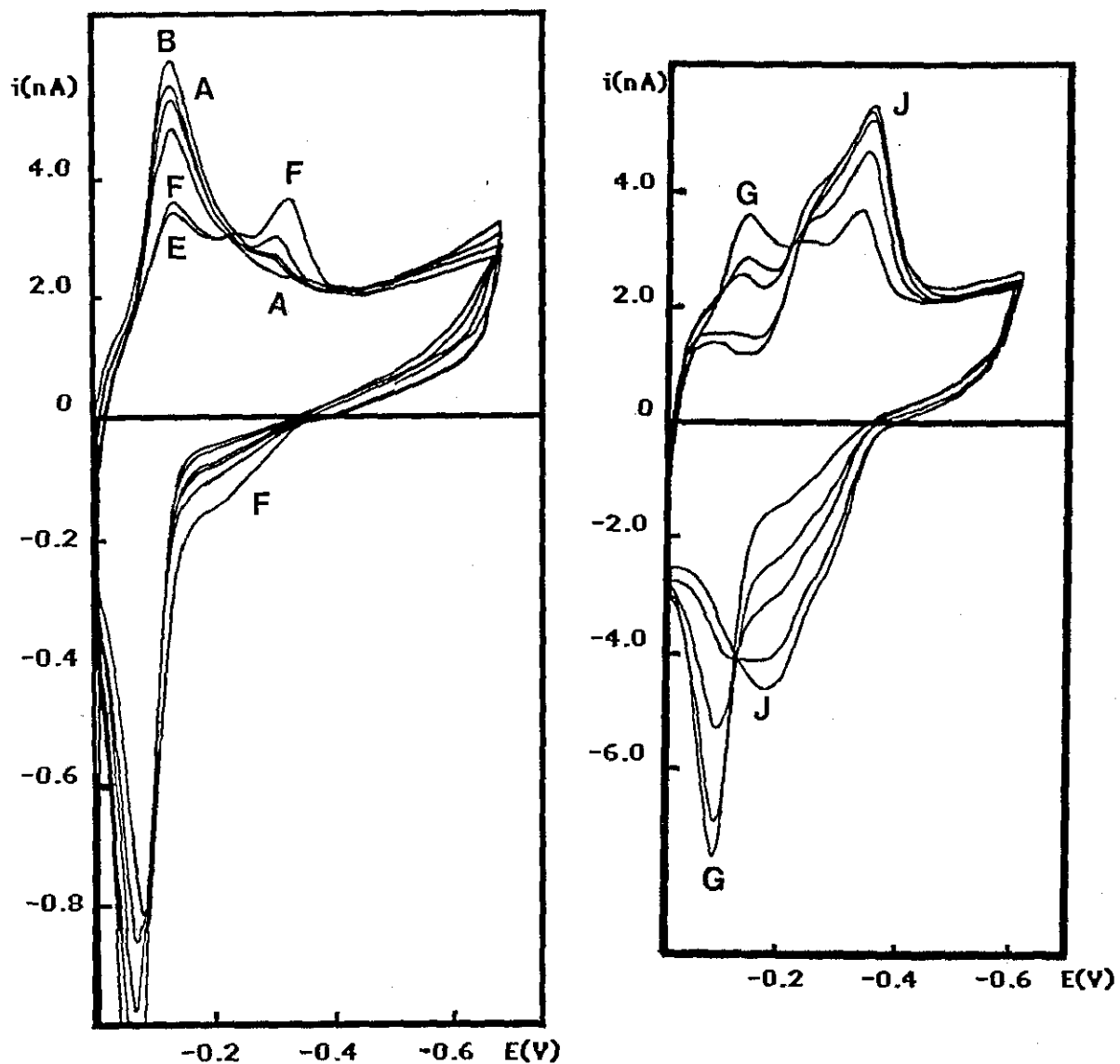


Figure.7.5- Cyclic voltammograms of  $5 \times 10^{-7}$  M copper(II) in the presence of increasing excess of GH at pH 8.3. Accumulation potential: -0.4 (120 s). Scan rate: 20 mV/s. (A) copper(II) only; (B)  $2 \times 10^{-7}$ ; (C)  $4 \times 10^{-7}$ ; (D)  $6 \times 10^{-7}$ ; (E)  $1 \times 10^{-6}$ ; (F)  $2 \times 10^{-6}$ ; (G)  $4 \times 10^{-6}$ ; (H)  $6 \times 10^{-6}$ ; (I)  $8 \times 10^{-6}$  and (J)  $1 \times 10^{-5}$  M GH.

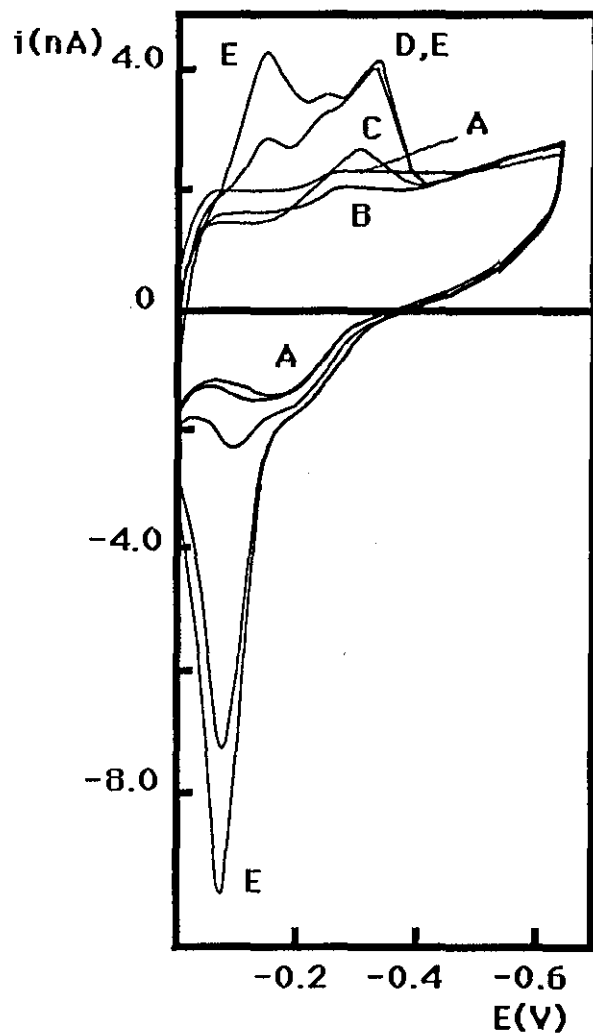


Figure.7.6- The effect of accumulation potential on the cyclic voltammograms for  $2 \times 10^{-5}$  M GH in the presence of  $1 \times 10^{-6}$  M copper(II). Scan rate : 20 mV/s. Accumulation potential: (A) 0; (B) -0.1 and (C) -0.2 V; (D) -0.3 and (E) -0.4 V. Accumulation time : 120 s.

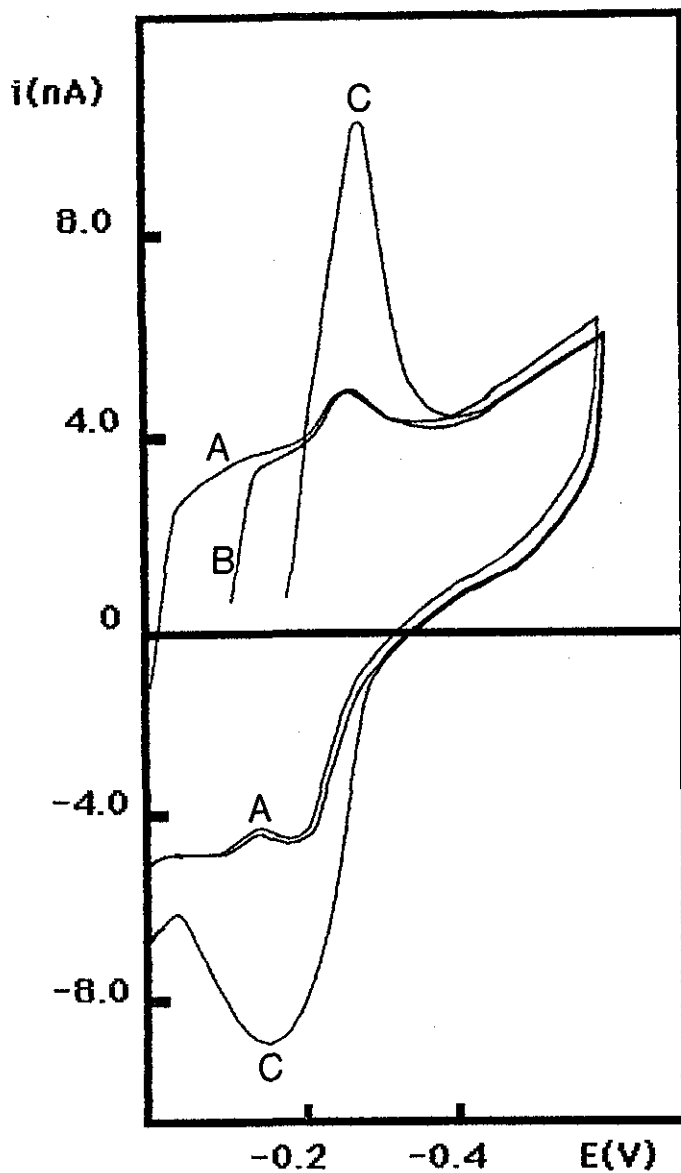


Figure.7.7- The effect of accumulation potential on the complex peak heights of  $2 \times 10^{-5}$  M GH in the presence of  $1 \times 10^{-6}$  M copper(II). Scan rate : 20 mV/s. Accumulation potential: (A) 0 ; (B) -0.1 and (C) -0.2 V. Accumulation time : 120 s. Scan was initiated from the accumulation potential.

Effect of accumulation time at  $-0.4$  V, and of multiple scans gave signs of the first peak, more so during the anodic scan, but less so than for the HG complex. From these studies the very weak adsorption of the complexes can be concluded. The linear relationship of square root of scan rate with the peak currents confirms the diffusion controlled character of the reduction peaks.

Similar to the GHG-copper complexes studied before this, the dependence on the accumulation potential for HG and GH complexes suggests two subsequential one electron reduction processes of the copper(II) complexes are involved with these dipeptides. However, the absence of the first peak in the voltammograms which were recorded after accumulations at potentials more positive than  $-0.2$  V rules out this assumption. These two peaks therefore seem to correspond to different complexes of the peptides with copper. This electrogeneration of the species responsible from the first peak by successive scanning or accumulating at sufficiently negative potentials resembles the formation of the copper(I) complex which can be stabilised by adsorption in the presence of excess ligand solution. On the other hand, the position of the anodic peaks cannot be assigned with this reduction mechanism since the second cathodic peak is related to the anodic peak at more negative potentials and the sequence of the reoxidation of copper amalgam cannot be explained by this mechanism. Another type of complex formation, possibly polynuclear species formation, should be considered. Aiba et al<sup>26</sup> studied the copper complexes of simple histidyl peptides and polymer

formation was reported for GH and GHG copper(II) systems in which the imidazole ring acts as a bridge to connect copper atoms.

On the other hand, Philp and co-workers<sup>60,61</sup> studied the effect of low total ligand concentration on potential shifts and shapes of cyclic voltammograms. For reversible systems with one predominant complex at substoichiometric ligand concentration distorted double peaks were observed for  $\log \beta$  values higher than 11. The copper(II) ions, produced from the amalgamated copper upon switching of the potential to 0 V prior to initiating the scan, changes the concentration ratio around the drop and another possibly lower complex is formed.

#### Cathodic stripping differential pulse voltammetric studies

Cathodic stripping dp voltammetric studies of the reduction process of the complexes were carried out at the same pH with a -50 mV pulse amplitude. The effect of accumulation time at -0.4 V on the peak current was studied in a  $5 \times 10^{-7}$  M copper(II) solution with an added ten fold excess of ligand. The peak currents plotted against time gave a maximum at 90 s indicating the saturation of the drop with longer accumulation times(Figure.7.8) .

From the above studies, it is apparent that dipeptides can be determined in the presence of an excess of copper(II). HG can be determined in submicromolar levels by accumulating at -0.1 V in the presence of  $1 \times 10^{-6}$  M copper(II) and the calibration curve was linear for  $1-10 \times 10^{-8}$  M concentration range with a slope of 0.15 A/M and intercept 5.4 nA. Figure.7.9 shows the

cathodic stripping voltammograms used for determination of HG at pH 8.3. For  $2 \times 10^{-8}$  M HG solution in  $1 \times 10^{-6}$  M copper(II) relative standard deviation was less than 2%.

GH can be determined in pH 8.3 bicarbonate solutions by accumulating at -0.2 V and scanning in the negative direction. A calibration curve for a concentration range of  $1-10 \times 10^{-7}$  M GH can be obtained in the presence of  $1 \times 10^{-6}$  M copper(II) solution measuring the height of the peak at -0.30 V (Figure.7.10).

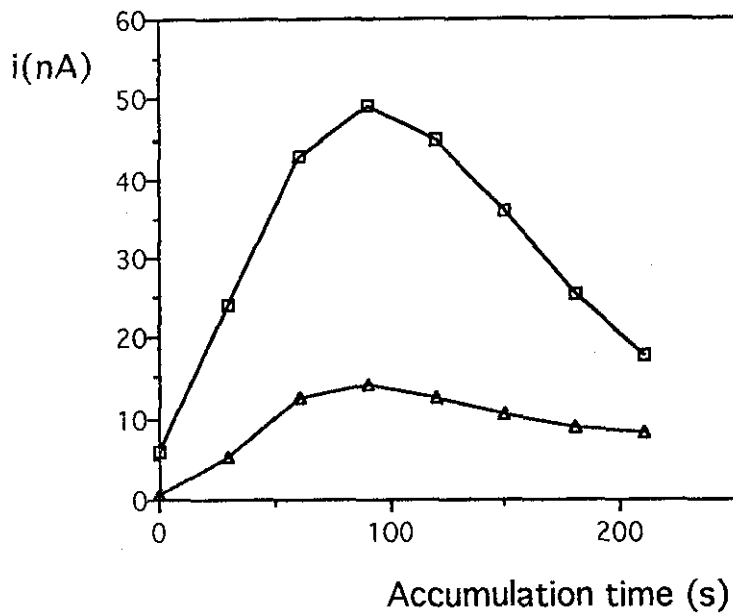


Figure 7.7- Effect of accumulation time on the complex peak heights of ( $\square$ )  $5 \times 10^{-6}$  M GH in the presence of  $5 \times 10^{-7}$  M copper(II) and ( $\Delta$ )  $1 \times 10^{-7}$  M HG in the presence of  $1 \times 10^{-6}$  M copper(II) at pH 8.3. Accumulation was influenced at -0.4 V and -0.1 V, respectively.

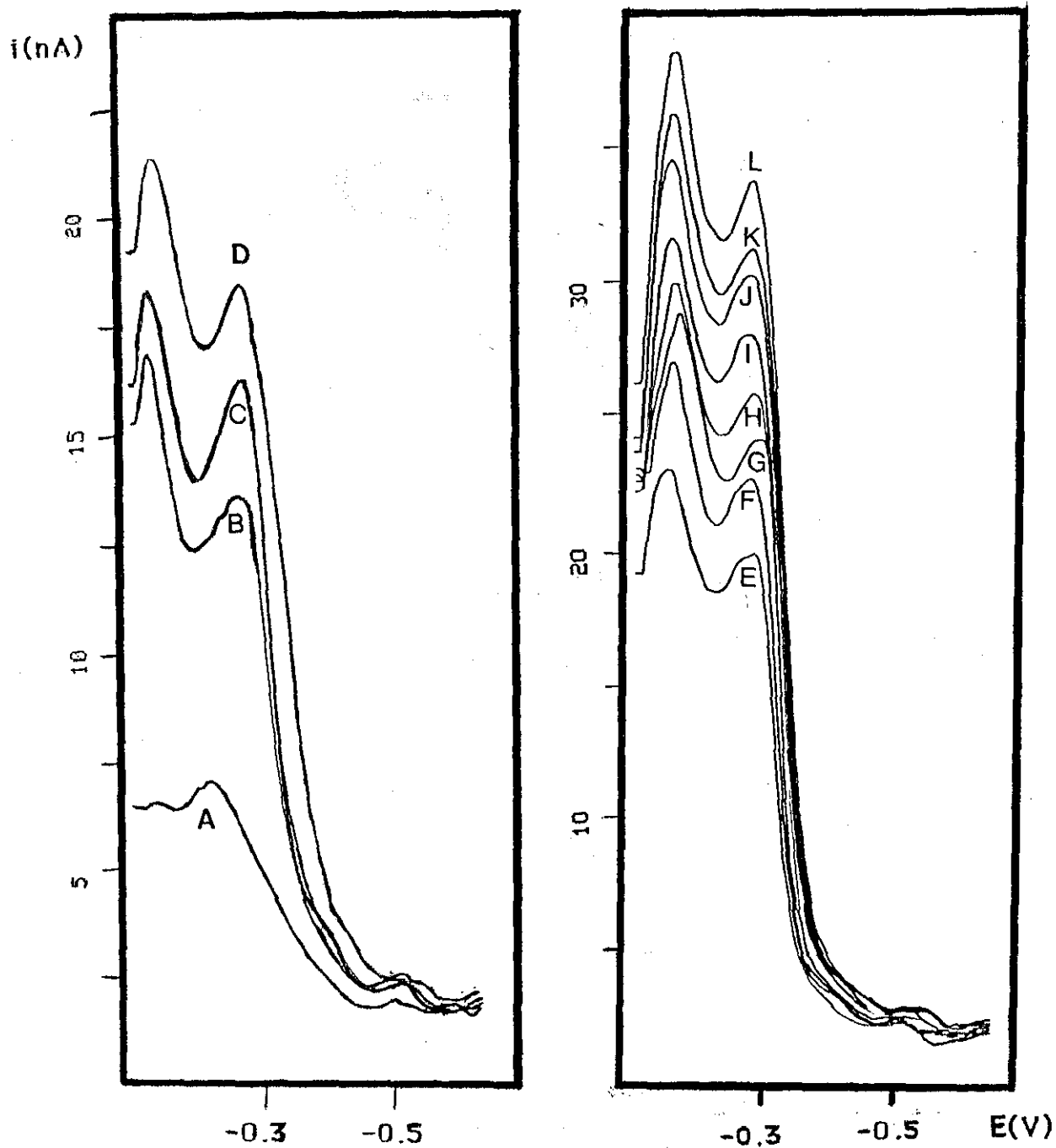


Figure.7.9- Voltammograms used for cathodic stripping determination of HG. (A) 0.1 M sodium hydrogencarbonate solution only, (B)  $1 \times 10^{-6}$  M copper(II); (C-L)  $(1-10) \times 10^{-8}$  M HG. Accumulation was performed at -0.1 V for 120 s.



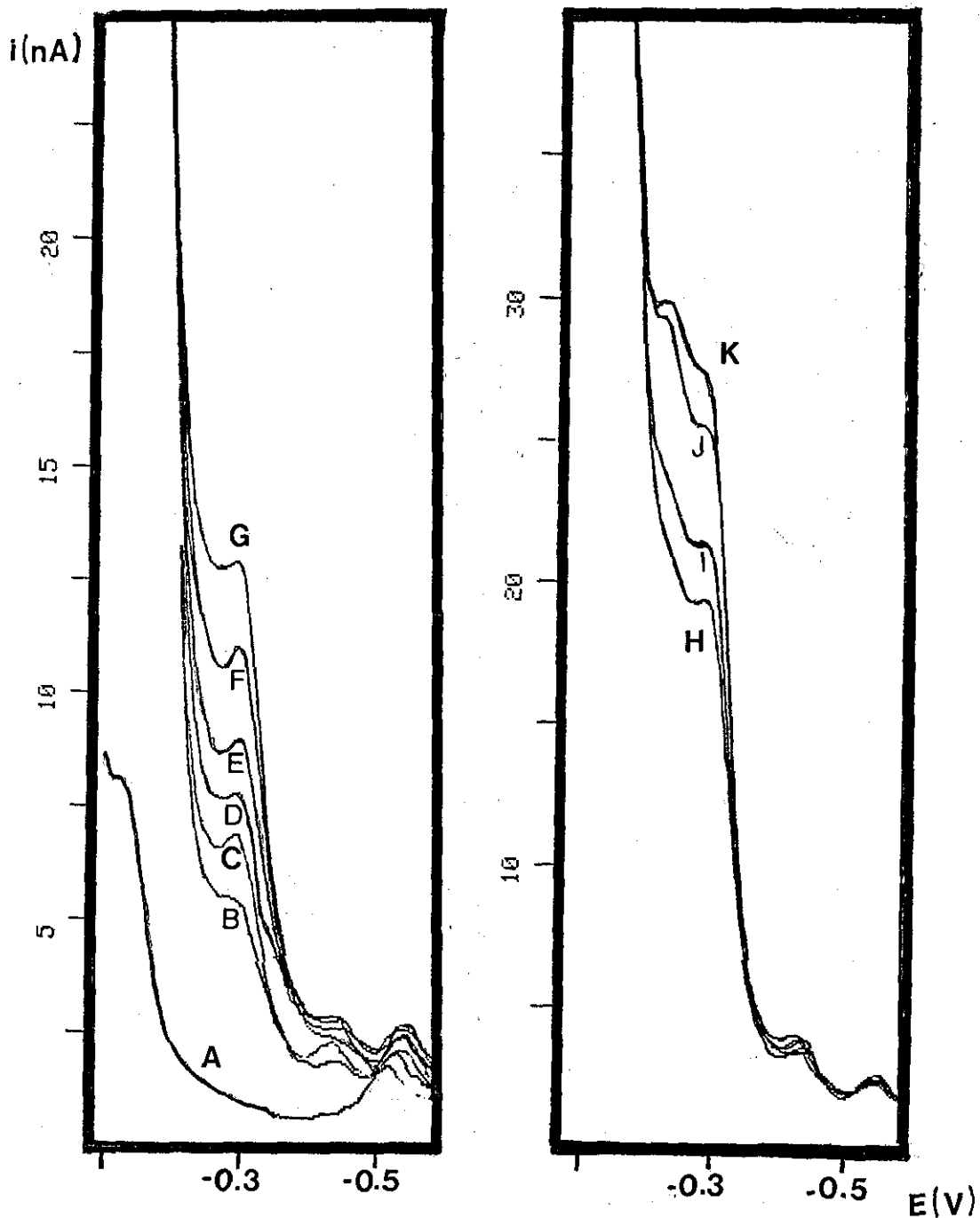


Figure.7.10- Cathodic stripping dp voltammograms used for determination of GH at pH 8.3. (A) hydrogen carbonate solution only, (B)  $1 \times 10^{-6}$  M copper(II); GH concentration : (C-K)  $(1-10) \times 10^{-7}$  M. Accumulation potential : -0.3 V, accumulation time : 120 s.

## Conclusion

The similarity in the peak potentials and dependence on the accumulation conditions indicates a similar type of binding of these dipeptides with copper ions. The accumulation potential and hence the amalgam formation was found to have a great influence on the peak heights and the type of the collected species. Additional peak formation was observed for both complex systems when the accumulation was performed at potentials more negative than  $-0.2$  V. The copper(II) ions, produced from the amalgamated copper upon switching of the potential to  $0$  V prior to initiating the scan, changes the concentration ratio around the drop and another, possibly a lower complex is formed.

The above determined conditions provide a sensitive method for the determination of the dipeptides using the complex peak which occurs around  $-0.3$  V in buffered solutions. Better sensitivity was obtained for the HG complex under the conditions applied. The similarity of the peak potentials of these dipeptide complexes to those of other compounds which can complex with either copper(II) ion or the analyte, limits the selectivity of the method, and a pre-separation would be required.

## CHAPTER 8

### CATHODIC STRIPPING BEHAVIOUR OF CARNOSINE AND THYROTROPINE RELEASING FACTOR AT A HANGING DROP MERCURY ELECTRODE IN THE PRESENCE OF COPPER(II) IONS

#### Introduction

Tyrotropin-releasing factor (TRF), L-pyroglutamyl-L-histidyl-prolinamide is one of the important histidine containing peptides providing a simple model for bioactive peptides and proteins. Its interaction with copper(II) was investigated by Farkas et al<sup>32</sup> by pH metric and spectrophotometric methods. The complex structure is shown in Figure.2.6.

Carnosine (Car) complexes (see Figure.2.5 for structure) with copper(II) were also investigated by pH metric studies and a dimeric complex structure has been reported for the complex<sup>18,24</sup>. A CSV study has shown that the complex can be accumulated as the copper(I) complex at an HMDE<sup>36</sup>. The effect of accumulation time on the complex was monitored by dp voltammetry but no utilisation of this effect for quantitative analysis was reported.

The present study aims to investigate the reduction mechanism of the copper(II) complexes of Car and TRF by use of cathodic stripping and cyclic voltammetric techniques and describes the utilisation of the accumulation in the determination of these ligand systems using dp cathodic stripping voltammetry.

## Results and Discussion

An analytically useful reduction peak of the copper complex of Car was obtained by dp CSV at around -0.33 V in the presence of  $1 \times 10^{-5}$  M copper in the solution. The determination studies of Car were carried out in 0.1 M hydrogen carbonate solutions with a 2 min deposition at -0.1 V. A linear calibration curve was obtained for a  $2-20 \times 10^{-9}$  M Car concentration range with a slope of 1.4 A/M and intercept 1.2 nA. Coefficients of variation at the  $2 \times 10^{-8}$  M level are typically 3 % for 4 determinations. Figure.8.1 shows the cathodic stripping dp voltammograms used for Car determination.

The determination method of TRF was not quite as good as that for Car. The complex peak appears at -0.32 V in the presence of  $1 \times 10^{-6}$  M copper(II) in pH 9.2 borate buffer (Figure.8.2). A calibration curve was obtained in a concentration range of  $1-10 \times 10^{-8}$  M TRF with a slope of 4.47 A/M. The blank current was  $8.2 \pm 0.17$  nA and the rsd (for 4 determinations) was 2.4 % for  $1 \times 10^{-8}$  M TRF.

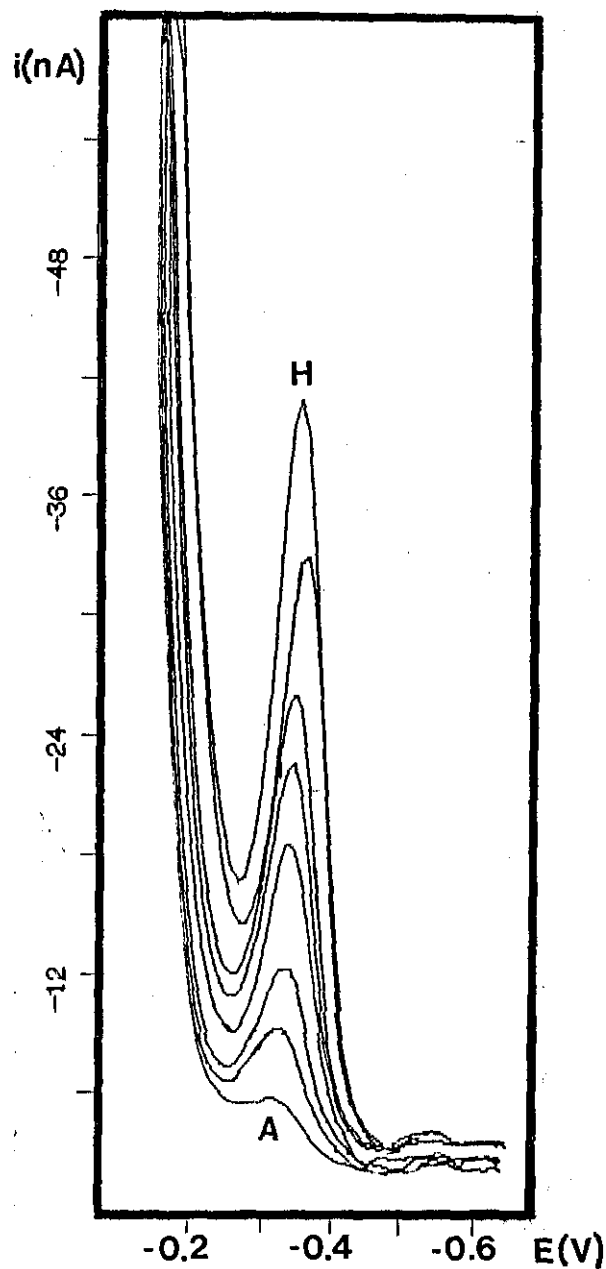


Figure.8.1- Cathodic stripping voltammograms used for Car determination. (A)  $1 \times 10^{-5}$  M copper(II) in 0.1 M  $\text{NaHCO}_3$  solution. Car concentrations : (B) 2; (C) 4; (D) 8; (E) 10; (F) 12; (G) 16 and (H)  $20 \times 10^{-9}$  M. Accumulation potential : -0.1 V, accumulation time : 2 min.

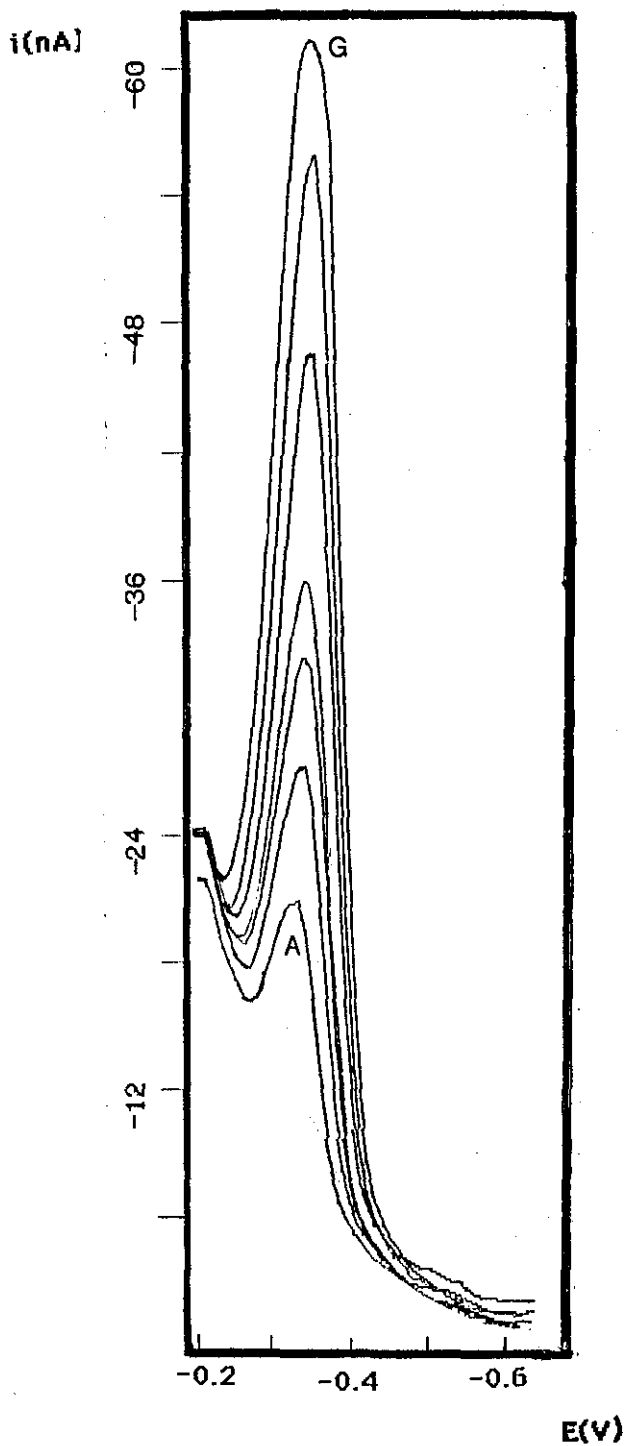


Figure.8.2- Voltammograms used for cathodic stripping determination of TRF at pH 9.2 borate buffer. (A)  $1 \times 10^{-6}$  M copper(II); (B-G)  $(1-6) \times 10^{-8}$  M TRF. Accumulation was performed at -0.2 V for 2 min.

The effect of accumulation conditions on the determination was investigated for a  $1 \times 10^{-8}$  M Car in 0.1 M  $\text{NaHCO}_3$  solution containing  $1 \times 10^{-5}$  M copper(II). The dependence of the complex peak heights at -0.40 V on the accumulation potential is shown in Figure.8.3. The potential was scanned in the negative direction from the accumulation potential. The signal increased as accumulation potential made more negative, indicating a potential dependent adsorption of the complex, and then gave a decrease for the accumulation potentials more negative than the peak potential as expected (Figure.8.3). Similar dependence was observed for the copper(II)-TRF system in 1:10 molar ratio. The peak height of the TRF complex at -0.42 V decreases for accumulation potentials more negative than -0.2 V (Figure.8.4).

Figure.8.5 shows the effect of accumulation time on the complex peak heights for both complex systems. For dilute concentrations of Car the peak heights increased linearly in time range of 0-3 min, but for more concentrate Car and TRF complex systems deviation from the linearity was observed for accumulation times more than 2 min (Figure.8.5) probably due to the saturation of the drop.

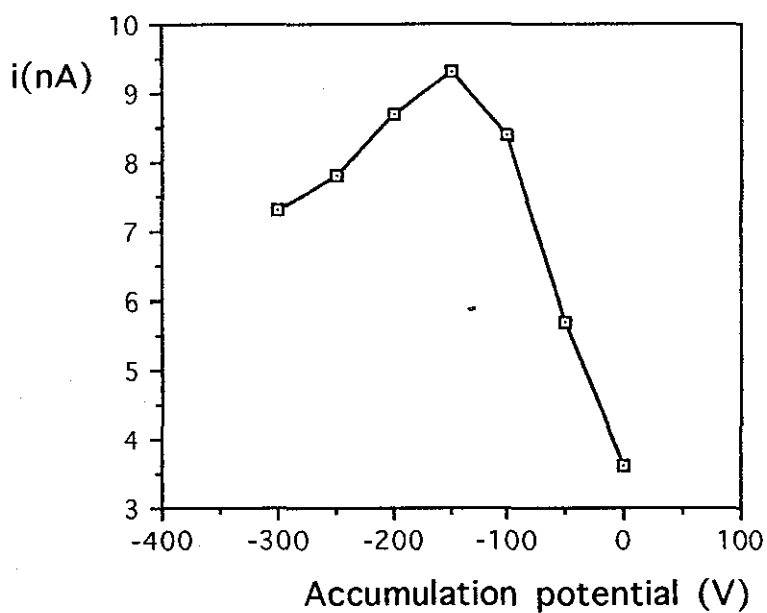


Figure.8.3- The influence of accumulation potential on the complex peak heights of  $1 \times 10^{-8}$  M Car in the presence of  $1 \times 10^{-5}$  M copper(II) solution at pH 8.3. Scan was made from the accumulation potential.

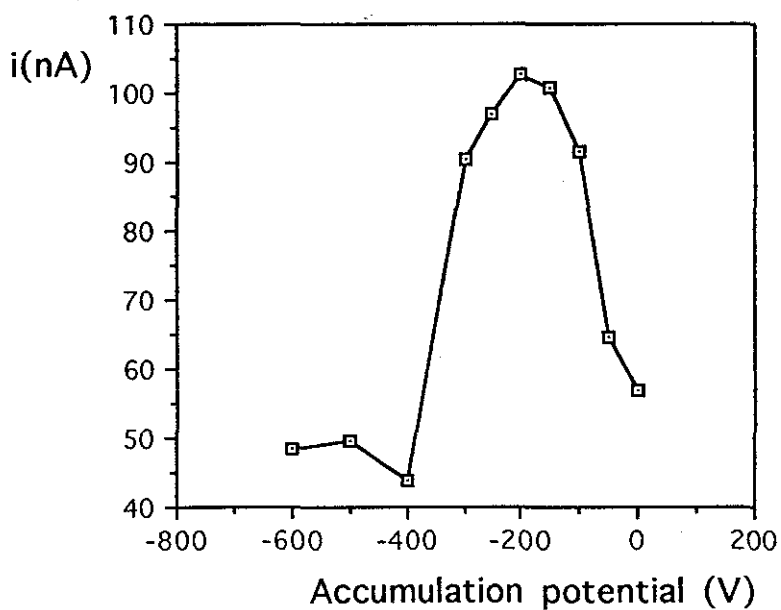


Figure.8.4- The effect of accumulation potential on the peak heights of the TRF complex in 1:10 molar ratio. Initial concentration of copper(II) is  $5 \times 10^{-7}$  M at pH 8.3.



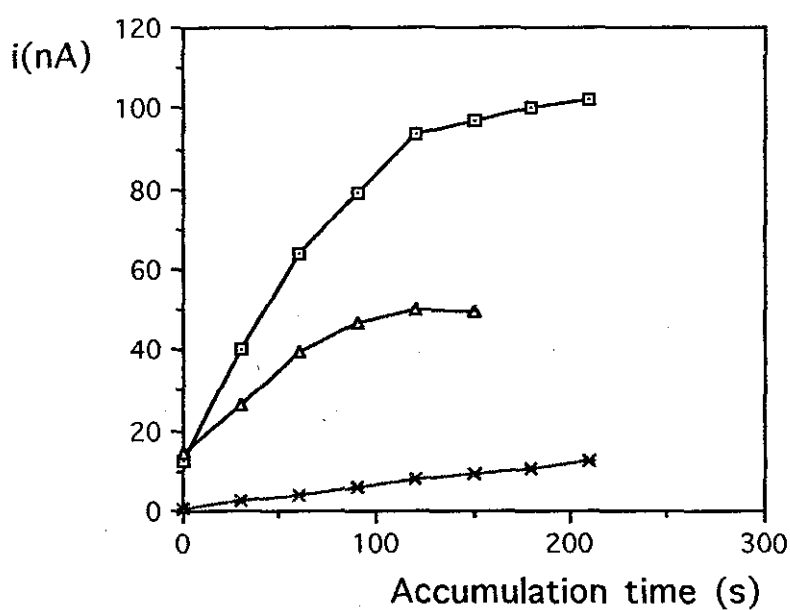


Figure.8.5- The effect of accumulation time at -0.1 V on the complex peak heights of (-□-)  $5 \times 10^{-7}$  M copper(II) containing  $1 \times 10^{-5}$  M TRF; (-Δ-)  $5 \times 10^{-6}$  M Car in the presence of  $5 \times 10^{-7}$  M copper(II) and (-\*-)  $1 \times 10^{-8}$  M Car in the presence of  $1 \times 10^{-5}$  M copper(II) at pH 8.3.

## Adsorptive Stripping Cyclic Voltammetric Behaviour of The Car and TRF Complex Systems

The reduction process of both complex systems was investigated by using cyclic voltammetry and dp polarography. Adsorption controlled characteristic of the reduction process for carnosine and TRF complex systems was confirmed with the linear relation between the peak currents and the scan rate. Peak potentials have shifted to negative potentials a few mVs for the latter showing a small degree of irreversibility.

Stripping cyclic voltammograms recorded at a HMDE for a 1:1 copper(II)-Car system in 0.1 M hydrogen carbonate solutions show a single peak at -0.31 V for a 2 min accumulation at -0.1 V (Figure.8.6). The complex peak increased on adding more ligand to the copper(II) solution shifting a few mVs to more negative potentials and an anodic peak became more apparent around -0.3 V while the oxidation peak of copper amalgam at more positive potentials decrease. Similarly, a shift in the peak potential was observed for the TRF complex by ligand addition (not shown). The reduction peak potential of the TRF complex, monitored by AdSC dp voltammetry, shifted from -0.38 V to -0.44 V by addition of  $5 \times 10^{-7}$ - $5 \times 10^{-5}$  M TRF on  $5 \times 10^{-7}$  M copper(II) in pH 9.2 borate buffer.

Successive scans of potential for the same drop in the Car-copper(II) system are shown in Figure.8.7. Accumulation at 0 V and then cycling between 0 and -0.7 V with a 20 mV/s scan rate gave the complex peak at -0.33 V. This peak increased in size with further scanning as does the additional peak at

-0.17 V which comes from the dissolution of amalgam formed during the scan to negative potentials (Figure.8.7). This effect was also observed with TRF complex system while the complex peak at -0.40 V decreases in height (Figure.8.8). No additional complex peak was observed for both complex systems with cycling to negative potentials. It was not possible to obtain evidence for formation of copper(I) complex of Car, as proposed earlier<sup>37</sup>.

Polarographic experiments were carried out on the Car-copper(II) system to compare with the voltammetric data. A single polarographic peak was obtained which is shifting to more negative potentials with a slight increase in peak height as pH increases (Table.8.1). The polarographic peak corresponds to the voltammetric peak which takes place at more positive potentials in agreement with the theory<sup>1</sup>. The presence of the single polarographic peak for the complex system indicates a one step two electron reduction of the copper(II) complex and excludes the copper(I) complex formation as this species usually forms on the electrode surface and is stabilised by adsorption.

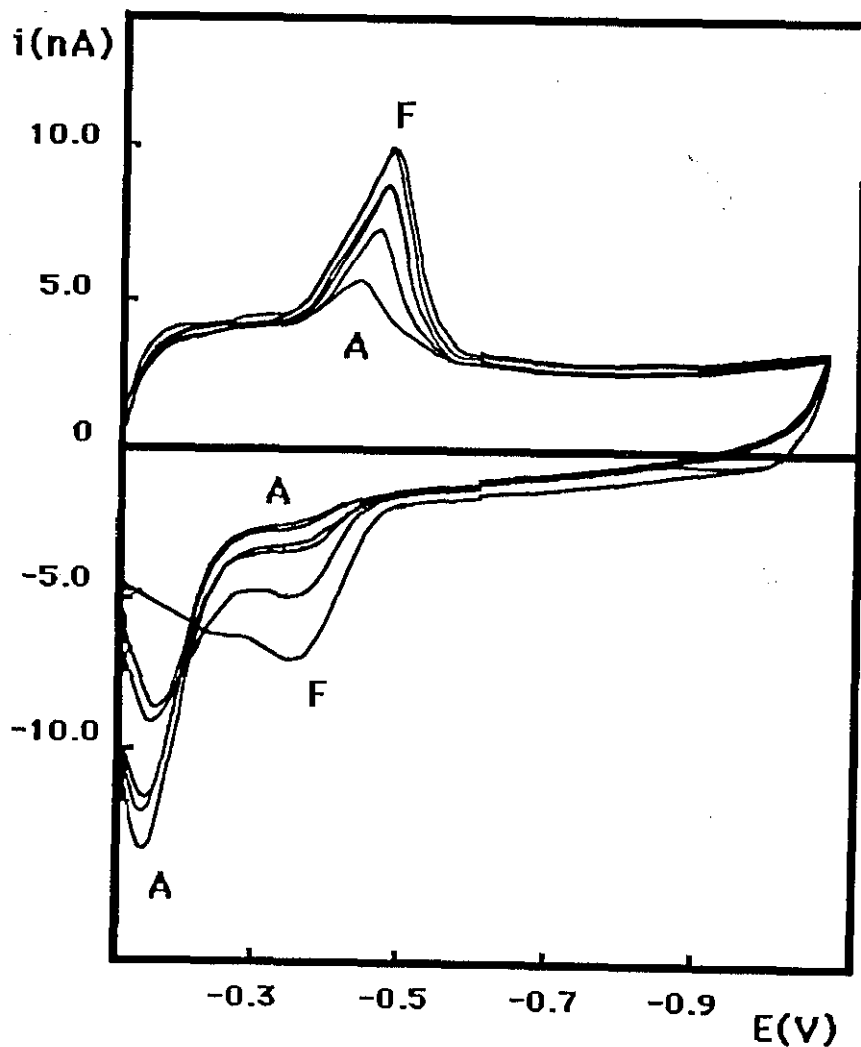


Figure.8.6- The influence of ligand addition on the complex peak of copper(II)-Car system at pH 8.3. (A)  $5 \times 10^{-7}$ ; (B)  $1 \times 10^{-6}$ ; (C)  $1.5 \times 10^{-6}$ ; (D)  $2.5 \times 10^{-6}$ ; (E)  $5 \times 10^{-6}$ ; (F)  $1 \times 10^{-5}$  M Car in the presence of  $5 \times 10^{-7}$  M copper(II). The accumulation was performed at  $-0.1$  V for 2 min. Scan rate : 20 mV/s.

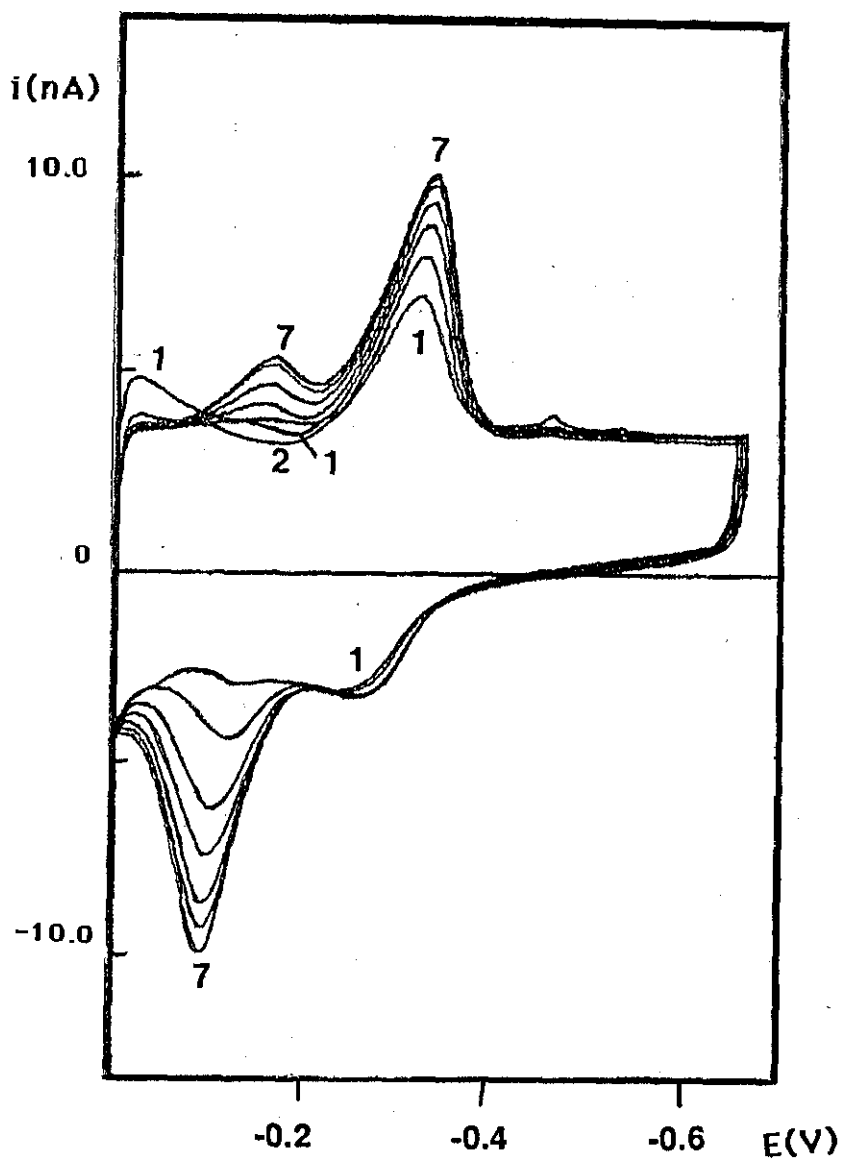


Figure.8.7- Successive scan cyclic voltammograms of  $5 \times 10^{-7}$  M copper(II) in the presence of  $5 \times 10^{-6}$  M Car in pH 8.3; scan rate : 20 mV/s. Accumulation was performed at 0 V for 2 min in stirred solutions. The scan number was indicated on the plot.

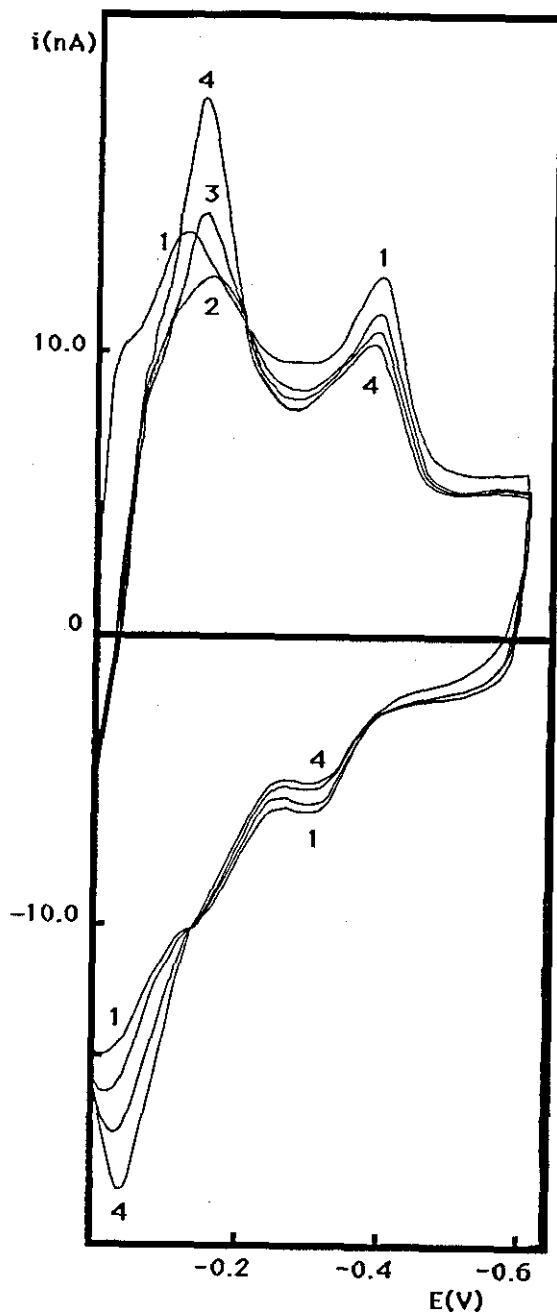


Figure.8.8- Successive scan cyclic voltammograms of TRF complex at an HMDE. Initial concentrations :  $1 \times 10^{-5}$  M TRF and;  $5 \times 10^{-7}$  M copper(II) in pH 9.2 borate buffer; scan rate : 50 mV/s; Accumulation was made at 0 V for 2 min in stirred solution. The scan number was indicated on the plot.

Table.8.1- The polarographic data of Car complex system. Initial concentrations; [Car] :  $5 \times 10^{-4}$  M; [Copper(II)] :  $1 \times 10^{-4}$  M.

pH	$E_p$ (V)	$i_p$ (nA)
6.1	-0.20	140
7.0	-0.32	150
7.6	-0.35	225
8.3	-0.45	285
9.2	-0.46	305
12.0	-0.59	390

### Conclusion

Very low levels of Car can be determined by using dp cathodic stripping voltammetry in the presence of copper ions. The similarity in the complex peak potentials precludes the practical determination in a complex mixture of the other simple peptides. It was not possible to obtain evidence for the formation of copper(I) complex as proposed for Car complex. Successive scans and accumulating at negative potentials and scanning from relatively positive potentials only results in the free copper(II) reduction peak in addition to the complex reduction peak. The increase in the peak potentials with accumulation at more negative potentials can be explained by the reoxidation of the copper amalgam to free copper(II) ions which can readily complexes with the ligand which is in excess in the solution.

## CHAPTER 9

### SOLID PHASE REMOVAL OF CHLORIDE INTERFERENCE IN THE DIFFERENTIAL PULSE POLAROGRAPHIC DETERMINATION OF NITRATE USING NITRATION REACTIONS

#### Introduction

Nitrate determination in a variety of fluids is important because of the conversion of nitrate to cancerous nitrosamines within the human body. The determination of nitrate by reacting it with a suitable organic reagent in a nitration reaction is very convenient and rapid. There are several UV-visible spectroscopic methods for nitrate determinations based on nitroderivatives which are formed with several organic reagents such as phenol<sup>62</sup>, dimethylphenols<sup>63-65</sup>, salicylic acid<sup>66</sup>, 2-sec-butylphenol<sup>67</sup> and resorcinol<sup>68</sup>. Alternatively diazotisation and coupling reactions follow the reduction of nitrate to nitrite in a copperised cadmium column<sup>69</sup>.

Nitroderivatives also have been determined with chromatographic methods including GC<sup>70,71</sup>, HPLC<sup>72</sup> and IC<sup>73</sup>. Ion chromatography is generally the best technique for the determination of a range of ions but the instrumentation is expensive and rapid alternative methods are needed.

Polarographic determination of nitrate in this laboratory has been based on a study of the reduction of the nitroderivatives of more than fifteen compounds<sup>74</sup>. The most satisfactory reagent was found to be benzoic acid giving a single product



which is reduced at a low negative potential. Chloride was noted to be an interferent reducing the nitrate to nitrosyl bromide whilst being oxidised to chlorine in concentrated sulphuric acid solution. A flow injection amperometric method of determining nitrate<sup>75</sup> was developed in this laboratory based on this latter reaction occurring on-line with monitoring of the combined reduction signal of nitrosyl bromide and chlorine.

In the literature the interference of chloride in nitrate samples is not clearly illustrated. Here the interference of chloride on the nitration reaction of benzoic acid is shown graphically and the study was repeated with thiophene-2-carboxylic acid which was reported to react more rapidly than benzoic acid on line<sup>76</sup> and might react more quickly than the chloride. Preliminary studies showed that this is not the case and pre-separation is needed to eliminate the interference. Dionex produce extraction cartridges based on a silver(I) loaded cation exchange resin for removing chloride prior to ion chromatography. The present study shows that these cartridges can be used effectively prior to the developed polarographic method for nitrate determination.

### Results and Discussion

The major product of the nitration reaction of benzoic acid is 3-nitrobenzoic acid which gives a reduction peak around -0.1 V. The influence of chloride on the nitration reaction was investigated using the developed procedure with a  $4 \times 10^{-4}$  M nitrate solution containing chloride (see Chapter 3). Figure.9.1

shows the decrease in reduction peak heights with increasing chloride contents. It is clearly seen that chloride at sufficiently high levels interferes with the determination by causing some nitrate to be reduced to nitrite and this loss of signal is listed in Table.9.1.

Alternatively thiophene-2-carboxylic acid was examined as a nitration reagent. Thiophene-2-carboxylic acid was observed to react very rapidly with nitrate<sup>15</sup> but the nitroderivative gives several peaks at +0.06, -0.03, -0.21, -0.45 and -0.64 V. The first two peaks at the more positive potentials were much larger and were used in this investigation. Both peaks gave a rectilinear response (Figure.9.2) over the nitrate range studied ( $1 \times 10^{-5}$ - $1 \times 10^{-3}$  M), but the reproducibility was poor at lower nitrate levels as shown in Table.9.2.

The influence of chloride was investigated in a similar way to benzoic acid and the loss of the signals were shown in Figure.9.3 and listed in Table.9.3. These results agree that chloride considerably effects the nitration reaction of these two selected reagents reducing some nitrate to nitrosyl chloride in sulphuric acid medium and separation of chloride prior to the developed procedure is needed.

The use of cartridges to eliminate the chloride interference was examined for  $4 \times 10^{-4}$  M nitrate (in final solution) in a range of chloride solutions. Table-9.4 gives the recovery data in terms of the reduction current of 3-nitro-benzoic acid.

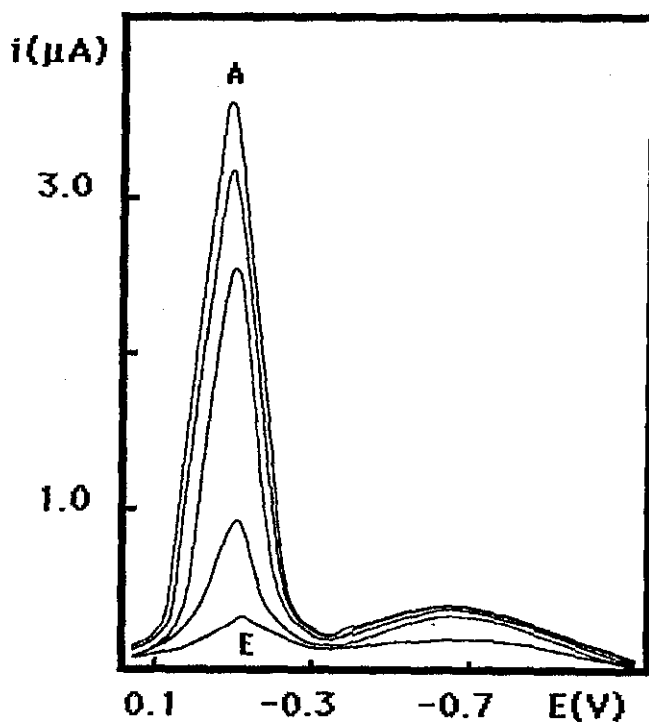


Figure.9.1- The influence of chloride on dpp signal of 3-nitrobenzoic acid formed using the procedure with  $4 \times 10^{-4}$  M nitrate solution containing (A) 0; (B)  $4 \times 10^{-4}$ ; (C)  $8 \times 10^{-4}$ ; (D)  $2 \times 10^{-3}$  and (E)  $4 \times 10^{-3}$  M chloride.

Table-9.1. The effect of chloride on the nitration product of benzoic acid as indicated by dpp. Initial nitrate concentration :  $4 \times 10^{-4}$  M.

[Cl <sup>-</sup> ](M)	Peak current (μA)	Loss of signal (%)
-	3.5	-
$4 \times 10^{-4}$	3.1	10
$8 \times 10^{-4}$	2.6	26
$2 \times 10^{-3}$	0.9	74
$4 \times 10^{-3}$	0.3	91

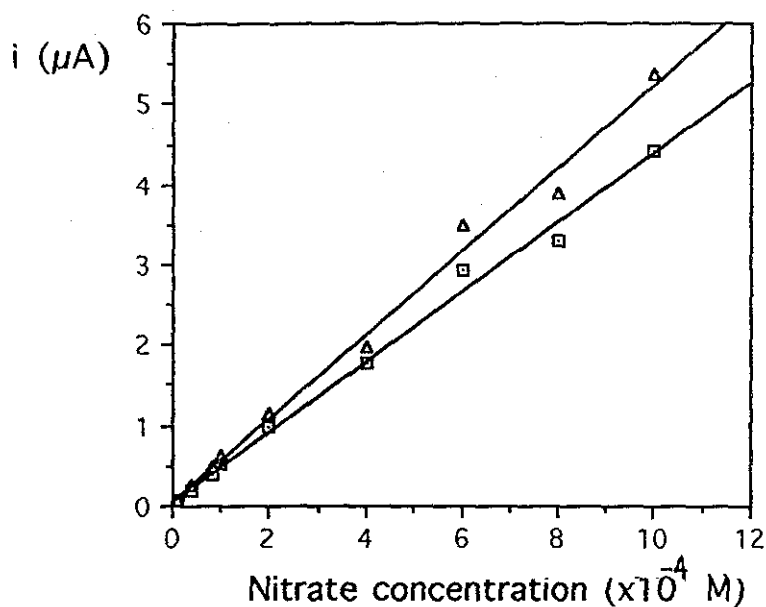


Figure.9.2- Calibration curve for nitrate determination using the procedure with T-2-CA. The peak currents were measured at (-□-) +0.06 and (-Δ-) -0.03 V.

Table.9.2-Reproducibility of the nitration reaction with thiophene-2-carboxylic acid as indicated by dpp.

[NO <sub>3</sub> <sup>-</sup> ](M)	rsd (%) (n=3)	
	First peak	Second peak
1x10 <sup>-5</sup>	16.0	2.5
1x10 <sup>-4</sup>	9.9	3.2
1x10 <sup>-3</sup>	2.9	1.8

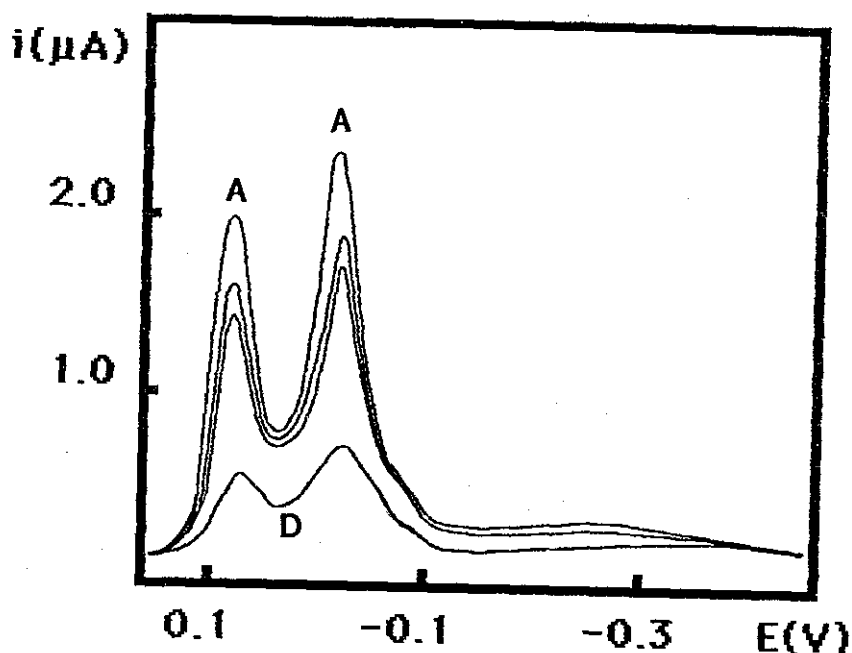


Figure.9.3- The influence of chloride concentration on the dp polarographic signal of nitration product of thiophene-2-carboxylic acid in the presence of  $4 \times 10^{-4}$  M nitrate. Chloride concentration : (A) 0; (B)  $4 \times 10^{-4}$ ; (C)  $8 \times 10^{-4}$  and (D)  $2 \times 10^{-3}$  M.

Table-9.3. The effect of chloride concentration on the peak heights of nitroderivative of thiophene-2-carboxylic acid obtained from  $4 \times 10^{-4}$  M nitrate solution.

[Cl <sup>-</sup> ](M)	Peak currents (μA)		Loss of signal (%)	
	First peak	Second peak	First peak	Second peak
-	1.95	2.10	-	-
$4 \times 10^{-4}$	1.60	1.90	18	9
$8 \times 10^{-4}$	1.48	1.70	29	19
$2 \times 10^{-3}$	0.58	0.70	70	67

Table.9.4. Recovery data for OnGuard-Ag

[Cl <sup>-</sup> ] (M)	Recovery (%)	rsd (%)
-	99.7	1.25
4 x10 <sup>-4</sup>	97.5	1.75
8 x10 <sup>-4</sup>	99.7	0.50
2 x10 <sup>-3</sup>	97.5	2.09
4 x10 <sup>-3</sup>	99.7	0.50

### Conclusion

Chloride was shown to be a source of serious interference in the determinations of nitrate in water samples by using two selected reagents. The removal of chloride from sample solutions using solid phase extraction cartridges prior to the derivatisation reaction gives satisfactory recovery data.

## CHAPTER 10

### CONCLUSION

A number of histidyl peptides were shown to be determined sensitively as their copper complexes at a HMDE by using cathodic stripping voltammetry. In view of the importance of compounds containing the imidazole ring, and the affinity of this ring for co-ordinating copper ions, the adsorptive stripping voltammetric behaviour of these complexes was investigated to gain a better understanding of the redox behaviour on the surface of mercury drop. Copper(I) complex formation was observed with the complexes of imidazole and GGH which reduce at more positive potentials than that of the copper(II) complex. The dependence of the formation of the copper(I) species on the accumulation potential indicates that the copper(Hg) formation plays a role in the generation of the copper(I) species which reoxidises to the complex in the presence of excess of ligand. A stepwise reduction was observed for GHG complex in which the intermediate copper(I) complex was stabilised by adsorption. Similar cathodic stripping voltammetric behaviour was observed for the GH and HG complexes in which the size and the number of the complex peaks depends on the accumulation potential. On the basis of the polarographic and stripping cyclic voltammetric behaviour of these dipeptide complexes, the possibility of the formation of other types of copper(II) complex was kept in mind : this is due to the effect of preconcentration of both ligand and copper ions on the surface

of the drop. A single reduction peak was observed for the Car and TRF complexes and this has been used for their determination.

The selectivity of the determination method is limited by the interference of surface active substances which can form complexes with copper(II). A preliminary separation step would be required in the presence of these interferents. For analysis of these compounds in a complex matrix, prior separation with an appropriate column can provide a very selective determination. However, in many model biological studies in a simple matrix, the developed method can provide a very sensitive tool for the determination of trace amounts of histidine containing compounds.

The cathodic stripping behaviour of other metal complexes of histidyl peptides could be investigated in further studies. The stability constants of cobalt complexes with these ligand systems are comparable to those of copper(II) complexes, and preliminary investigations with the cobalt complexes of GGH showed that the complex adsorbs on the electrode surface and gives two distinct peaks with adsorptive stripping voltammetry.



## REFERENCES

- 1- A. J. Bard and L. R. Faulkner, *Electrochemical Methods, Fundamentals and Applications*, John Wiley & Sons, New York, 1980.
- 2- J. A. Plambeck, *Electroanalytical Chemistry*, Wiley Interscience Publication, 1982.
- 3- Southampton Electrochemistry Group, *Instrumental Methods in Electrochemistry*, Ellis Horwood Limited, 1985
- 4- J. P. Hart, *Electroanalysis of Biologically Important Compounds*, Ellis Horwood Limited, 1990
- 5- W. F. Smyth, *Crit. Rev. in Anal. Chem.*, 1987, 18, 155
- 6- P. M. Bersier, *CRC Crit. Rev. in Anal. Chem.*, 1985, 16, 15
- 7- J. Wang, in *Electroanalytical Chemistry*, A.J. Bard, Ed., Vol.16, Marcel Deccer, New York, 198
- 8- F. Vydra, K. Stulik and E. Julakova, *Electrochemical Stripping Analysis*, Ellis Horwood Limited, Halsted Pres. 1976
- 9- C. M. G. van den Berg, *Anal. Chim. Acta*, 1991, 250, 265
- 10- E. Laviron, in *Electroanalytical Chemistry*, A.J. Bard, Ed., Vol.12, Marcel Deccer, New York, 1982
- 11- J. Wang, *Inter. Lab.*, October, 1985, 68
- 12- B. Pihlar, P. Valenta and H. W. Nürnberg, *Fresenius' Z. Anal. Chem.*, 1981, 307, 337
- 13- J. Wang, J. Zadeii and M. S. Lin, *J. Electroanal. Chem.*, 1987, 237, 281
- 14- C. M. G. van den Berg and G. S. Jacinto, *Anal. Chim. Acta*, 1988, 211, 129

- 15- S. Glodowski, R. Bilewicz and Z. Kublik, *Anal. Chim. Acta*, 1986, 186, 39.
- 16- U. Forsman, *Anal. Chim. Acta*, 1983, 146, 71
- 17- R. Österberg, *Coord. Chem. Rev.*, 1974, 12, 309
- 18- R. J. Sundberg and R. B. Martin, *Chem. Rev.*, 1974, 74, 471
- 19- H. Sigel and R. B. Martin, *Chem. Rev.*, 1982, 82, 385
- 20- S-J Lau, T. P. A. Kruck and B. Sarkar, *J. Biol. Chem.*, 1974, 249, 5878
- 21- S-J Lau and B. Sarkar, *Can. J. Chem.*, 1975, 53, 710
- 22- S-J Lau and B. Sarkar, *J. Chem. Soc. Dalton*, 1981, 491
- 23- H. Aiba, A. Yokoyama and H. Tanaka, *Bull. Chem. Soc. Jpn.*, 1975, 47, 112
- 24- R. P. Agarwall and D. D. Perrin, *J. Chem. Soc. Dalton*, 1975, 268
- 25- R. P. Agarwall and D. D. Perrin, *J. Chem. Soc. Dalton*, 1977, 53
- 26- H. Aiba, A. Yokoyama and H. Tanaka, *Bull. Chem. Soc. Jpn.*, 1974, 47, 1437
- 27- R. Österberg, B. Sjöberg and R. Soderquist, *Acta Chem. Scan.*, 1972, 26, 4184
- 28- R. Österberg and B. Sjöberg, *J. Inorg. nucl. Chem.*, 1975, 37, 815
- 29- H. Aiba, A. Yokoyama and H. Tanaka, *Bull. Chem. Soc. Jpn.*, 1974, 47, 136
- 30- H. C. Freeman and J. T. Szymanski, *Acta Crystal.*, 1967, 22, 406
- 31- I. Sovago, E. Farkas and A. Gergely, *J. Chem. Soc. Dalton Trans.*, 1982, 2159

- 32- E. Farkas, I. Sovago and A. Gergely, *J.Chem. Soc. Dalton*, 1984, 611
- 33- M. Aihara, Y. Nakamura, Y. Nishida and K. Noda, *Inorg. Chim. Acta*, 1968, 124, 169
- 34- M. P. Youngblood and D.W. Margerum, *J.Coord. Chem.*, 1981, 11, 103
- 35- K. Takehara and Y. Ide, *Inorg. Chim. Acta*, 1991, 183, 195
- 36- K. Takehara and Y. Ide, *Inorg. Chim. Acta*, 1991, 186, 73
- 37- R. Bilewicz, *J. Electroanal. Chem. Interfacial Electrochem.*, 1989, 267, 231
- 38- N. C. Li, J. M. White and E. J. Doody, *J. Am. Chem. Soc.*, 1954, 76, 6219.
- 39- F. Fenwick, *J. of Am. Chem. Soc.*, 1926, 48, 860
- 40- C. J. Hawkins and D. D. Perrin, *J. Chem. Soc. London*, 1962, 1351
- 41- J. Crouser, L. Pardessus and J. P. Crouser, *Electrochimica Acta*, 1988, 33, 1039
- 42- R. Bilewicz and Z. Kublik, *Anal. Chim. Acta*, 1981, 123, 201
- 43- A. Nelson, *Anal. Chim. Acta*, 1984, 169, 273
- 44- M. J. Pinchin and J. Newham, 1977, 90, 91
- 45- C. Sigwart, P. Kroneck and P. Hemmeric, *Helv. Chim. Acta*, 1970, 53, 177
- 46- B. C. Househam, C.M.G. van den Berg, J.P. Riley, *Anal. Chim. Acta*, 1987, 200, 291
- 47- G. Thomas and P.S. Zackarias, *Polyhedron*, 1985, 4, 811
- 48- J. C. Moreira and A. G. Fogg, *Analyst*, 1990, 115, 41
- 49- G. Svehla, *Vogel's Qualitative Inorganic Analysis*, Longmans, Singapore, 6th ed., 1979, p.288.
- 50- C. Tanford, *J. Am. Chem. Soc.*, 1952, 74, 211

- 51- D. G. Davis and W. R. Bordelon, *Anal. Lett.*, 1970, 3(8), 449
- 52- J.C. Moreira, R. Zhao and A.G. Fogg, *Analyst*, 1990, 115, 1561.
- 53- Y. Nozaki, F.R.N. Gurd, R.F. Chen, R. F. and J.T. Edsall, *J. Am. Chem. Soc.*, 1957, 79, 2123.
- 54- C.M.G. van den Berg, *Anal Chim Acta*, 1984, 164, 195.
- 55- C.M.G. van den Berg, *J. Electroanal. Chem.*, 1986, 215, 111.
- 56- C.M.G. van den Berg, *Analyst*, 1989, 114, 1527.
- 57- S. Kitagawa and M. Munakata, *Bull. Chem. Soc. Jpn.*, 1986, 59, 2751.
- 58- L. Casella and I. Rigoni, *J. Chem. Soc., Chem. Commun.*, 1985, 1668.
- 59- R. Osterberg and B. Sjöberg, *Acta Chem. Scan.*, 1968, 22, 639.
- 60- H. M. Killa and R. H. Philip, *J. Electroanal. Chem.*, 1984, 175, 223.
- 61- A. A. Castleberry, E. E. Mercer and R. H. Philip, *J. Electroanal. Chem.*, 1987, 216, 1.
- 62- N. Velghe and A. Claeys, *Analyst*, 1983, 108, 1018.
- 63- A. C. Holler and R. V. Huch, *Anal. Chem.*, 1949, 21, 1385.
- 64- A. M. Hartley and R. I. Asai, *Anal. Chem.*, 1963, 35, 1207
- 65- P. R. Elton-Bott, *Anal. Chim. Acta*, 1977, 90, 215.
- 66- D. A. Cataldo, M. Haroon., L. E. Schrader and V. L. Youngs, *Commun. Soil Sci. Plant Anal.*, 1975, 6, 71.
- 67- A. Tanaka, N. Nose and H. Iwasaki, *Analyst*, 1982, 107, 190.
- 68- N. Velge and A. Claeys, *Analyst*, 1985, 110, 313.
- 69- M. Okada, H. Miyata and K. Toei, *Analyst*, 1979, 104, 1195.
- 70- R. L. Tanner, R. Fajer and J. Gaffney, *Anal. Chem.*, 1979, 51, 865.

- 71- P. Englmaier, J. Chromatogr., 1983, 270, 243.
- 72- M. A. Alawi, Fresenius'Z. Anal. Chem., 1982, 313, 239.
- 73- D. T. Gjerde, "Ion Chromatography" Huthig, Heidelberg, 1983
- 74- A. G. Fogg, S. P. Scullion and T.E. Edmonds, Analyst, 1989, 113, 979
- 75- A. G. Fogg, S. P. Scullion and T.E. Edmonds, Analyst, 1989, 114, 579
- 76- B. K. Afghan, R. Leung, A. Kulkarni and J. F. Ryan, Anal. Chem., 1975, 47, 556.
- 77- A. G. Fogg, S. P. Scullion and T.E. Edmonds, Analyst, 1990, 115 599.

## Publications and Presentations

### Publications

Adsorptive stripping voltammetric behaviour of copper(II) at a hanging mercury drop electrode in the presence of excess of imidazole, F. Nil Ertas, Josino C. Moreira and Arnold G. Fogg, *Analyst*, 1991, 116, 369.

Cathodic stripping voltammetry at a hanging mercury drop electrode: use of polyaminoacid films, copper(II), derivatization of large molecules and sample cleanup, Arnold G. Fogg, Josino C. Moreira and F. Nil Ertas, *Portugaliae Electrochimica Acta*, 1991, 9, 65.

Adsorptive stripping voltammetry is interesting : is it useful ? Arnold G. Fogg, F. Nil Ertas, Josino C. Moreira and Jiri Barek, *Portugaliae Electrochimica Acta*, 1993, 278, 41.

Cathodic stripping voltammetric behaviour of copper complexes of glycyglycyl-L-histidine at a hanging mercury drop electrode, Arnold G. Fogg, F. Nil Ertas, Josino C. Moreira and Jiri Barek, *Anal. Chim. Acta*, 1993, 278, 41

Differential pulse cathodic stripping voltammetry of the copper complexes of glycyl-L-histidylglycine at a hanging mercury drop electrode, F. Nil Ertas, Arnold G. Fogg, Josino C. Moreira and Jiri Barek, *Talanta*, in press.

Solid phase extraction of chloride interference in differential pulse polarographic determination of nitrate using nitration reaction, Arnold G. Fogg and F. Nil Ertas, in preparation.

## Poster Presentations

Derivatization and adsorptive stripping voltammetry of some biological molecules, modification of HMDE with adsorbed polyaminoacids, Josino C. Moreira, F. Nil Ertas and Arnold G. Fogg, R&D Topics meeting, Analytical division, RSC, Runcorn, July, 1990.

Adsorptive stripping voltammetry of metal complexes of some simple peptides, F. Nil Ertas, Josino C. Moreira and Arnold G. Fogg, R&D Topics meeting, Analytical division, RSC, Aberdeen, July, 1991.

Adsorptive stripping voltammetry of metal complexes of heterocyclic compounds and anti-asthma drugs, F. Nil Ertas, Ramin Pirzad, Josino C. Moreira and Arnold G. Fogg, R&D Topics meeting Analytical division, RSC, Birmingham, July, 1992.

Cathodic stripping voltammetry of copper complexes of histidine-containing peptides, F. Nil Ertas, Josino C. Moreira and Arnold G. Fogg, International symposium on electroanalysis in biomedical, environmental and industrial sciences, Electroanalytical group, Analytical division, RSC, Loughborough, 1993.

